TRANSCRIPTIONAL CONTROL OF T CELL TOLERANCE AND IMMUNITY

by

Chong Luo

A Dissertation

Presented to the Faculty of the Louis V. Gerstner, Jr.

Graduate School of Biomedical Sciences,

Memorial Sloan Kettering Cancer Center

in Partial Fulfillment of the Requirements for the Degree of

Doctor of Philosophy

New York, NY

February, 2016

_____   _____
Ming Li, PhD   Date
Dissertation Mentor

For my parents, grandma and Dazhi

ABSTRACT

The immune system has evolved to mount effective defense against pathogens or tumors yet prevent misguided or excessive responses that could be detrimental to the host. Maintenance of immune homeostasis involves tight control of expansion, differentiation, survival and trafficking of conventional and regulatory lineages of T lymphocytes. This dissertation focuses on T cell receptor (TCR)-induced cell signaling and transcriptional regulation, with a particular interest on how forkhead box O1 (Foxo1)- and GA-binding protein alpha (GABPα)-dependent programs control T cell tolerance and immunity.

We found that the migration of activated-phenotype regulatory T cells (aTregs), the predominant Treg population in non-lymphoid tissues, was associated with repression of Foxo1-dependent transcriptional program. Treg-specific expression of a constitutively active mutant of Foxo1 (Foxo1CA) impeded Treg homing to non-lymphoid organs, causing $CD8^+$ T cell-mediated autoimmune diseases. Compared to Tregs from healthy tissues, tumor-infiltrating Tregs were more susceptible to Foxo1CA-induced depletion. Therefore, the Akt/Foxo signaling in Tregs could be titrated to specifically boost anti-tumor immunity without inflicting autoimmunity.

Using a mouse model that ablates the Ets family transcription factor GABPα specifically in T cells, we showed that GABPα was crucial for T cell proliferation, cellular redox homeostasis and cell survival, both in response to antigen stimulation *in vitro* and upon *Listeria Monocytogenes* infection *in vivo*.

The work in this dissertation will provide novel molecular insights into T cell biology and shed light on future T cell-dependent therapy against cancer and infectious diseases.

ACKNOWLEDGEMENTS

TABLE OF CONTENTS

CHAPTER III

GABP-DEPENDENT REGULATION OF EFFECTOR T CELL RESPONSES

LIST OF FIGURES

CHAPTER I

INTRODUCTION AND OVERVIEW

1.1 T cell overview

The immune system has evolved to mount an effective defense against invading pathogens and to minimize deleterious reactions attacking healthy self-tissues and commensal microorganisms. T lymphocytes, a crucial component of the adaptive immune system, orchestrate antigen-specific immune responses and immunological memory. T cells are composed of two distinct lineages, αβ and γδ T cells, which contain different types of T-cell receptor (TCR) chains and are committed early in T cell development. Later, αβ T cells develop into two distinct functional subsets, CD4$^+$ or CD8$^+$ T cells, identified by their cell surface expression of co-receptors. Cytotoxic CD8$^+$ T cells are crucial in mediating pathogen clearance during various bacterial and viral infections. Full activation and differentiation of these cells requires the help of CD4$^+$ T cells. CD4$^+$ T cells, or helper T cells, also provide help to B cells to produce antibodies and regulate innate immune cells such as macrophages. Immunity mediated by the CD4$^+$ and CD8$^+$ T cells includes a primary response by naive T cells, effector functions by activated T cells, and persistence and reactivation of antigen-specific memory T cells.

1.2 T cell-mediated immunity

1.2.1 T cell development

T cells are derived from multipotent lymphoid progenitors in the bone marrow and differentiate into mature T cells through a series of lineage commitment steps occurring in specific locations of the thymus (*1, 2*). The major stages of thymocyte development can be delineated by the expression of co-receptors, CD4, CD8, which define the CD4$^-$CD8$^-$ (double-negative, DN), CD4$^+$CD8$^+$ (double-positive, DP), CD4$^+$CD8$^-$ or CD4$^-$CD8$^+$ single-positive (SP) subsets. During their early development stages, DN thymocytes can be further subdivided into four stages of differentiation (DN1-DN4), which are identified by their surface expression of CD44 and CD25 (*3*). Early committed T cells (DN1) lack expression of TCR, and they begin to rearrange the γ, δ and β TCR loci simultaneously as they progress through the DN2 to DN4 stages. If a complete γδ TCR is formed before a successful β-chain gene rearrangement, the thymocyte matures into a γδ T cell. If a functional pre-TCR, which is composed of a rearranged β-chain and the non-rearranging pre-T α chain, is formed before a complete γδ TCR, the signal through the pre-TCR commits the cell to the αβ lineage. Successful pre-TCR expression leads to substantial cell proliferation during the DN4 to DP transition and replacement of the pre-TCR α-chain with a newly rearranged TCR α-chain, which yields a complete αβ TCR (*3*).

The αβ TCR$^+$ DP thymocytes then interact with thymic cortical epithelial cells (cTECs) and the bone marrow-derived antigen presenting cells such as dendritic cells

(DCs) that express a high density of major histocompatibility complex (MHC) class I and class II molecules associated with self-peptides. The diversely rearranged TCRs recognize self-peptide MHC (self-pMHC) ligands at various intensities and durations, and the signaling mediated by this TCR-self-pMHC interaction dictates the fate of the DP thymocytes. Too little signaling results in delayed apoptosis (death by neglect), while too much signaling can promote elimination of the thymocyte by negative selection. The appropriate, intermediate level of TCR signaling initiates effective maturation into SP thymocytes, a process known as positive selection (*4*). SP cells migrate from the cortex to the medulla, where they continue to sample antigen presented by DCs and medullary TECs (mTECs). Thymocytes that express TCRs that bind self-pMHC-class-I complexes become CD8$^+$ T cells, whereas those with TCRs that contact self-pMHC-class-II ligands develop into CD4$^+$ T cells (*5*). Among the CD4$^+$ SP cells, one subset that receives strong TCR signal differentiates to thymic regulatory T cells (tTregs), which is marked by the expression of forkhead family of transcription factor Foxp3 (*6*). The CD4$^+$ and CD8$^+$ SP cells are then ready to emigrate from the thymus.

1.2.2 Naive T cell homeostasis

Once T cells have completed their development in the thymus, they enter the bloodstream and continually recirculate through secondary lymphoid organs, the lymph and the blood (*7*). Mature recirculating T cells that have not yet encountered their cognate antigens are known as naive T cells. They are characterized by low expression of CD44 (CD44^{lo}) and high expression of the lymph node-homing receptors L-selectin (CD62L)

3

and CC-chemokine receptor 7 (CCR7) ($CD62L^{hi}CCR7^{hi}$). Naive T cells are relatively long-lived and can remain in interphase for several weeks (*8, 9*).

The numbers of naive T cells in the periphery remain fairly stable in young adult animals, despite continuous output from the thymus, suggesting balanced loss and replacement. In addition to the stable size of the entire pool, naive T cell homeostasis requires the maintenance of diversity and functional competence. A large number of unique antigen receptors are needed in a limited physical space in order to recognize a multitude of potential foreign antigens (*9*). Maintenance of both the naive T cell number and the diverse TCR repertoire relies on signals from TCR-self-pMHC interaction and members of the common gamma chain (γ_C) family of cytokines, including interleukin 7 (IL-7) and to a lesser degree IL-15 (*10-12*). IL-7 and related cytokines promote survival of naive T cells by preventing the mitochondrial pathway of apoptosis, primarily through increasing expression of the anti-apoptotic factor Bcl-2 (*13, 14*).

Naive T cells undergo spontaneous homeostatic proliferation in response to severe depletion of T cells or upon transfer into lymphopenic environment. This homeostatic proliferation is dependent on the TCR-self-pMHC interaction and/or IL-7, the same factors required for survival of naive T cells, but have increased availability under lymphopenic conditions (*15*). Other common γ_C cytokines such as IL-15 and IL-2 can also provoke proliferation of naive T cells (*16*).

1.2.3 T cell activation and differentiation

Upon encountering of foreign antigens presented by antigen-presenting cells (APCs), naive T cells become activated and differentiate into effector T cells. This process is accompanied by robust proliferation, transcriptional, epigenetic and metabolic reprogramming, and the acquisition of cardinal features of effector T cells such as effector function and altered migratory pattern.

Naive T cells are small resting cells with condensed chromatin. Antigen sensing, together with costimulation and cytokine signaling trigger the quiescent T cell to rapidly proliferate and differentiate into effector T cells (*17*). Their proliferation and differentiation are driven by the cytokine IL-2, which is produced by the activated T cells themselves (*18*). Initiation and progression of cell cycle is tightly controlled by the ordered expression and degradation of cyclins, cyclin-dependent kinase (CDKs) and their negative regulators, the CDK inhibitors. Extracellular cues are first integrated through the D-type cyclins and their catalytic partners, CDK4 and CDK6. The D-type cyclins are rate-limiting factors cell cycle progression from the G1 to the S phase. The induction of cyclin E occurs at the late G1 restriction point, and cyclin A is expressed at S phase entry. CDK inhibitors, such as p27^{kip1} and p21^{cip1}, negatively modulate the kinase activities of CDKs. Cyclin-CDK complexes phosphorylate the retinoblastoma tumor suppressor (Rb), releasing the E2F transcription factor from Rb-mediated inhibition, which is required for the transcription of S phase genes (*19*).

T cell activation is also accompanied with dramatic metabolic changes (*20, 21*). Naive T cells exhibit basal levels of nutrient uptake and primarily use mitochondrial

oxidative phosphorylation (OXPHOS) and fatty acid oxidation (FAO) to generate energy in the form of ATP (*17, 22*). Antigen stimulation leads to increased uptake of nutrients and a metabolic switch to a program of anabolic growth and biomass accumulation. Notably, activated T cells show enhanced facilitated glucose transport and a marked increase in aerobic glycolysis, a process in which glucose is converted into lactate even though sufficient oxygen is present to support glucose catabolism via the tricarboxylic acid (TCA) cycle and OXPHOS (*20, 23*). Although less efficient in producing ATP, aerobic glycolysis is thought to provide activated T cells with intermediate substrates to fuel *de novo* nucleotide synthesis and fatty acid synthesis (FAS), and to serve as a way to maintain the redox balance (NAD^+/NADH) in the cell (*22, 24*). In addition, T cell activation results in increased facilitated amino acid transport and augmented glutaminolysis to support the need of biosynthetic precursors required for rapid cell growth (*23*). Moreover, Tregs exhibit distinct metabolic profiles from conventional effector T cells – they depend more on the oxidation of lipids rather than strongly engaging glycolysis (*25*).

Activated T cells differentiate into diverse effector subsets, which is optimally tailored to provide an appropriate response to the broad array of infectious agents that the host encounters. Depending on the particular cytokine milieu, naive $CD4^+$ T cells can differentiate into T helper 1 (Th1), Th2, Th17, T follicular helper (Tfh) and peripherally derived Tregs (pTregs) (*26, 27*). These subsets require the transcription factors T-bet, GATA-binding protein 3 (GATA3), retinoic acid receptor-related orphan receptor-γt (RORγt), B cell lymphoma 6 (BCL-6) and forkhead box P3 (FOXP3), respectively, for their development (*27*). They also play distinct roles in the regulation of immune

responses: Th1 cells preferentially produce the cytokine IFN-γ, and are important for eradicating intracellular pathogens. Th2 cells produce large quantities of IL-4, IL-5 and IL-13, and are crucial in the regulation of humoral immune responses to extracellular pathogens, such as helminth worms. Th17 cells are known for their secretion of IL-17, and they are important in the elimination of extracellular bacteria and fungi. Tfh locate in the germinal center, and are specialized providers of B cell help in the lymphoid follicles. pTregs, together with tTregs, restrain effector T cell responses and keep autoimmunity in check (*27*). CD8$^+$ T cells have a less versatile repertoire of effector functions. They differentiate into cytotoxic effector T cells that recognize and kill cells infected by intercellular pathogens like virus and bacteria. CD8$^+$ T cells accomplish killing through molecules including the granzymes and perforin, and Fas-mediated cell death mechanisms. Effector CD8$^+$ T cells secrete inflammatory cytokines such as IFN-γ and tumor necrosis factor TNF as well (*28, 29*).

T cell activation also leads to altered migration – naive T cells recirculate through secondary lymphoid organs, whereas activated T cells disseminate broadly to sites of infection to exert effector functions (*7*). Cell surface proteins including CD62L, CCR7 and lymphocyte function-associated antigen 1 (LFA1) mediate the entry of naive T cells into secondary lymph organs. These molecules are downregulated upon antigen stimulation (*30, 31*). In addition, specific homing molecules are induced in effector T cells to dictate their tissue-selective homing, for instance, CCR9 and integrin α4β7 are preferentially upregulated in T cells migrating to the gut, and CCR10 is induced to guide T cells to the skin (*32, 33*).

1.2.4 Memory T cells

Following the peak of effector expansion, the resolution of inflammation and pathogen eradication, the majority of effector T cells die, leaving behind a heterogeneous pool of memory T cells (*34, 35*). On the basis of their function, proliferative capacity, anatomical location and migration pattern, memory T cells can be divided into discrete subsets, including two circulating populations – effector memory T (T_{EM}) cells and central memory T (T_{CM}) cells – as well as non-circulating tissue-resident memory T cells (*36*). T_{CM} cells express high levels of lymph node homing molecules, CCR7 and CD62L, and home to secondary lymphoid organs and bone marrow. T_{EM} cells lack the expression of these lymph homing molecules, and are most commonly found in non-lymphoid tissues (*37, 38*). Functionally, T_{CM} cells can proliferate extensively and produce IL-2, whereas T_{EM} cells possess heightened effector functions such as cytolytic activity among $CD8^+$ T cells, and they are commonly the immediate responders. Both T_{CM} and T_{EM} populations continuously circulate through blood vessels, and they might interconvert as they pass through lymphoid and non-lymphoid tissues (*37*).

Memory T cells downregulate much of the activation program of effector T cells, yet they maintain the ability to rapidly reactivate effector functions upon restimulation. They primarily rely on fatty acid metabolism, and are maintained in an antigen-independent, cytokine-dependent manner mainly through IL-7 and IL-15, which promote the cell survival and self-renewal proliferation (*8*).

1.3 Molecular insights into T cell signaling

Immunological inputs in form of antigen recognition (signal 1), co-stimulatory ligand engagement (signal 2) and cytokine stimulation (signal 3) guide the outcomes of T cell development, homeostasis, activation and differentiation (*39*). The responses are highly coordinated and context-dependent. A number of evolutionarily conserved signaling modules have been rewired by T lymphocytes to interpret these environmental cues and to orchestrate the wide array of responses.

1.3.1 T cell receptor (TCR) signaling

The signaling network downstream of TCR signaling has a central role in adaptive immune response (Fig. 1-1). The extracellular portion of TCR recognizes cognate pMHC, which is facilitated by the binding of coreceptors, CD4 and CD8. TCR-pMHC interaction induces conformational changes of associated CD3 chains and phosphorylation of the immunoreceptor tyrosine-based activation motifs (ITAMs) of CD3 δ-, γ-, ε-, and ζ-chains, which is mediated by the Src kinases leukocyte-specific tyrosine kinase (Lck) (*14*). A significant proportion of Lck in the cell constitutively associates with the intracellular domain of CD4, thus CD4 "primes" TCR signaling upon recruitment to the TCR-CD3 complexes. Phosphorylated CD3 ITAMs recruit the Syk family kinase Zeta activated protein 70 kDa (Zap70) via Src-homology-2 (SH2)-domain interactions (*40*).

Upon localization to the TCR complex, Zap70 propagates TCR signaling by phosphorylating multiple downstream targets, among which include the activation of T cells (Lat), a membrane-associated scaffolding protein (*41*). Phosphorylated Lat recruits a second molecular scaffold, SH2-domain-containing leukocyte protein of 76 kDa (Slp76), via the protein Grb2-related adapter proteins (Gads) (*42*). Slp76 is subsequently phosphorylated by Zap70, and the resulting LAT-Slp76 complex serves as a platform for the recruitment of downstream effector molecules to further amplify the TCR-induced signaling, among which include phospholipase C-γ (PLCγ) and the Tec family kinase interleukin-2-inducible T-cell kinase (ITK) (*42*).

PLCγ transduces TCR signals by hydrolyzing phosphatidylinositol (4,5)-bisphosphate (PIP_2) to yield diacylglycerol (DAG), a membrane-associated lipid, and inositol (1,4,5)-trisphophate (IP_3), a diffusible second messenger. DAG recruits a number of downstream proteins to the plasma membrane, among them protein kinase C (PKC) and RAS guanyl nucleotide-releasing protein (RasGRP) (*43*). PKC activates a protein complex comprising the adaptors caspase recruitment domain containing membrane-associated guanylate kinase protein 1 (CARMA1), Bcl10 and mucosa-associated lymphoid tissue lymphoma translocation gene 1 (MALT1), and modulates the nuclear factor of kappa light chain enhancer in B cells (NF-κB)-dependent signaling pathway (*44, 45*). Under resting conditions, NF-κB is sequestered in the cytoplasm by inhibitor of κB (IκB). Phosphorylation of IκB by the IκB kinase (IKK) complex leads to the ubiquitylation and degradation of IκB, allowing NF-κB to translocate the nucleus. Activation of the CARMA1/Bcl10/MALT1 complex by PKC stimulates IKK, which then phosphorylates IκB and results in activation of NF-κB-dependent transcription (*46*).

10

RasGRP is a guanine nucleotide-exchange factor (GEF) for the small GTPase Ras, which crucial in transmitting signals from cell-surface receptor tyrosine kinases (RTKs) to activate downstream signaling cascades. In its active, GTP-bound confirmation, Ras has high affinity for numerous downstream effectors of RTK signal transduction pathways, including Raf, thereby activating a mitogen-activated protein kinase (MAPK) signaling cascades. Raf is a MAPK kinase kinase (MAPKKK) that phosphorylates and activates MAPK kinase (MAPKKs), which in turn phosphorylate and activate the effector MAPK, extracellular signal-regulated kinase (ERK) (*43*). ERK phosphorylates the ETS family transcription factors to induce the expression of immediate early genes such as c-Fos, a component of the AP-1 transcription complex (*47*).

The IP_3 generated by TCR-stimulated PLCγ activity stimulates the opening of Ca^{2+}-permeable ion channel receptors (IP_3R) on the endoplasmic reticulum (ER) membrane, leading to the release of ER Ca^{2+} stores into the cytoplasm (*48*). Depletion of ER Ca^{2+} triggers the aggregation of Ca^{2+} sensors stromal interaction molecules (STIMs) in regions of close ER-plasma-membrane apposition (*49, 50*). These STIM clusters induce the opening of Orail channels in the cell membrane, leading to a large and sustained influx of extracellular Ca^{2+} into the cytoplasm (*51*). The activity of nuclear factor of activated T cells (NFAT) is regulated by the concentration of intracellular Ca^{2+} (*52*). When Ca^{2+} levels are low, phosphorylation by the kinase glycogen synthase kinase 3 (GSK3) promotes nuclear export of NFAT. Increases in cytoplasmic Ca^{2+} lead to the dephosphorylation and nuclear import of NFAT, which is mediated by the binding of Ca^{2+} to calmodulin and subsequent activation of the phosphatase calcineurin (CN) that dephosphorylates NFAT (*53*).

In addition to the hydrolysis mediated by PLC, PIP_2 can be modified by phosphatidylinositol 3-kinase (PI3K). Several TCR signaling effectors, including Ras, activate PI3K, which then phosphorylates PIP_2 to generate phosphatidylinositol (3,4,5)-trisphosphate (PIP_3). Localized PIP_3 generation serves as a docking site for the PH domains of 3-phosphoinositide-dependent protein kinase 1 (PDK1) and its target Akt (*54*). Phosphorylation of Akt by PDK1 and the mechanistic target of rapamycin complex 2 (mTORC2) leads to its activation, allowing it to phosphorylate multiple downstream proteins including the Foxo family of transcription factors and the tuberous sclerosis complex (TSC) (*55*). Phosphorylation of Foxo proteins by Akt induces their nuclear export and transcriptional inactivation (*56*). Phosphorylation of TSC by Akt represses its function as a GTPase-activating protein (GAP) towards the small GTPase Rheb, which activates the mTORC1 kinase that is important in the regulation of cellular growth and metabolic responses (*57*). Activation of Akt also enhances the nuclear translocation of NF-κB by facilitating the assembly of the CARMA1/Bcl10/MALT1 complex (*58*). In addition, Akt affects optimal transcription of NFAT-regulated genes by inactivating GSK-3, the kinase that triggers nuclear export of NFAT (*53*).

Besides the downstream proteins that amplify the TCR-induced signaling, several pathways are involved in the downregulation of this signaling network. PLCγ-mediated signaling is attenuated by diacyglycerol kinases (DGKs), which phosphorylate DAG to yield phosphatidic acid (PA) (*59*). PI3K signaling is regulated by the opposing activity of the phosphate and tensin homology (Pten), which converts PIP_3 to PIP_2 (*55*).
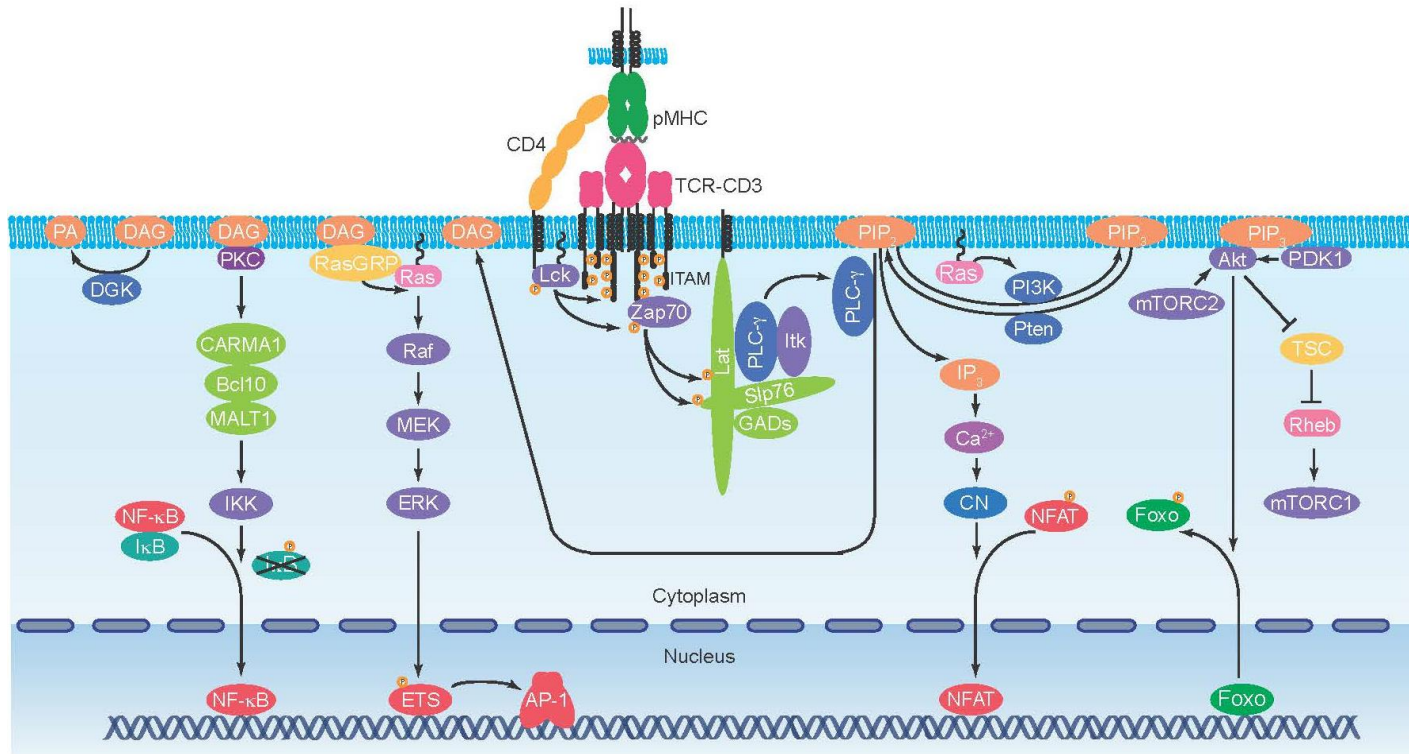
Figure 1-1: The T cell receptor (TCR) signaling network. Abbreviations: TCR, T cell receptor; MHC, major histocompatibility complex; ITAM, immunoreceptor tyrosine-based activation motif; Zap70, Zeta-associated protein 70 kDa; Slp76, SH2-domain-containing leukocyte protein of 76 kDa; GAD, Grb2-related adapter protein; PLCγ, phospholipase C-γ; Itk, interleukin-2-inducible T-cell kinase; PIP2, phosphatidylinositol (4,5)-bisphosphate; DAG, diacylglycerol; IP3, inositol (1,4,5)-triphosphate; Ca^{2+}, calcium; STIM, stromal interaction molecule; CN, calcineurin; PKC, protein kinase C; RasGRP, RAS guanyl nucleotide-releasing protein; CARMA1, caspase recruiting domain-containing membrane-associated guanylate kinase protein 1; Bcl10, B-cell lymphoma 10; MALT1, mucosa-associated lymphoid tissue lymphoma translocation gene 1; IKK, IκB kinase; PI3K, phosphatidylinositol 3-kinase; PIP3, PtdIns(3,4,5)P$_3$; mTORC1/2, the mechanistic target of repamycin complex 1/2; TSC, tuberous sclerosis complex; Foxo, Forkhead family O; GAP, GTPase-activating protein; PA, phosphatidic acid; DGK, diacylglycerol kinase.

1.3.2 Co-stimulation

Signaling solely through the TCR results in a nonresponsive state (anergy) in which T cells are refractory to restimulation. Optimal T cell stimulation that leads to productive T cell activation and proliferation requires a second signal delivered by the colligation of other cell surface receptors. Although many cell surface receptors can provide costimulatory signal, CD28, upon binding to B7-1 and B7-2 (also known as CD80 and CD86) expressed by APCs, transmits the most robust signal. Ligand binding of CD28 induces phosphorylation of its cytoplasmic tail, which recruits several downstream proteins, including PI3K and ITK (*60*). Since these molecules are also recruited to the activated TCR complex, it's speculated that CD28 engagement primarily enhance T cell signaling in a quantitative manner rather than a qualitative manner.

In addition to CD28, a number of other transmembrane proteins, such as inducible costimulator (ICOS), 4-1BB and OX40, have been described as having costimulatory functions (*61*). ICOS belongs to the CD28 superfamily of costimulatory molecules, and it binds to the B7-H2 ligand (*62*). Unlike CD28, which is constitutively expressed on naive and activated T cells, expression of ICOS is induced on activated T cells. Ligand engagement of ICOS also leads to phosphorylation of its cytoplasmic tail and stimulation of the PI3K signaling. 4-1BB and OX40 are members of the TNF receptor superfamily, and they transmit costimulatory signal in a distinct pattern from CD28 and ICOS. Colligation of 4-1BB and OX40 with their ligands 4-1BBL and OX40L, respectively, link downstream signaling through the TNFR-associated factor (TRAF) family of adapter proteins (*63*).

Besides the receptors that deliver positive signals, a group of co-inhibitory receptors function to limit the expansion and activation of TCR-triggered cells. Cytotoxic T-lymphocyte antigen 4 (CTLA4) and programmed death-1 (PD1) represent two well-studied co-inhibitory receptors (*64, 65*). CTLA4 is closely related to CD28, but it binds to B7-1 and B7-2 with significantly higher affinity (*66*). It is sequestered in intracellular compartment in resting T cells, and traffics to the cell surface following TCR stimulation. One mechanism of CTLA4 exerting its inhibitory function is through competing with CD28 for binding to the B7 ligands. Additionally, ligand binding of CTLA4 leads to phosphorylation of its cytoplasmic tail, which recruits phosphatases, such as SH2-domain-containing tyrosine phosphate 2 (SHP2) and serine/threonine protein phosphatase 2A (PP2A), to dephosphorylate membrane-proximal effectors. Binding of PD1 to its ligand (PD1-L) recruits SHP2 and PP2A in a similar manner as CTLA4 (*61*).

1.3.3 Cytokine signaling

Along with antigen recognition and costimulation, a third signal that is mediated by cytokines plays crucial roles in T cell development, differentiation and function. For instance, CD8$^+$ T cells that do not receive a third signal from inflammatory cytokines, pre-dominantly IL-12 and type I interferons (IFNα/β), fail to develop cytolytic function, and become unresponsive (*67*). Additionally, the particular cytokine milieu experienced by antigen-activated CD4$^+$ T cells instructs the differentiation into distinct effector lineages.

Cytokines can be grouped into families based on their structures and downstream signaling modules. One large class of cytokines, including interleukins, interferons (IFNs), and hemotopoietins, employ the Janus kinase (JAK)-signal transducers and activators of transcription (STAT) pathway (*68, 69*). The receptors of these cytokines lack intrinsic kinase activity and are associated with JAK family of tyrosine kinase. Ligand binding to cytokine receptors and subsequent receptor dimerization lead to activation of associated JAKs. There are four JAK proteins, JAK1, JAK2, JAK3 and Tyk2, which selectively bind different receptor chains. The activated JAKs then phosphorylate the receptor cytoplasmic domains, creating docking sites for Sh2-containing signaling proteins, most representatively, the STATs. STATs are a family of transcription factors composed of seven members (STAT1-4, 5a, 5b and 6), and they dimerize upon activation by JAKs. The STAT-STAT dimer translocate to the nucleus, where it can directly bind DNA and regulate gene expression. One subfamily of cytokines that stimulates the JAK-STAT pathway include IL-2, IL-4, IL-7, IL-9, and IL-15, and they interact with a shared receptor subunit, the common γ chain (γ_C, CD132) (*70*). JAK3 binds γ_C, and JAK1 interact with the ligand specific subunit that is associated with γ_C. All interferons signal through the JAK/STAT pathway, and different JAK and STAT members mediate distinct downstream responses. Type I IFNs, including IFN-α, β activate TYK2 and JAK1, resulting in STAT1-2 heterodimerization, whereas type II IFN (IFN-γ) activates JAK1 and JAK2 to induce STAT1 homodimerizaion (*71*). The JAK/STAT pathway is negatively regulated by a family of JAK kinase inhibitor proteins referred to as suppressors of cytokine signaling (SOCS). SOCS members inhibit

JAK/STAT signaling via binding to phosphorylated JAK to suppress its kinase activity or interacting with cytokine receptors to block STAT recruitment (*72*).

Tumor necrosis factors (TNFs), such as TNF-α and lymphotoxin (LT), represent another important class of pro-inflammatory cytokines (*73*). TNF is primarily produced as a trimeric type II transmembrane protein, and the soluble TNF is released via proteolytic cleavage. Both TNF and LT bind to two receptors: TNF receptor 1 (TNFR1) and TNFR2, which differ in their structure and expression patterns. The intracellular domains of the two receptors are devoid of intrinsic enzyme activity, and they transduce signaling by recruiting distinct signaling modules. TNFR1 contains a cytoplasmic death domain (DD), which recruits the adaptor molecule TNFR1-associated death domain protein (TRADD). TNFR2 lacks the cytoplasmic DD sequence and binds TNFR-associated factor 1 (TRAF1) and TRAF2. Both TNFR1-TRADD and TNFR2-TRAF1/TRAF2 signaling lead to activation of NF-κB pathway, through the recruitment of receptor-interacting serine threonine-protein kinase 1 (RIPK1), and transforming growth factor β (TGF-β)-activated kinase 1 and MAP3K7-binding protein 2 (TAB2) and TAB3 and TGF-β-activated kinase 1 (TAK1). The activated TAK1 also stimulate the JNK and p38 signaling (*74*).

TGF-β belongs to a family of regulatory cytokine that have pleiotropic functions (*75*). Three members of TGF-β proteins (TGF-β1-3) have been identified in mammals, and TGF-β1 is the predominant form expressed in the immune system. TGF-β is synthesized in an inactive form composed of a TGF-β dimer in association with the latency-associated protein (LAP), which is subsequently degraded by a TGF-β activator (*76*). Active TGF-β initiates signaling by binding to and bringing together type I and type

II receptors (TGF-βRI and TGF-βRII) that contain serine/threonine kinase activity. This allows TGF-βRII to phosphorylate and activate TGF-βRI, which then propagates the signal through phosphorylation of the Smad proteins, such as Smad2 and Smad3. Phosphorylated Smad2/3 interact with the co-Smad, Smad4, and translocate into the nucleus. In conjunction with other nuclear cofactors, the active Smad complex binds to DNA and regulate the transcription of target genes (*77*). In addition, TGF-β activates a number of Smad-independent signaling pathways, such as MAPK and PI3K/Akt signaling.

1.4 T lymphocytes in health and disease

1.4.1 T cell tolerance under steady-state conditions

As a key component of the adaptive immune system, T lymphocytes are capable of recognizing enormously diverse antigens, mounting vigorous effector responses, and developing long-lasting immunological memory. Due to this high potency, they can cause severe damage to the host if inappropriately directed. Therefore, a major challenge for the immune system under steady-state conditions is the maintenance of self-tolerance.

Multiple mechanisms are involved in the immune self-tolerance. Central tolerance refers to the deletion of autoreactive T cells during development in the thymus (*78*). Single positive thymocytes binding with overly high avidity to self-peptide MHC complex undergo apoptosis in the thymic medulla, a process named clonal deletion (*79*). This process relies in part on ectopic expression and presentation of proteins usually

restricted to peripheral tissues, by medullary thymic epithelial cells (mTEC). Promiscuous expression of tissue-restricted antigens (TRAs) by mTEC is regulated by a transcription factor called the autoimmune regulator (AIRE), mutation of which causes autoimmune polyendocrinopathy, candidiasis, and ectodermal dysplasia (APECED) (*80, 81*). In addition to clonal deletion, clonal diversion also occurs in the thymus – some self-reactive clones differentiate into Tregs (*6, 82, 83*). Finally, a group of thymocytes expressing high affinity TCR for self-peptide MHC complexes can avoid the deletion or diversion fate via secondary gene rearrangement at the TCRα loci, a process is known as receptor editing, thereby changing the TCR specificity (*84*).

Despite extensive pruning of self-reactive cells in the thymus, potentially self-destructive T cells escape into the periphery, necessitating additional peripheral tolerance mechanisms. Self-reactive T cells can be rendered anergic upon exposure to cognate self-antigen in the peripheral (*85*). Alternatively, their activation threshold may be raised by the expression of inhibitory receptors or negative signaling molecules (*85*). In addition, deletion of self-reactive T lymphocytes through apoptotic cell death also occurs in the peripheral, a process that is termed peripheral deletion (*61*). Mutation in FAS, a member of the TNF receptor family that is crucial for both the central and peripheral deletion, causes autoimmune lymphoproliferative syndrome (*86*).

In addition to these cell-intrinsic or recessive mechanisms, cell-extrinsic or dominant mechanisms, by which suppressive populations acting in *trans* to restrain aberrant or over-reactive lymphocytes, play pivotal roles in the maintenance of peripheral tolerance. A most extensively studied suppressive population is Tregs. Mutations of the *Foxp3* gene, which encodes the lineage-specifying transcription factor of Tregs, result in

a lethal lymphoproliferative disorder in *Scurfy* mice, and are associated with immunedysregulation, polyendocrinopathy, enteropathy and X-linked syndrome (IPEX) in human patients (*87-89*). Tregs depend on IL-2 signaling for development and function. IPEX-like syndrome is also manifested in animals possessing defects in IL-2 signaling such as mutations in the IL-2 receptor α chain (CD25) or the intracellular signaling mediator STAT5b (*90, 91*).

1.4.2 T cell responses to infection

The goal of immune responses in infectious diseases is to eliminate pathogens through inflammatory reactions without collateral damage. T cells are not only the key mediators of adaptive immune reactions, but they also orchestrate the delicate balance between nonproductive and exaggerated responses. Depending on the particular pathogenic insults, naive CD4$^+$ T cells can differentiate into Th1, Th2 and Th17 cells, which are important for eradicating intracellular pathogens, helmith, and extracellular bacteria/fungi, respectively. Tfh and Treg cells are two other CD4$^+$ T cell subsets that can provide help to B cells or limit immune reactions, respectively. CD8$^+$ T cells differentiate into cytotoxic lymphocytes that participate in defense against intracellular viral, bacterial and protozoal infections.

The differentiation fate of effector CD4$^+$ T cells involves integration of antigen, costimulatory, and cytokine signals that influence the expression of lineage-specific transcription factors (*26, 27*). During Th1 polarization, IL-12 produced by dendritic cells and macrophages binds to IL-12 receptor, a heterodimer of IL-12Rβ1 and IL-12Rβ2, on

the cell surface of naive CD4$^+$ T cells, and stimulates IFN-γ production via STAT4 activation. IFN-γ produced by developing Th1 cells functions through an autocrine route, binds to IFN-γ receptor (IFN-γR), elicits downstream STAT1 signaling and induces T-bet expression (*92*). T-bet is a lineage specific transcription factor of Th1 program, which functions to enhance IFN-γ production and induce IL-12Rβ2 expression. IFN-γ produced by Th1 cells then activates macrophages that are infected by or have ingested pathogens to eliminate the intracellular pathogen (*92*). Th1 cells are of particular importance in the defense against intracellular bacteria, most notably, mycobacterial species, as deficiencies in human *IFNGR1, IFNGR2, STAT1, IL12RB1,* and *IL12B* genes causes susceptibility to those infections (*93*).

IL-4 is a crucial cytokine for Th2 lineage commitment. Parasite infection triggers the production of IL-4 in cells such as eosinophils and basophils. Binding of IL-4 to the IL-4 receptor on naive CD4$^+$ T cells activates STAT6, which upregulates the expression of the master regulator GATA3. GATA3 induces its own expression, reinforcing Th2 differentiation. GATA3 also induces the expression of type 2 cytokines, IL-4, IL-5 and IL-13 that required for the switching of B cells to produce the IgE class of antibody and recruitment of eosinophils. Besides GATA3, IL-2-mediated activation of STAT5 is indispensible for the production of Th2 cytokines as well (*94, 95*). Mutations of GATA3 have been detected in human populations, and in the heterozygous form they account for the hypoparathyroidism, deafness, and renal dysplasia (HDR) syndrome (*96*). Mice lacking IL-4 receptor α chain (IL-4Rα), STAT6 or GATA3 show highly compromised anti-helminth immunity (*97, 98*).

IL6, IL21, IL23 and TGF-β are the major signaling cytokines involved in Th17 cell differentiation, and RORγt is the master regulator. The differentiation process can be divided into three stages – differentiation, amplification and stabilization. TGF-β in the presence of IL-6 initiates the differentiation of Th17 lineage, inducing the expression of RORγt, production of IL-21 as well as upregulation of IL-23 receptor (IL-23R) (*99*). IL-21 produced by developing Th17 cells then mediates the amplification step, and IL-23 expands and stabilizes the Th17 lineage. STAT3, activated downstream of IL-6, IL-21 and IL-23, is crucial in the Th17 differentiation process (*100, 101*). Th17 cells help protect against extracellular bacteria and fungi through stimulating the neutrophil response that helps to clear such pathogens. Mutations in IL-12Rβ1, the signal transduction chain of both IL-12 and IL-23 receptors, in humans lead to impaired immunity to mycobacteria and Candidia (*102*). Similarly, mutations in STAT3, or RORC, the human version of mouse RORγ, trigger heightened susceptibility to fungi infection, such as *Staphylococcus aureus* and *Candida albicans (102, 103)*. Besides the protective responses in infection, Th17 cells have been implicated in many autoimmune diseases, including psoriasis, rheumatoid arthritis and Crohn's disease (*104-106*).

CD4^{+} Tfh cells are recently recognized as a distinct T cell subset. They are identified mainly by their location in the B cell follicles, and by the expression of surface markers including chemokine (C-X-C motif) receptor 5 (CXCR5) and ICOS. Bcl-6, a transcription factor that is induced by antigen stimulation and ICOS signaling, plays a crucial role in Tfh differentiation. Tfh cells express CD40 ligand, and produce IL-21 and IL-4 (*107*). They drive B cell proliferation, antibody affinity maturation, isotype class switching, and the formation of memory B cells and plasma cells. Increased populations

of virus-specific Tfh cells are observed during chronic lymphocytic choriomeningitis virus (LCMV) infection of mice, as well as human immunodeficiency virus (HIV), hepatitis B and hepatitis C virus infections of humans, yet they exhibit impaired activity partly due to PD-1 ligation (*108*). Additionally, aberrant expansion of circulating Tfh cells has been reported to correlate with numerous autoimmune diseases in humans, including rheumatoid arthritis and systemic lupus erythematosus (*109*).

Cytotoxic CD8+ T cells are important in the defense against intracellular pathogens, including virus, bacteria and protozoa. They recognize pathogen-derived peptides complexed with MHC class I molecules on the surface of infected cells, and trigger apoptosis of the target cells. The principle mechanism of CTL killing is the release of cytotoxic granules, which includes granzymes that induces apoptosis of target cells, and perforin that delivers granzymes into the cells (*28*). CD8+ T cells also perform killing via Fas-Fas ligand-dependent cell death. Additionally, they secrete cytokines such as TNF-α and IFN-γ, which play important roles in antimicrobial defense. Durable memory CD8+ T cells can be established after the eradication of pathogen, conferring protection against subsequent reinfection (*28*). Mutations in genes coding for proteins that transport MHC I to the cell surface, for example TAP1 and TAP2, impair CD8+ T cell development and function (*110*). Increased susceptibility to a broad spectrum of infections has been observed in patients harboring these mutations, underlying the crucial function for CD8+ T cells in host defense (*110*).

In addition to the effector CD4+ and CD8+ T cell populations that carry out host defense against invading pathogens, Tregs also participate in the responses to infection. They play both negative and positive roles − excessive Treg activity restrains effector T

23

cell responses and impairs clearance of harmful pathogens, yet adequate Treg activity is required to limit the immunopathology (*111*). The deleterious role of Tregs has been implicated by the association of elevated Treg number with higher viral burden in patients infected with hepatitis C virus (*112*). On the other hand, Tregs exert protective function by regulating the quality and quantity of effector response. For instance, in a murine infection model of herpes simplex virus-2 (HSV-2), depletion of Tregs triggers uncontrolled T cell activation that prevents effector T cell migration to the site of infection (*112*). Furthermore, Tregs increase the avidity of primary $CD8^+$ T cell responses by destabilizing low-affinity T cell-DC interactions in mice following *Listeria monocytogenes* infection (*113*). Tregs also promote memory responses in a murine *Leishmania* infection model through blocking the sterile eradication of the pathogen, thereby providing long-term persistence of the antigen that is needed for the maintenance of memory responses (*114*).

1.4.3 T lymphocytes in cancer

The idea that immune system has negative effects in tumor development may trace back to the 1900s, but it has been under debate ever since. Extensive work over the past two decades has ended the argument, and demonstrated the dual host-protective and tumor-promoting roles of immunity (*115*). The immune system can not only suppress tumor growth by recognizing and destroying cancer cells (cancer immunosurveillance), but also facilitate tumor progression either by selecting for tumor cells that are more fit to survive in an immunocompetent host (possibly through shaping the immunogenicity), or

by establishing conditions within the tumor microenvironment that are beneficial for tumor growth (*116*). T lymphocytes have central functions in the many facets of immune-tumor interactions.

The host-protective role of T cells is supported by the observations that mice lacking T cells, such as $Tcrb^{-/-}Tcrd^{-/-}$ and Nude strains, develop more carcinogen-induced tumors and spontaneous cancer than wild-type mice (*117, 118*). CD8$^+$ T cells are at the core of adaptive response. They recognize and destroy the tumor cells expressing peptide-MHC class I complexes on the surface. CD8α^+ DC can take up and cross-present tumor antigens to T cells, a process that is promoted by type I IFNs (*119*). Activated effector CD8$^+$ T cells release IFN-γ that can mediate anti-tumor effects by inhibiting tumor cell proliferation and angiogenesis, or by activating macrophages (*119*). Additionally, CD8$^+$ T cells can induce tumor cell apoptosis by interacting with Fas and TRAIL receptors on tumor cells, or through secreting perforin and granzymes. Depleting effector molecules including IFN-γ, perforin, Fas Ligand, TRAIL in mice causes increased susceptibility to carcinogen-induced or spontaneous tumors (*120-122*). On the other hand, contribution of CD4$^+$ T helper cells to host protection against tumors has been typically attributed to Th1 cells, whereas the functions of Th2, Th17 and Tfh cells remain elusive (*123*).

Conversely, T cells can promote tumor evasion. One such mechanism is through immunoediting that selects outgrowth of tumor cells that lack strong rejection antigens (*124*). Another mechanism is mediated by Tregs, which dampen effector responses and prevent immune-mediated rejection of cancer (*125*). In murine tumor models, transient ablation of Tregs results in activation of CD4$^+$ or CD8$^+$ effector T cells and rejection of

solid tumors (*126*). In human patients, low Treg to Teff ratios are associated with better prognosis in multiple cancers including ovarian cancer, breast cancer, renal cell carcinoma, and colorectal carcinoma (*127, 128*).

Growing knowledge on the interplay between T cells and tumor cells has attracted enormous interest to T cell-based cancer therapies. One early approach focuses on developing therapeutic vaccines to expand T cells against shared antigens expressed on tumors (*129*). Nevertheless, such trials elicited minimal clinical benefits, which might be caused by cell-extrinsic suppressive mechanisms in the tumor microenvironment such as Tregs. Another contributing factor to the failure of cancer vaccines is cell intrinsic – the anergic or irresponsive status of tumor-infiltrating lymphocytes triggered by activation of inhibitory pathways such as CTLA-4 and PD-1 (*61*). Blocking CTLA-4 and/or PD-1 unleashes T cell responses against tumor, and has generated outstanding responses in patients with a variety of tumor types, including melanoma, renal cell carcinoma, prostate cancer and ovarian cancer (*130-132*).

Adoptive T cell transfer represents another type of T cell manipulation in cancer treatment. In one approach, tumor-infiltrating lymphocytes (TILs) are isolated, expanded, and in some cases, selected for TCR specificity before being reinfused into the same patient (*133*). TIL transfer has so far showed remarkable efficacy in patients with metastatic melanoma (*134*). In a second approach, host T cells are genetically engineered with antitumor T cell receptors or chimeric antigen receptors (CARs) before subsequent administration to the patient. CARs can be constructed by linking the antigen-binding domain of an antibody to the intracellular signaling molecules such as CD3-ζ and other costimulatory signaling domains to fully activate T cells (*135*). CD19-targeted CAR-T

cells have generated marvelous responses in B cell malignancies, and CAR-T cells targeting other cancer types are under active investigation (*136-138*).

1.5 Conclusion

With the mapping of human genome and rapidly evolving technologies in animal modeling, our knowledge of the pervasive influence T lymphocytes exert on health and diseases has increased at an exponential rate. Understanding the molecular mechanisms that dictate T cell fate and behavior could lead to novel approaches to treating human diseases.

CHAPTER II

THE PI3K/AKT/FOXO SIGNALING PATHWAY CONTROLS REGULATORY T CELL HOMEOSTASIS AND FUNCTION*

2.1 Introduction

2.1.1 PI3K/Akt/Foxo signaling pathway

The PI3Ks are a family of kinases that regulate diverse biological process, including cell growth, differentiation, proliferation, survival, metabolism and migration, through the generation of lipid second messengers. On the basis of the structural similarities, the PI3K family can be divided into four classes, among which class IA and class IB PI3Ks have been most extensively studied in immune cells (*139*). Class I PI3Ks phosphorylate PIP_2 into PIP_3, which mediates the recruitment and activation of numerous signaling molecules. Class IA PI3Ks are activated by receptor tyrosine kinases such as the TCR, costimulatory receptors and cytokine receptors, whereas class IB PI3Ks are primarily stimulated by G-protein-coupled receptors such as chemokine receptors (*139*). Each PI3K comprises a regulatory subunit and a catalytic subunit. Most studies in the immune system focus on the p110δ class IA and p110γ class IB catalytic subunits due to their high expression (*140*).

Luo C.T., Liao W., Dadi S., Toure A., Li M.O. (2016) Graded Foxo1 activity in Treg cells differentiates tumour immunity from spontaneous autoimmunity. Nature. 529, 532-6.

PIP$_3$ recruits PDK1 and Akt to the plasma membrane. PDK1 phosphorylates Akt at Thr308, and the full activation of Akt requires a second phosphorylation by mTORC2 or DNA-PK at Ser473 (*141, 142*). In the nucleus, activated Akt phosphorylates and triggers nuclear exclusion of Foxo transcription factors (*143*). Phosphorylated Akt also activates mTORC1 via Rheb-GTPase (*144*). Several phosphatases negatively regulate the PI3K pathway, including the lipid phosphatases Pten and SHIP that dephosphorylate PIP$_3$ (*145*), and the PH-domain leucine-rich-repeat protein phosphatase (PHLPP) that dephosphorylates Akt (*146*).

2.1.2 Foxo family of transcription factors

Foxo transcription factors are key players in an evolutionary conserved pathway downstream of insulin and insulin-like growth factors. They regulate a variety of processes including cellular metabolism, organ development, cell cycle progression or apoptosis (*56*). In mammals, the Foxo subclass is comprised of four members, Foxo1, Foxo3, Foxo4 and Foxo6 (*147*). Foxo6 expression is confined to specific region of the brain, whereas Foxo1, 3 and 4 are ubiquitously expressed, but among different cell types and organs, a heterogeneous pattern of expression has been described (*148*). Foxo1 is highly expressed in B cells, T cells and ovaries. Constitutive deletion of *Foxo1* gene causes embryonic lethality in mice at day 10.5 due to impaired vascular development (*149-151*). Lymphocytes and myeloid cells express high levels of Foxo3. *Foxo3*-mutant mice exhibit minimally noticeable phenotype with the exception of early ovarian follicle

depletion in female mice (*150, 152*). Foxo4 is expressed at a lower level, and no apparent phenotype has been reported in the Foxo4 knockout animal (*151*).

One mechanism by which Foxo proteins regulate gene transcription is through their binding as monomers to cognate DNA-binding sequence (5'-TTGTTAC-3') (*153*). Besides, they can associate with many transcriptional cofactors, including STATs, Smad3, p300 and β-catenin, to regulate context-dependent transcription programs (*154*). The activity of Foxo proteins is tightly regulated by post-translational modifications, primarily phosphorylation and acetylation, which alter the subcellular localization and protein abundance of Foxo (*153*). In response to growth factors, insulin or cytokines stimulation, kinases downstream of PI3K, such as Akt and serum glucocorticoid kinase (SGK1) phosphorylate Foxo proteins, resulting in their nuclear export into the cytoplasm and potentially proteasomal degradation (*56, 155*). Conversely, oxidative stress stimulates JNK signaling, activates Foxo and triggers the relocalization of Foxo members from the cytoplasm to the nucleus (*56*). Cell starvation results in nuclear transportation of Foxo proteins as well (*147*).

2.1.3 Foxo proteins in conventional T cells

A number of studies have implied that the evolutionarily ancient Akt-Foxo signaling has been co-opted to play a highly specialized role in the immune system. Foxo1 controls the homing of T cells to secondary lymphoid organs. Activation of Foxo1 promotes expression of trafficking molecules S1P1, CD62L and CCR7, potentially through induction of Klf2, the transcription factor known to have a specialized function

in regulating T cell trafficking (*151, 156, 157*). In addition, Foxo1 is required to sustain naive T cell survival. Adult mice with T cell specific Foxo1-deficiency harbor a significantly reduced population of naive T cells, mainly due to the loss of IL-7R expression and anti-apoptotic protein Bcl2 (*151, 157*).

Besides naive T cell homeostasis, Foxo proteins are involved in the differentiation and function of effector and memory T cells. Foxo1 interacts with RORγt and suppresses its activity, thereby serving as a negative regulator of Th17 cell differentiation (*158, 159*). Activation of the salt-sensing kinase SGK1 phosphorylates Foxo1, relieving RORγt from Foxo1-mediated inhibition (*159*). In acute viral and bacterial infection models, Foxo1 and Foxo3 have been shown to promote the differentiation and maturation of memory CTLs, via positive regulation of genes involved in memory T cell survival and trafficking, including *Il7r*, *Ccr7*, *Tcf7*, *Eomes* and *Bcl2 (160-166)*. Moreover, Foxo proteins might counterbalance effector CTL differentiation by repressing the expression of T-bet, IFN-γ and granzyme B (*160, 166, 167*). In a chronic infection model, Foxo1 is shown to sustain the expression of PD-1 and survival of virus-specific CTLs (*168*).

2.1.4 Foxo proteins in regulatory T cells

In addition to the control of conventional T cell responses, Foxo proteins are crucial regulators of T cell tolerance. Foxo1 and Foxo3 cooperatively induce Foxp3 expression during thymic Treg cell development as well as TGF-β-induced Treg cell differentiation *in vitro (169-171)*. Mechanistic studies reveal that Foxo1 and Foxo3 bind to the promoter and a conserved intronic enhancer region (conserved noncoding sequence

2: CNS2) of Foxp3 locus, and regulate the transcription of Foxp3 gene (*170, 171*). In mature Tregs, Foxo1 rather than Foxo3, is highly expressed (*172*). Disruption of Foxo1 in mature Tregs triggers a fatal lymphoproliferative disease in mice, which is in part caused by the loss of Foxo1-dependent repression of IFN-γ (*172*).

2.1.5 Other PI3K/Akt signaling molecules in regulatory T cells

Dynamic regulation of the PI3K/Akt signaling pathway has central functions in the differentiation, maintenance and function of Tregs. Compared to conventional T cells, Treg exhibit dampened activation of PI3K/Akt signaling in response to TCR, costimulatory and γc cytokine stimulation (*172-174*). The distinct signaling regulation is associated with heightened expression of negative regulators in Tregs, such as Pten and the protein phosphatase PHLPP (*173-175*). Recruitment of Pten to the immunological synapse relies on the scaffold protein Disc large homolog 1 (Dlgh1), depletion of which impairs the suppressive function of human Tregs *in vitro (176)*.

Consistent with the reduced PI3K/Akt signaling in Tregs, numerous studies have shown that activation of PI3K/Akt pathway is inhibitory to the differentiation of Tregs, including tTreg development in the thymus, conversion of Treg from naive CD4$^+$ T cells in the peripheral (pTreg), as well as TGF-β-dependent induction of Tregs *in vitro* (iTreg) (*177-182*). These reports utilized various models to introduce elevated PI3K/Akt signaling, for instance, overexpression of a constitutively active form of Akt or sphingosine 1-phosphate receptor (S1P1), or inactivation of negative regulators such as Cbl-b or PTEN, which all resulted in profound defects in Foxp3 induction (*169, 178-181*).

Conversely, blockade of the PI3K/Akt signaling, either through pharmacological inhibition, limitation of essential amino acid, expression of a kinase-inactive version of PI3K p110δ, or disruption of mTOR or S1P1, facilitates differentiation of Tregs (*177, 180-185*). Mechanistically, the PI3K/Akt/mTOR signaling and the transcriptional regulation of Foxp3 can be connected by aligning the Foxo family of transcription factors in this pathway (*170, 171*).

Beyond the differentiation stage, the maintenance of Treg population as well as their suppressive activity depends on the PI3K/Akt signaling axis. Compared to conventional T cells, Tregs have elevated steady-state mTORC1 activity (*186*). Depletion of Raptor, the defining element of mTORC1, results in loss of Treg suppressive activity, which is associated with mTORC1-mediated regulation of lipid metabolism (*186*). Additionally, activation of the Treg-enriched receptor neuropilin-1 by semaphoring-4a potentiates Treg function by recruiting Pten at the immunological synapse, which limits Akt phosphorylation and retains nuclear localization of Foxo proteins (*187*). Recent studies on Pten revealed that it is required for the maintenance of Treg stability as well as its suppressive function. Treg-specific disruption of Pten triggers unrestrained Th1 and Tfh cell responses in mice (*188, 189*). Moreover, depletion of Pten in Tregs or pharmacologic inhibition reverses the Treg-induced immune suppression, resulting in tumor regression (*190*).

2.1.6 Regulatory T cells heterogeneity

The PI3K/Akt signaling pathway controls many aspects of Treg biology –
differentiation, proliferation, stability and function – perturbation of any of these causes a
wide spread of deleterious consequences, such as rampant autoimmunity, abnormal
responses to infection and cancer. Therefore, in order to accomplish such a plethora of
tasks, an emerging concept in the field of Tregs implies that Tregs are broadly distributed
and possess context-specific functions. Rather than a homogenous population, Tregs are a
diverse collection of phenotypically and functionally specialized subsets (*191, 192*). The
Tregs heterogeneity includes distinct developmental origins, antigen-specificities, tissue-
tropisms, homeostatic requirements and functions (*193, 194*). Accordingly, expression of
adhesion and chemoattractant receptors directs preferential migration of Tregs, for
instance, integrin α4β7 for intestinal Tregs and CCR4 for skin Tregs (*195, 196*).
Moreover, colonic Tregs mainly exhibit peripherally converted phenotype (*197-199*), and
environmental factors such as the metabolites of commensal organisms influence their
development and homeostasis (*200-202*). Sequencing studies revealed that the TCR
repertoire of colonic Tregs is distinct from that of Tregs in other tissue sites (*203*).

Aside from the phenotypical diversity, Tregs also exhibit distinct functional
specificity – specialized Treg populations are recruited to control different types of
inflammation. Expression of the helper T cell lineage-specific transcription factors, T-bet,
IRF4 and Stat3, in Tregs has been shown to be indispensible for the control of Th1, Th2
and Th17 responses, respectively (*204-206*). Additionally, Blimp-1, a transcription factor
induced upon Treg activation is required for effector Treg function (*207*). Blimp-1

promotes IL-10 expression in Tregs, disruption of which causes exaggerated immune responses in the intestine, skin and lung (*208*).

2.2 Results

2.2.1 Resting and activated Treg subsets with distinct homeostatic characteristics

Despite the incredibly complicated heterogeneity, Tregs can be broadly divided into two subsets based on differential expression of the lymph node homing molecule CD62L and the T cell activation marker CD44. Similar as conventional CD4$^+$ T cells, the CD62L^{hi}CD44^{lo} subset represents the resting phenotype Tregs (rTregs), whereas the CD62L^{lo}CD44^{hi} population is considered as activated Tregs (aTregs) (*209-211*). rTreg and aTreg subsets reside at different anatomic sites and possess distinct homeostatic characteristics. rTregs were abundant in secondary lymphoid tissues, including lymph nodes (LNs) and spleens (Fig. 2-1). aTregs were present in secondary lymphoid organs as well, and they were the predominant Treg population in nonlymphoid organs, such as the liver and lamina propria (LP) of the intestine (Fig. 2-1). Since Tregs in the nonlymphoid organs contained a very minor rTreg subset (Fig. 2-1), we treat them as one population without further dividing into rTregs and aTregs for the sake of simplicity.

To examine the homeostatic characteristics of different Treg subsets, we established parabiosis between mice expressing two distinct CD45 allotypes, CD45.1 and CD45.2 (Fig. 2-2a). In line with a recent study (*212*), rTregs as well as naïve CD4$^+$ T cells were completely exchanged, whereas aTregs, in particular LP Tregs, were skewed

towards the host at 2 weeks post-surgery (Fig. 2-2b and Fig. 2-3a). Nevertheless, in contrast to liver-resident CD49a⁺NK1.1⁺ innate lymphoid cells (213), all Treg populations were mixed by 4 weeks after initiation of parabiosis (Fig. 2-2b and Fig. 2-3a). These observations reveal that despite different kinetics, both rTregs and aTregs cells recirculated through the blood and/or the lymph, and they were not locally sustained for an extended period.

Antigen-experienced conventional T cells that recirculate through non-lymphoid tissues, the blood and the lymph can be either short-lived effector cells or long-lived effector memory cells (35). To directly determine homeostatic characteristics of rTregs and aTregs, we separated parabiotic mice after Treg equilibration (4 weeks), and measured the rate of Tregs loss that was originated from the non-host parabiont (Fig. 2-2a). LN or splenic rTregs turned over at a rate close to that of naïve CD4⁺ T cells with a decay half time between 4 to 7 weeks (Fig. 2-2b and Fig. 2-3b). In contrast, aTregs from these tissues turned over at a substantially slower rate with a half time of around 14 weeks (Fig. 1b, p=0.0025 for LN and p=0.0335 for spleen). Notably, liver or LP Tregs had a comparable decay half time between 13 to 15 weeks (Fig. 2-3b). Thus, compared to rTregs, aTregs from both lymphoid and non-lymphoid tissues turn over more slowly, resembling the homeostatic features of effector memory T cells.
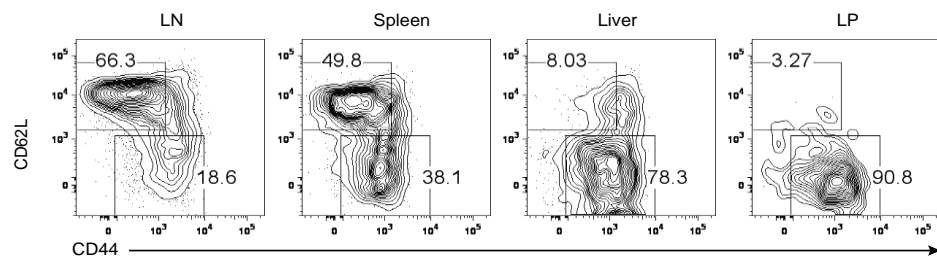
Figure 2-1: rTregs and aTregs reside in distinct anatomic locations. Flow cytometric analysis of CD44 and CD62L in Tregs (CD4$^+$Foxp3$^+$) from lymph node (LN), spleen, liver, and colon lamina propria (LP) of C57BL/6 mice. Percentage of rTregs and aTregs are shown.
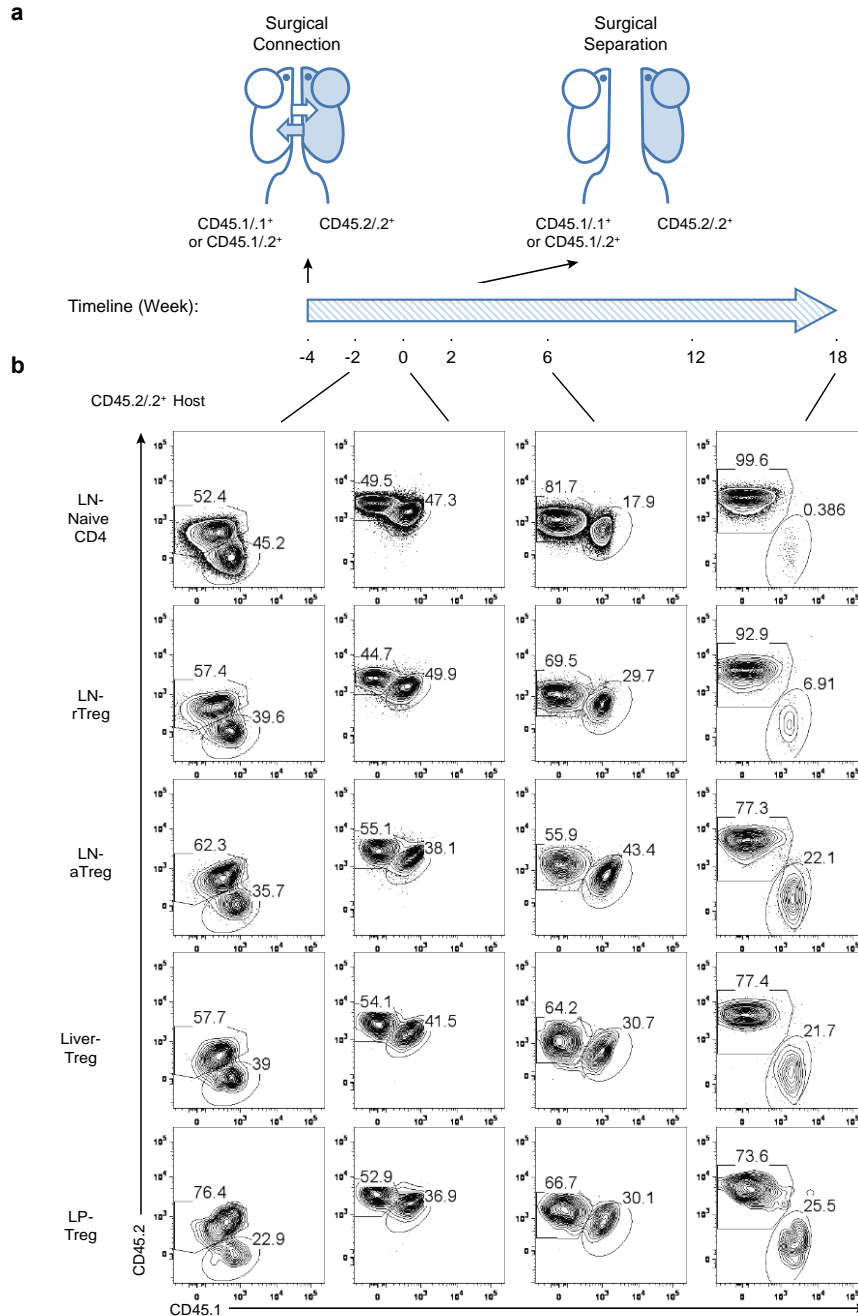
Figure 2-2: Parabiotic analysis of Tregs from different organs. a, Graphical representation of the parabiosis experiments. Congenically mismatched C57BL/6 mice were surgically connected (time point -4). Parabionts were analyzed 2 or 4 weeks post-surgery (time point -2 or 0). In separation experiments, parabiotic mice that had been connected for 4 weeks were surgically disconnected from each other (time point 0). Separated mice were analyzed 2, 6, 12 or 18 weeks after surgery (time point 2, 6, 12 18). **b**, Representative flow cytometric plots showing chimerism of naive CD4^{+} T cells or different Treg subsets in a CD45.2/2^{+} parabiont at various time points.
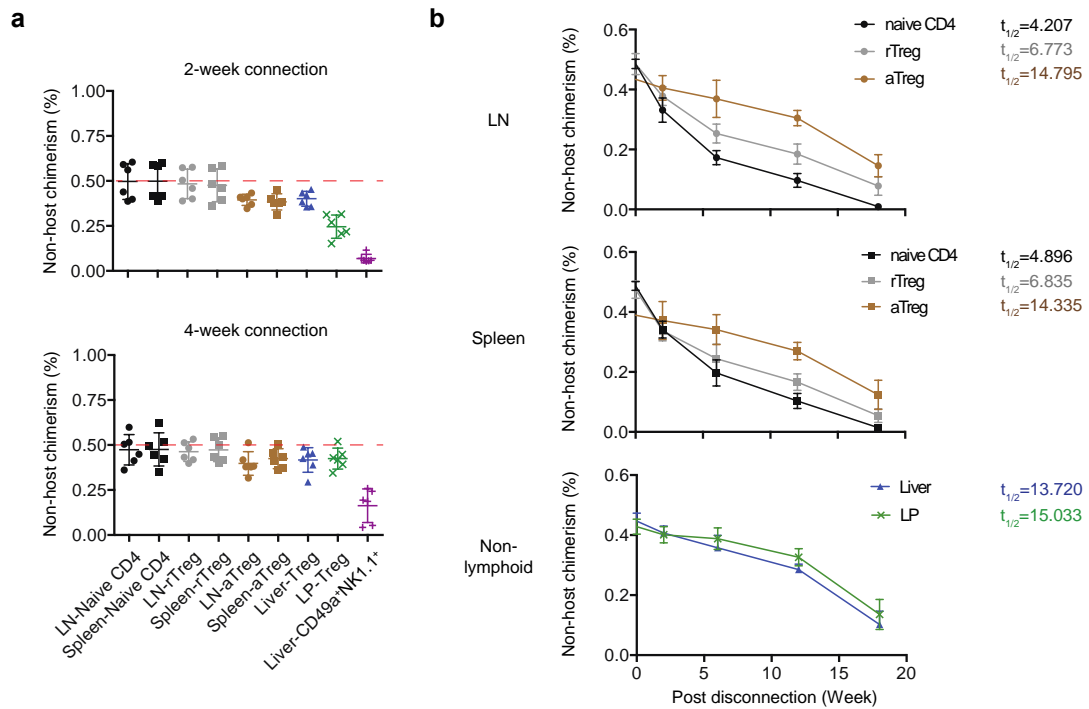
Figure 2-3: aTregs have a slow turnover, but are not locally maintained in nonlymphoid tissues. a, The frequencies of non-host derived cells in parabiotic mice 2 or 4 weeks after surgery, including naive $CD4^+$ T cells ($CD4^+Foxp3^-CD62L^{hi}CD44^{lo}$), rTregs ($CD4^+Foxp3^+CD62L^{hi}$ $CD44^{lo}$), aTregs ($CD4^+Foxp3^+CD62L^{lo}CD44^{hi}$) in the lymph node (LN) and spleen, total Tregs ($CD4^+Foxp3^+$) in the liver and colon lamina propria (LP), and $CD49a^+NK1.1^+$ innate lymphoid cells in the liver. n=6. **b**, Parabionts were separated 4 weeks after connection, and percentages of non-host chimerism at 2, 6, 12, 18 weeks post-separation are shown. $t_{1/2}$ depicts the amount of time it took until the population decayed to half of its original size. n=4 for each time point. Mean values ± SEM are shown. Two-way ANOVA.

2.2.2 Foxo1-dependent transcriptional program is repressed in aTregs

We wanted to understand how the distinct trafficking pattern and homeostasis features between rTregs and aTregs were established, and whether this process could be manipulated. The transcription factor Foxo1 integrates diverse environmental signals to control T cell homeostasis and differentiation (*143, 214*). Previous reports have shown that expression of Foxo1 is crucial for Treg function (*172, 215*), but whether it plays a role in differentiating the aTreg and rTreg subsets remains elusive.

To address this question, we purified splenic aTreg and rTreg subsets and performed gene-expression profiling experiments. By cross-referencing the differentially expressed genes between aTreg and rTreg and the Foxo1-regulated genes (*172*), we found that aTregs preferentially expressed the Foxo1-downregulated transcripts, whereas rTregs contain higher expression of Foxo1-upregulated genes (Fig. 2-4a). Furthermore, in reference to a Foxo1 direct target gene signature (*172*), the Foxo1-repressed or -activated transcripts were enriched in aTregs or rTregs, respectively (Fig. 2-4b), suggesting that Foxo1-dependent gene expression is repressed in aTregs.

In line with the different trafficking pattern between aTregs and rTregs, several Foxo1-activated genes that promote T cell homing to secondary lymphoid organs, including the transcription factor Klf2 and the cell trafficking receptors CCR7 and S1pr1, were highly expressed in rTregs (Fig. 2-5a). In addition, the Foxo1-repressed genes potentially involved in T cell migration or retention in tissues, such as the extracellular matrix glycoprotein Lamc1, the basement protein Nid2, and the matrix metalloproteinase Mmp9, were induced in aTregs (Fig. 2-5a and 5c). The attenuated expression of two

well-defined Foxo1-activated targets, CCR7 and Bim, in aTregs was validated on the protein level (Fig. 2-5b).

We then sought to understand the molecular mechanisms that contributed to the dampened Foxo1 program in aTregs. Using a report strain containing a *Foxo1^{tag}* allele that encodes an in-frame fusion of GFP (*172*), we could assess Foxo1 protein abundance by Foxo1tag-GFP. We found that compared to rTregs, aTregs expressed lower amounts of Foxo1 protein (Fig. 2-6a). Foxo1 protein stability and subcellular localization are negatively modulated by the PI3K/Akt signaling axis (*143*). Indeed, we found that the reduced protein level of Foxo1 in aTregs was associated with its cytosolic localization (Fig. 2-6b). In contrast, Foxo1 predominately resided in the nucleus of rTregs (Fig. 2-6b). Furthermore, phosphorylation of Akt, Foxo1, as well as the mTORC1 signaling pathway marker S6 ribosomal protein was elevated in aTregs (Fig. 2-6c to 6e). Together, these observations demonstrate that aTreg differentiation is associated with activation of the Akt kinase with concomitant repression of Foxo1 nuclear localization and expression. Accordingly, inclusion of an Akt inhibitor (MK-2206) in the *in vitro* culture diminished Foxo1 phosphorylation and prevented the conversion of rTregs into aTregs (Fig. 2-7d).

a Foxo1-regulated genes

b Foxo1 direct target genes
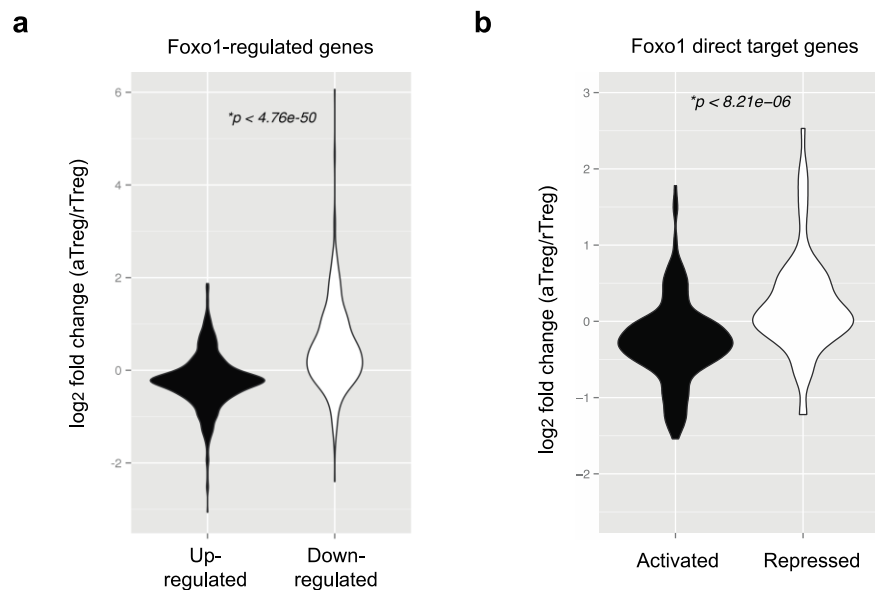
Figure 2-4: aTreg differentiation is associated with downregulation of Foxo1-dependent gene expression. a, Gene expression comparison of Foxo1-regulated genes in splenic aTregs (CD62L^{lo}CD44^{hi}) versus rTregs (CD62L^{hi}CD44^{lo}). Foxo1-regulated genes were defined by the following criteria: 1) differentially expressed between wild-type and Foxo1 knockout Tregs; 2) the expression was corrected by expression of a constitutively active mutant of Foxo1 (Foxo1CA). **b,** Gene expression comparison of Foxo1 direct target genes in splenic aTregs versus rTregs. Foxo1 direct target genes are defined as: 1) differentially expressed between wild-type and Foxo1 knockout Tregs; 2) the expression was corrected by Foxo1CA; 3) Foxo1 was recruited to the gene locus.
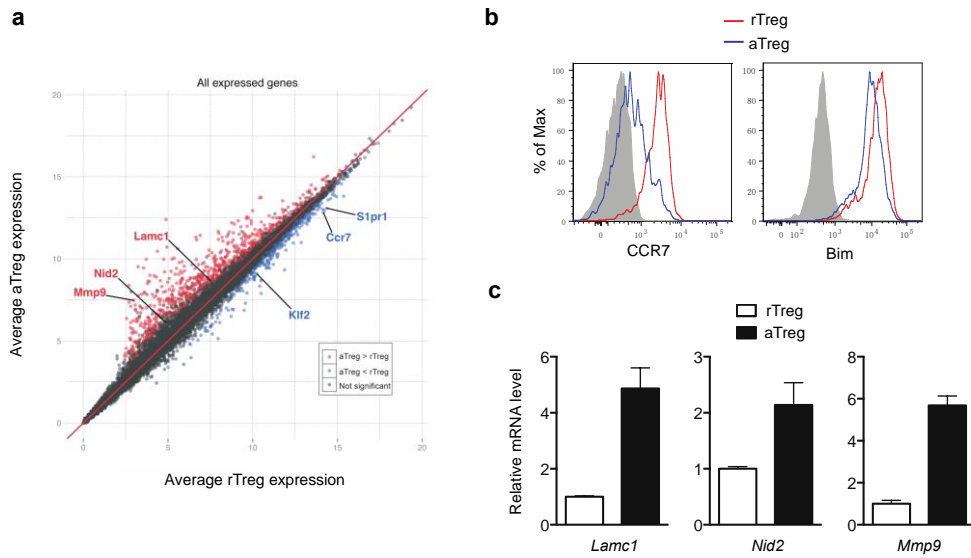
Figure 2-5: Differential expression of Foxo1-direct target genes in aTregs compared with rTregs. a, Normalized expression of all transcripts isolated from splenic aTregs were plotted against transcripts from splenic rTregs. Some of the Foxo1 direct target genes were highlighted. **b**, Flow cytometric analysis of Foxo1-activated target genes, CCR7 and Bim, in splenic aTregs and rTregs. **c,** Comparison of *Lamc1, Nid2, Mmp9* mRNA levels in rTreg versus aTreg subsets.
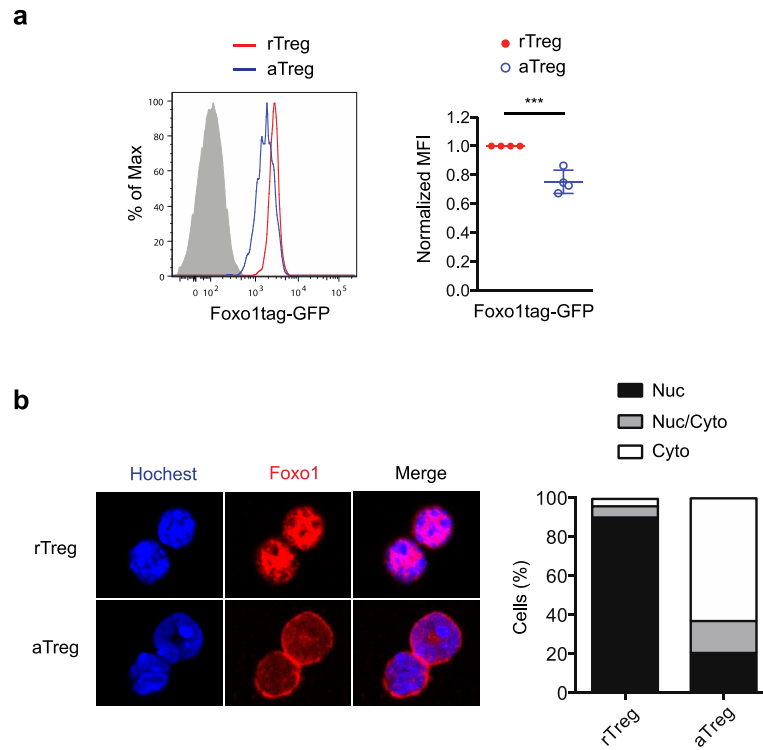
Figure 2-6: aTregs show reduced expression and cytoplasmic localization of Foxo1. **a,** Flow cytometric analysis of Foxo1 protein (Foxo1tag-GFP) in splenic aTregs and rTregs. Mean values ± SEM of mean fluorescence intensity (MFI), normalized to rTregs are shown. n=4. Paired *t*-test. **b**, Immunofluorescence staining of Foxo1 in splenic rTregs and aTregs. Original magnification, ×60. n=70. Nuc, Foxo1 in the nucleus; Nuc/Cyto, Foxo1 in both the nucleus and cytoplasm; Cyto, Foxo1 in the cytoplasm.
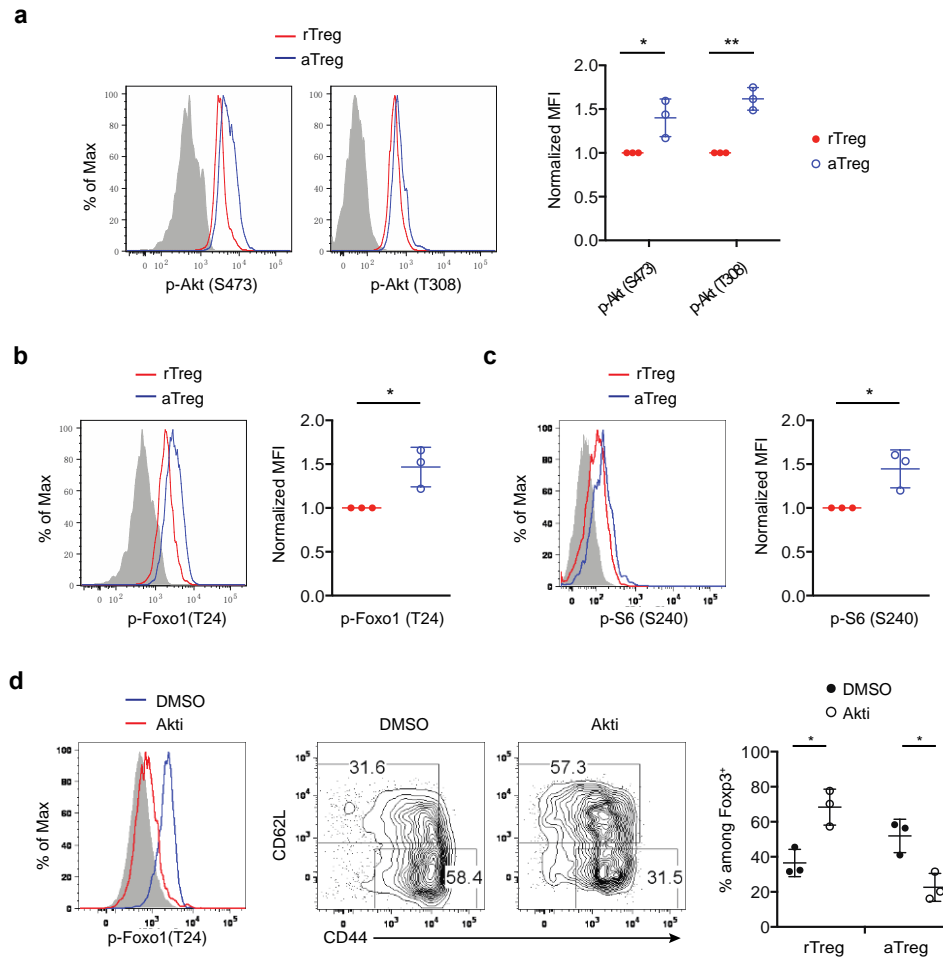
Figure 2-7: Conversion of rTreg to aTreg is associated with Akt-triggered suppression of Foxo1. a-c, Flow cytometric analysis of phosphorylated Akt (**a**), Foxo1 (**b**), and S6 ribosomal protein (**c**), in splenic aTregs and rTregs. Mean values $\pm$ SEM of mean fluorescence intensity (MFI), normalized to rTregs are shown. n=3. Paired *t*-test. **d**, aTreg differentiation experiments *in vitro*. rTregs (CD4$^+$Foxp3$^+$CD62L^{hi}CD44^{lo}) from spleen and LNs of Foxp3-YFP reporter mice were purified by flow cytometric sorting, and were stimulated with α-CD3/CD28 and IL-2 for 3 days. Akt inhibitor (Akti, MK-2206) or DMSO solvent control were added to the culture. Phospho-Foxo1, CD44 and CD62L levels were determined by flow cytometry. Quantification shows percentages of rTregs and aTregs in DMSO control or Akt inhibitor group. n=3. Unpaired *t*-test. All data are presented as the mean values $\pm$ SEM.

45

2.2.3 Mice with constitutively active Foxo1 contain reduced aTregs

To determine the specific role of Foxo1 inactivation in aTregs *in vivo*, we used a mouse strain carrying a mutant allele of *Foxo1* in which amino acids at the Akt phosphorylation sites are substituted with alanines, rendering the mutant protein refractory to Akt-triggered inhibition (*172*). The constitutively active Foxo1 mutant, herein designated as CA, preceded by a *loxP*-flanked '*neo*-STOP' cassette, was inserted into the *ROSA26* locus. Mice harboring CA were bred to the *Foxp3^{cre}* background to induce Treg-specific expression of CA. As expected, CA was expressed at increasing levels in CA/+ or CA/CA Tregs, and was constitutively localized in the nucleus (Fig. 2-8a and 8b). In addition, CA triggered a dose-dependent induction of its target gene expression, including CCR7 and Bim (Fig. 2-8c).

Thymocytes development or thymic Treg differentiation was unperturbed in CA/+ or CA/CA mice (Fig. 2-9). However, CD62L^{lo} aTreg phenotype cells in LNs were proportionally decreased in 9 to 12-day-old CA/+ or CA/CA mice (Fig. 2-10a), which is in line with a role for Foxo1 in inducing CD62L expression possibly via Klf2 (*151, 156, 157*). T cell activation markers CD69 and ICOS were comparably expressed among Tregs from wild-type (WT), CA/+, or CA/CA mice, yet a lower fraction of CD62L^{lo} aTreg phenotype cells in CA/+ or CA/CA mice expressed these molecules (Fig. 2-10b and 10c). Collectively, these data revealed a substantial reduction of aTreg population in CA-expressing mice.
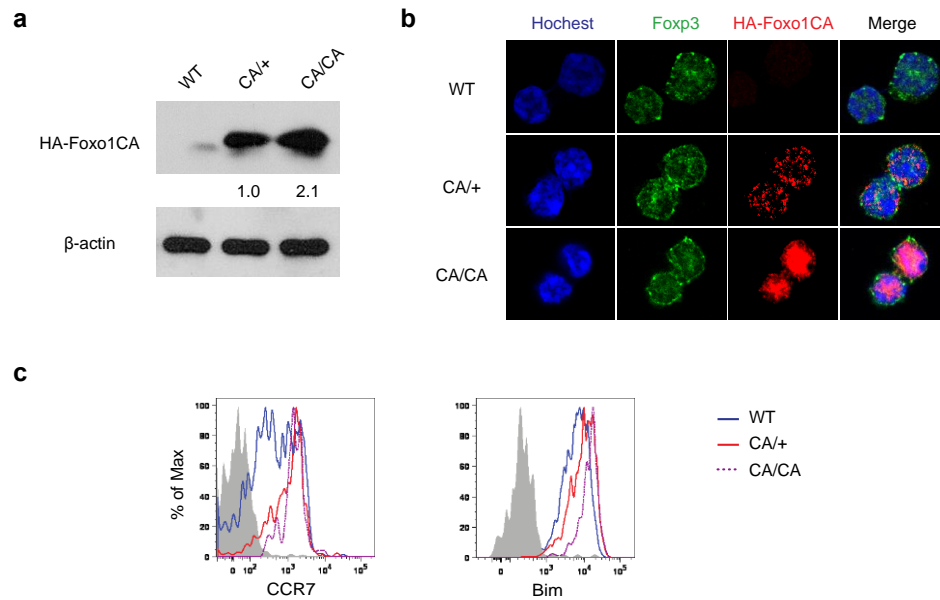
Figure 2-8: Mice expressing the constitutively nucleus-localized form of Foxo1. a-b, Tregs (CD4^{+}Foxp3^{+}) from spleens and lymph nodes (LNs) of wild-type (WT), *Foxp3^{Cre}Foxo1CA/+* (CA/+) or *Foxp3^{Cre}Foxo1CA/Foxo1CA* (CA/CA) mice were purified by flow cytometric sorting. **a**, HA-Foxo1CA protein in the whole cell lysate was measured by immunoblotting with α-HA. **b**, Subcellular localization of HA-Foxo1CA was determined by immunofluorescence staining with α-HA. **c**, Flow cytometric analysis of Foxo1-activated target genes CCR7 and Bim in LN Tregs from 9 to 12-day-old WT, CA/+, CA/CA mice. Grey shaded lines represent isotype controls.
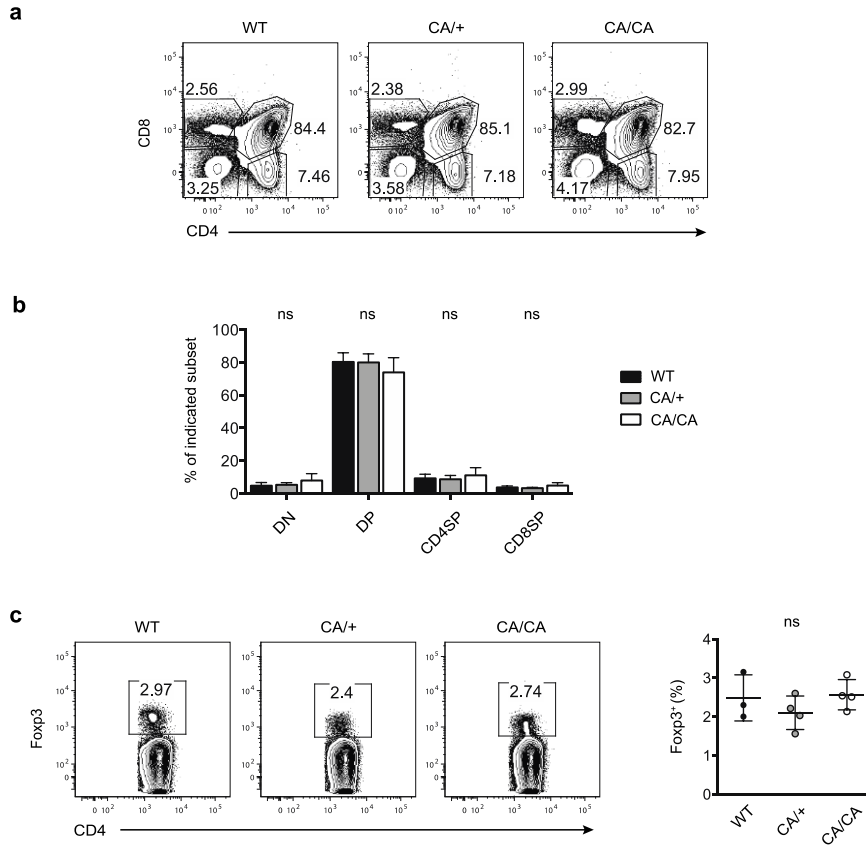
Figure 2-9: Thymic Treg differentiation is intact in mice expressing constitutively active Foxo1. a, Representative flow cytometric plots of thymocyte subsets, including CD4$^-$CD8$^-$ (DN), CD4$^+$CD8$^+$ (DP), CD4$^+$CD8$^-$ (CD4SP), and CD4$^-$CD8$^+$ (CD8SP) in WT, CA/+ and CA/CA mice. **b**, Percentages of thymic DN, DP, CD4SP and CD8SP populations from WT, CA/+ and CA/CA mice. **c**, Treg population in the thymi of TCRβ$^+$CD4$^+$ cells in WT, CA/+ and CA/CA mice. Mean ± SEM. WT: n=3, CA/+, CA/CA: n=4. Unpaired *t*-test.
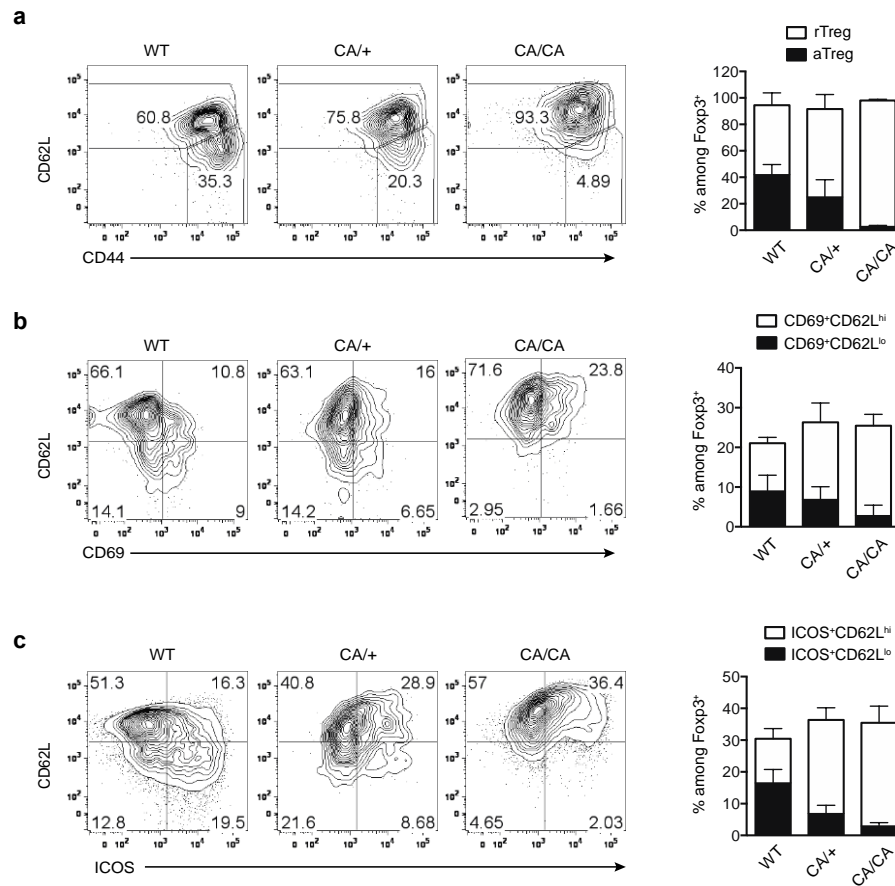
Figure 2-10: Reduction of CD62L^{lo} Tregs in mice containing the Foxo1 hyperactive mutant. Flow cytometric analysis of CD44, CD62L (**a**), CD69, CD62L (**b**), and ICOS, CD62L in lymph node (LN) Tregs (CD4$^+$Foxp3$^+$) from wild-type (WT), *Foxp3^{Cre}Foxo1CA/+* (CA/+) or *Foxp3^{Cre}Foxo1CA/Foxo1CA* (CA/CA) mice. Bar graphs show fractions of rTreg (CD62L^{hi}CD44^{lo}) and aTreg (CD62L^{lo}CD44^{hi}) subsets (**a**), CD69$^+$CD62L^{hi}, CD69$^+$CD62L^{lo} populations (**b**), and ICOS$^+$CD62L^{hi}, ICOS$^+$CD62L^{lo} subsets (**c**) among Tregs. n=6. All data are presented as the mean values $\pm$ SEM. Results represent at least three independent experiments.

2.2.4 Enhanced Foxo1 activity in Tregs alters cell migration

The diminished pool of CD62L^{lo} aTregs in CA-expressing mice could be explained by at least two possibilities: 1) expression of CA blocked the induction of aTregs from rTregs; or 2) CA-expressing aTregs had survival defects. To differentiate these possibilities and further dissect the effect of CA on Tregs, we purified CD62L^{hi}CD44^{lo}CD69$^-$ICOS$^-$ rTregs from WT, CA/+ and CA/CA mice, and performed *in vitro* cell culture experiments. Compared to WT rTregs, the CA-expressing rTregs were not defective in cell activation, proliferation or survival, but they failed to downregulate CD62L (Figure. 2-11). Considering the decrease of CCR7 expression was also attenuated in CA-expressing Tregs (Fig. 2-8c), we concluded that the relief of Akt-triggered Foxo1 inhibition was sufficient to maintain high expression of molecules that are involved in lymph node homing and intranodal T cell migration.

To determine whether the altered expression of migratory molecules, CD62L and CCR7, in CA-expressing Tregs resulted in a change of Treg trafficking, we performed *in vivo* T cell labeling experiments. We intravenously administered a Biotin-labeled CD4 antibody (RM4-4) into the WT, CA/+ or CA/CA mice, and analyzed the labeled cells in the spleens. The mouse spleen has a complex structure, with T and B cells predominantly found in the highly organized white pulp (WP), which is surrounded by the B cell-rich marginal zone (MZ) and the macrophage/granulocyte-rich red pulp (RP). The Biotin-labeled CD4 antibody predominantly labels cells in the RP or MZ, but not the WP, due to the relatively impermeant marginal sinus. We found that fewer CA-expressing Tregs were labeled by the CD4 RM4-4 antibody (Fig. 2-12a), whereas comparable percentages

of conventional T cells were labeled (Fig. 2-12b). These observations suggest that CA prevented the migration of Tregs from WP to RP/MZ.

rTregs and aTregs reside at different locations in secondary lymphoid organs, and engage discrete mechanisms of homeostatic maintenance (*212*). In 9 to 12-day-old CA/+ or CA/CA mice, whereas the total proportion or number of LN CD62L^{hi} Tregs were similar or elevated compared to that of WT mice, CD62L^{lo} Tregs were reduced with increasing doses of CA expression (Fig. 2-13c and 13d), resulting in reduced total LN Tregs (Fig. 2-13a). Therefore, although Foxo1 inactivation is not essential for Treg activation, proliferation or survival, it is required to control the expression of trafficking molecules that may promote aTregs to migrate away from the rTreg niche and further expand. Indeed, CA expression from one or two alleles caused a dose-dependent reduction of Tregs in the liver (Fig. 2-13b).
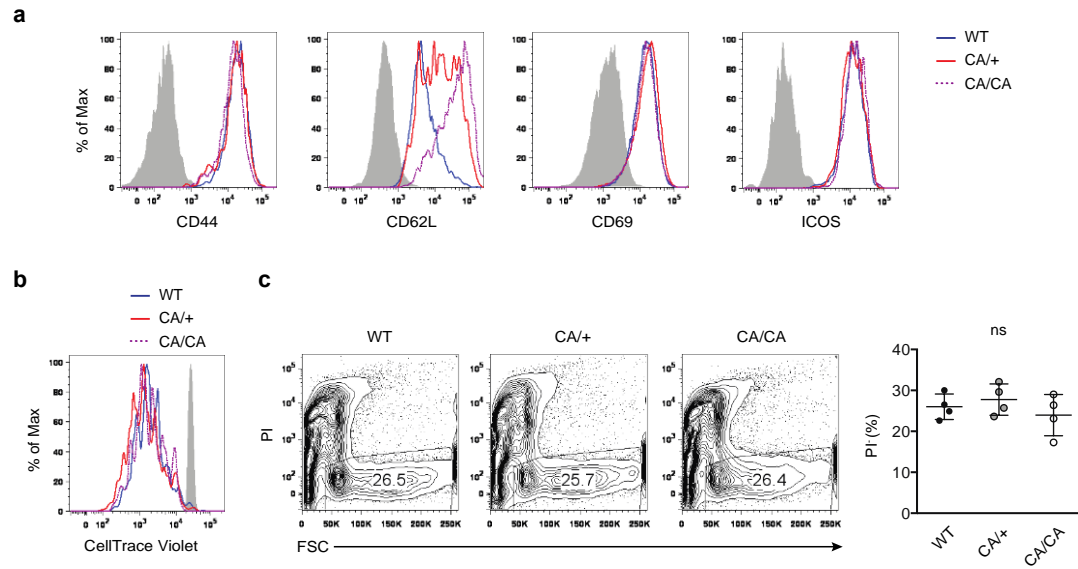
Figure 2-11: CA-expressing Tregs show intact activation, proliferation and survival *in vitro*. CD4$^+$Foxp3$^+$CD62L^{hi}CD44^{lo}CD69$^-$ICOS$^-$ rTregs were isolated from wild-type (WT), *Foxp3^{Cre}Foxo1CA/+* (CA/+) or *Foxp3^{Cre}Foxo1CA/Foxo1CA* (CA/CA) mice, and were stimulated with α-CD3, α-CD28 and IL-2 for 3 days. **a**, CD44, CD62L, CD69 and ICOS expression was determined by flow cytometry. Grey shaded lines represent isotype controls. **b**, Cells were stained with CellTrace Violet dye before culture, and cell division was tracked by dilution of the dye. Grey shaded line represents undivided cells. **c**, Cell death was measured by propidium iodide (PI) incorporation. Percentages of live cell fraction (PI$^-$) were compared. n=4. Unpaired *t*-test. All data are presented as the mean values ±SEM.
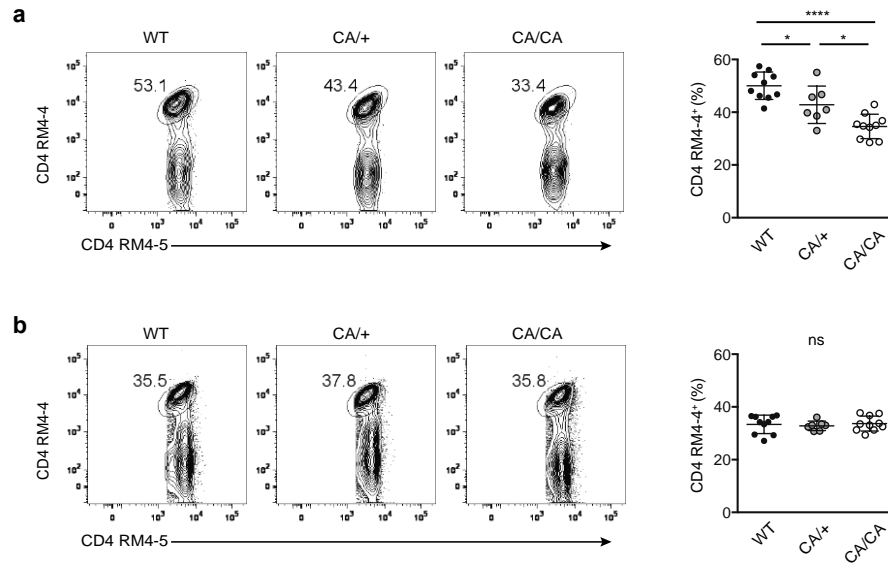
Figure 2-12: Expression of constitutively active Foxo1 leads to a change of Treg trafficking. *In vivo* labeling experiment: α-CD4-Biotin (RM4-4 clone) was injected intravenously into wild-type (WT), *Foxp3[Cre]Foxo1CA/+* (CA/+) or *Foxp3[Cre]Foxo1CA/Foxo1CA* (CA/CA) mice, and spleens were harvested 5 minutes post-injection. A non-competing clone of α-CD4 (RM4-5) was used in subsequent flow cytometric analysis to label total CD4$^+$ T cell. Representative flow cytometric plots from gated Tregs (CD4 RM4-5$^+$Foxp3$^+$) (**a**), and conventional CD4$^+$ T cells (CD4 RM4-5$^+$Foxp3$^-$) (**b**) are shown. Quantification shows percentage of RM4-4$^+$ cells among Tregs (**a**), and conventional CD4$^+$ T cells (**b**). WT, CA/CA, n=10; CA/+, n=7. All data are presented as the mean values ± SEM. Results represent at least three independent experiments. Unpaired *t*-test.
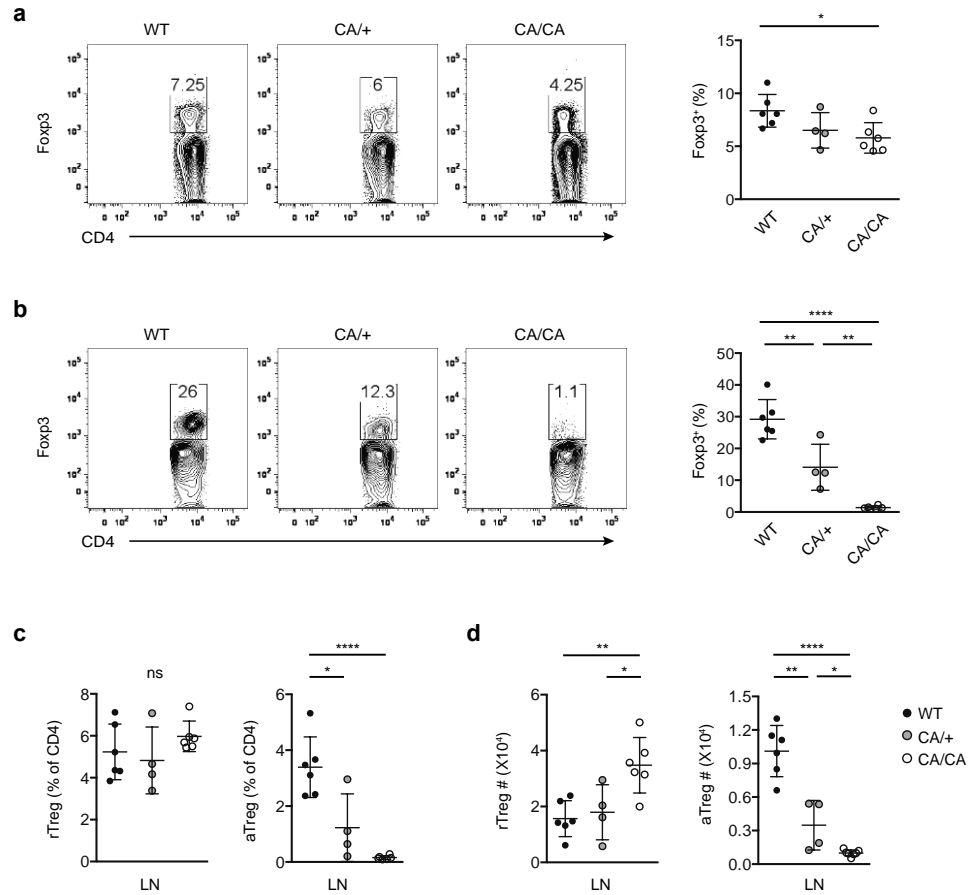
Figure 2-13: Foxo1 hyperactivation depletes aTregs and results in a reduced Treg population. a-b, Foxp3 expression in LN (**a**) or liver (**b**) CD4$^+$ T cells of 9 to 12-day-old wild-type (WT), *Foxp3^{Cre}Foxo1CA/+* (CA/+) or *Foxp3^{Cre}Foxo1CA/Foxo1CA* (CA/CA) mice. Quantification shows percentages of Tregs among total CD4$^+$ T cells. **c-d**, The frequencies (**c**) and numbers (**d**) of lymph node (LN) rTreg or aTreg cells among CD4$^+$ T cells of 9 to 12-day-old WT, CA/+ or CA/CA mice. WT, CA/CA, n=6; CA/+, n=4. All data are presented as the mean values $\pm$ SEM. Unpaired *t*-test.

2.2.5 aTregs are crucial for the suppression of CD8$^+$ T cell-mediated tissue destruction

To examine whether the aTreg defects were sustained beyond the neonatal stage, we analyzed 4 to 6-week-old mice. Expression of CA triggered a dose-dependent reduction of aTregs in lymphoid organs as well as in non-lymphoid tissues, leaving rTregs less affected (Fig. 2-14). Compared to WT and CA/+ mice, all CA/CA mice succumbed to a wasting disease and death by 4 months of age (Fig. 2-15a and 15d). CA/+ mice did not manifest overt disease symptoms, with the exception that about 60% of the CA/+ mice developed rectal prolapse at age of 4-5 months (data not shown). The drastically different disease severity between CA/+ and CA/CA mice was correlated with the magnitude of Treg reduction (Fig. 2-13a), as the mildly reduced Treg population in CA/+ mice was sufficient to keep overt autoimmunity in check while the scarce Treg pool in CA/CA mice failed to do so.

In contrast to Treg-specific Foxo1-deficient mice (*172*), CA/CA mice did not exhibit the typical inflammatory phenotype associated with the Scurfy mutation of *Foxp3* such as tail crusting, splenomegaly, or lymphadenopathy (Fig. 2-15b and 15c). However, a dense infiltrate of leukocytes were observed in multiple organs of CA/CA mice, including the liver and colon (Fig. 2-15e). Serum alanine aminotransferase (ALT) activity, a biomarker for liver injury, was elevated as well (Fig. 2-15f). Together, these data reveal that the immunopathology in the CA/CA mice had resulted in tissue damage.

In order to understand whether the immunopathology was caused by a compromised Treg suppressive activity, we examined the expression of several Treg suppression-associated molecules. Intriguingly, the ectopic expression of CA did not perturb the levels of CTLA4, LAG3 and GITR (Fig 2-16a). In addition, CA-expressing

Tregs possessed comparable suppressive activity as WT Tregs when assessed *in vitro* (Fig 2-16b).

The autoimmune lethal phenotype in CA/CA mice was associated with activation of CD4$^+$ and CD8$^+$ T cells in the secondary lymphoid organs (Fig. 2-17a and 17d). However, these hyper-activated T cells produced only modestly higher or comparable amounts of inflammatory cytokines, IFN-γ, IL-4 and IL-17, compared to T cells from WT or CA/+ mice (Fig. 16b-c and 17e-f). Splenic CD8$^+$ T cells, nevertheless, expressed markedly higher levels of the cytolytic molecule granzyme B (GzmB) (Fig. 2-18a and 18b). Such enhanced expression of GzmB was observed in CD8$^+$ T cells infiltrating the liver and LP as well (Fig. 2-18a and 18b). Intriguingly, IFN-γ production was not induced in the liver- and LP-infiltrating CD8$^+$ T cells (Fig. 2-18c and 18d). In the diseased CA/CA mice, T cell populations were skewed towards CD8$^+$ T cells in the spleen and peripheral non-lymphoid organs (Fig. 2-19a). This data together with the substantial expression of GzmB in CD8$^+$ T cells led us to hypothesize that the augmented effector CD8$^+$ T cell responses were responsible for the immunopathology developed in the CA/CA mice. To test this hypothesis, we crossed CA/CA mice to the CD8-deficient background. Depletion of CD8$^+$ T cells completely rescued the wasting disease and lethal phenotype of CA/CA mice (Fig. 2-19b and 19c). Serum ALT levels and tissue pathology were fully rectified as well (Fig. 2-19d and 19e). Collectively, these findings reveal that constitutively high activity of Foxo1 preferentially impair the aTreg subset, and aTregs have a particularly important function in suppressing CD8$^+$ T cell-mediated tissue destruction.
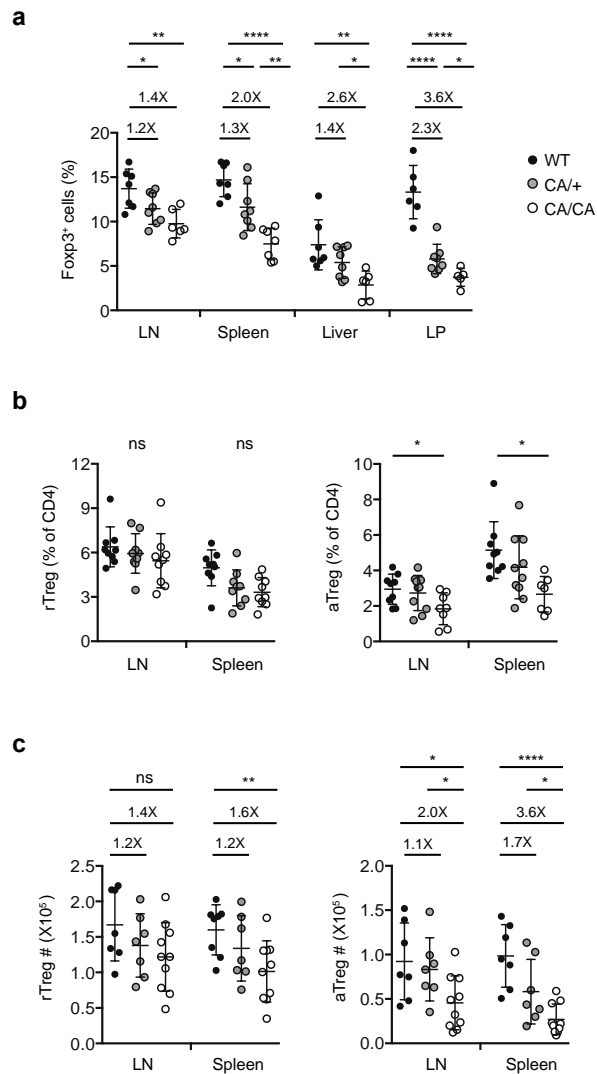
Figure 2-14: Foxo1 hyperactivation preferentially impairs aTregs in adult mice. a, The frequencies of Tregs among CD4^{+} T cells in lymph node (LN), spleen, liver and colon lamina propria (LP) of wild-type (WT), *Foxp3[Cre]Foxo1CA/+* (CA/+) or *Foxp3[Cre]Foxo1CA/Foxo1CA* (CA/CA) mice. WT, CA/CA, n=6; CA/+, n=8. Numbers above plots indicate fold changes in comparison to WT. **b**, The frequencies of LN and splenic rTreg or aTreg cells among CD4^{+} T cells of WT, CA/+ or CA/CA mice. n=10. **c**, The numbers of LN rTreg or aTreg cells of 4 to 6-week-old WT, CA/+ or CA/CA mice. n=10. Mice at 4 to 6-week-old of age were included. All data are presented as the mean values ±SEM. Unpaired *t*-test.
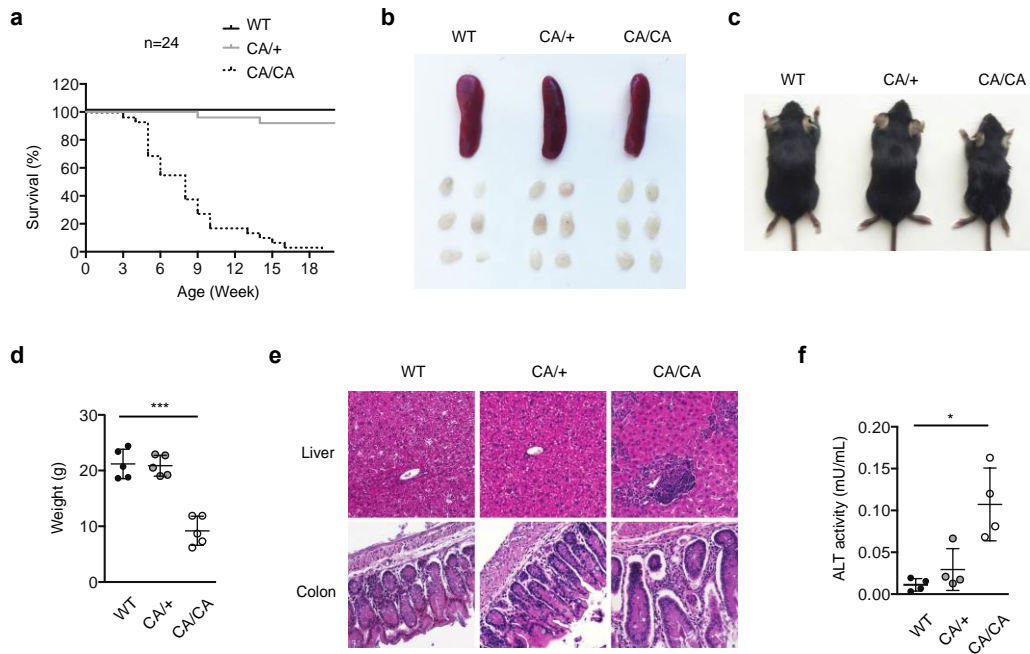
Figure 2-15: *Foxp3^{Cre}Foxo1CA/Foxo1CA* **mice succumb to a wasting disease. a**, Survival of wild-type (WT), *Foxp3^{Cre}Foxo1CA/+* (CA/+) or *Foxp3^{Cre}Foxo1CA/Foxo1CA* (CA/CA) mice. **b**, A representative picture of spleens and peripheral (axillary, brachial, and inguinal) LNs of 5-week-old WT, CA/+ or CA/CA mice. **c**, A representative picture of 5-week-old WT, CA/+ or CA/CA mice. **d**, Body weight of 4 to 6-week-old WT, CA/+, CA/CA mice. n=5. **e**, Haematoxylin and eosin staining of liver and colon sections of 5-week-old WT, CA/+ or CA/CA mice. **f**, Serum alanine aminotransferase (ALT) activity 4 to 6-week-old WT, CA/+, CA/CA mice. n=4. (**d, f**) Data is presented as the mean values ±SEM. Unpaired *t*-test used.
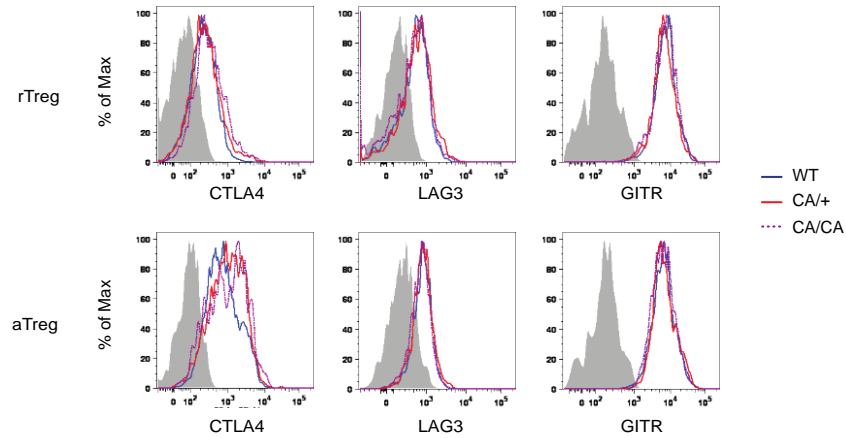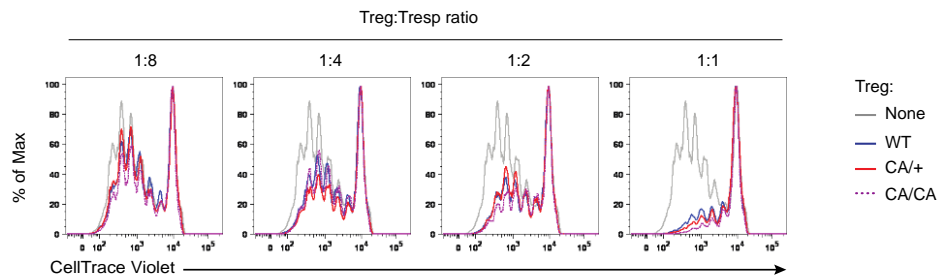
Figure 2-16: Foxo1 hyperactivation does not affect Treg suppressive function *in vitro*. a, Flow cytometric analysis of CTLA4, LAG3 and GITR expression in LN rTregs and aTregs from 4 to 6-week-old WT, CA/+, CA/CA mice. Grey shaded lines represent isotype controls. **b**, Suppression of WT naïve CD4$^+$ T cells, labeled with CellTrace Violet (Tresp, responding T cells), by WT, CA/+ or CA/CA Tregs. Tresp cell division was assessed by CellTrace Violet dilution at the indicated ratios of cell numbers between Treg and Tresp cells. Grey line represents conditions without Treg in culture. Results represent at least three independent experiments.
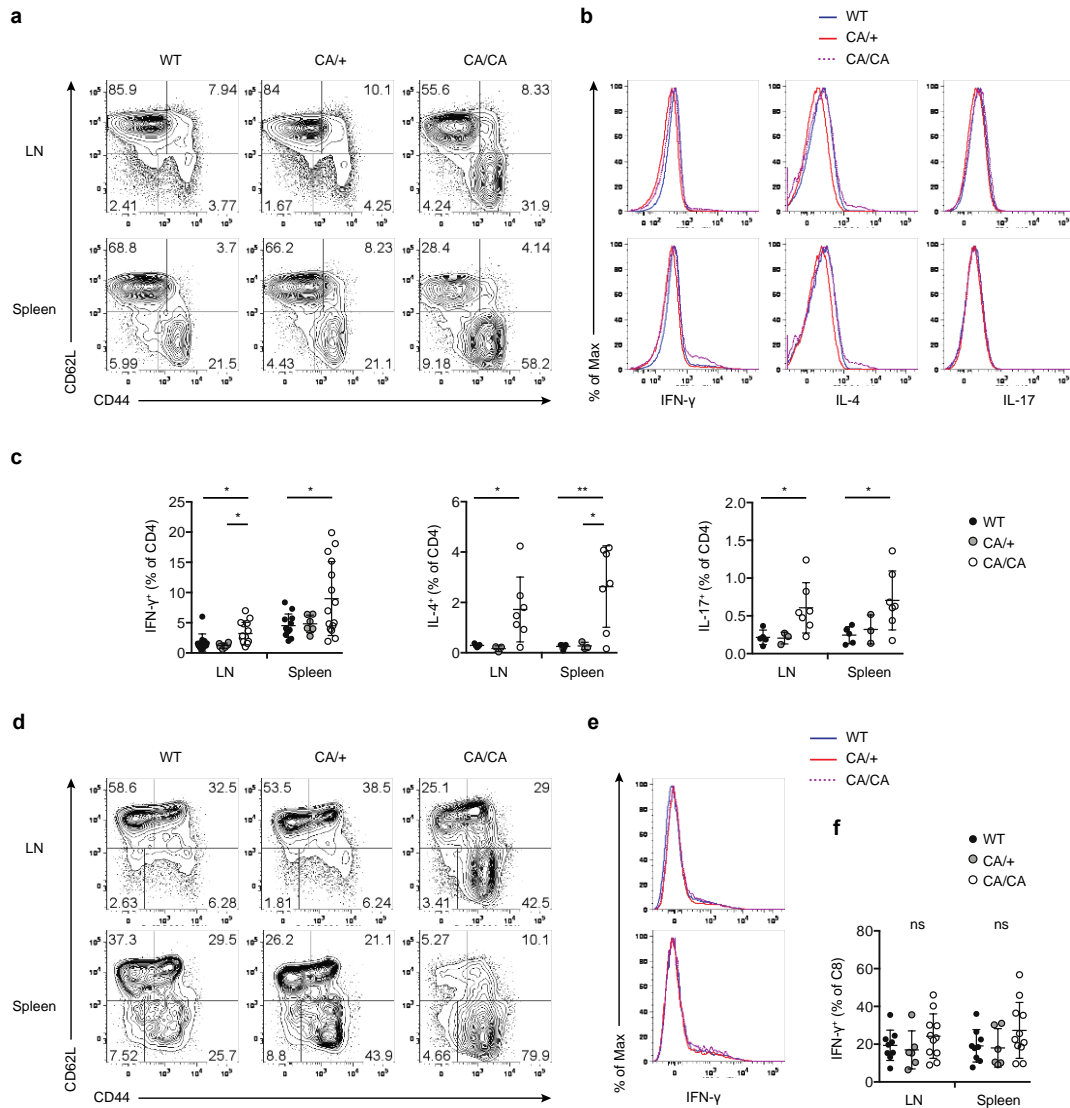
Figure 2-17: Modest increase of inflammatory cytokine production by CD4⁺ and CD8⁺ T cells in *Foxp3^{Cre}Foxo1CA/Foxo1CA* mice. a, **d,** Flow cytometric analysis of CD44 and CD62L expression in CD4⁺Foxp3⁻ conventional T cells (**a**) or CD8⁺ T cells (**d**) from lymph node (LN) and spleen of 4 to 6-week-old wild-type (WT), *Foxp3^{Cre}Foxo1CA/+* (CA/+) or *Foxp3^{Cre}Foxo1CA/Foxo1CA* (CA/CA) mice. **b-c**, Representative histogram (**b**), and quantification (**c**) of cytokine (IFN-γ, IL-4, IL-17) expression by CD4⁺Foxp3⁻ conventional T cells from LN and spleen of 4 to 6-week-old WT, CA/+, CA/CA mice. WT, CA/CA, n=14 for IFN-γ, n=7 for IL-4, IL-17; CA/+, n=3. **e-f**, Representative histogram (**e**), and quantification (**f**) of IFN-γ expression by CD8⁺ T cells from LN and spleen of 4 to 6-week-old WT, CA/+, CA/CA mice. WT, n=9; CA/+, n=6; CA/CA, n=11. (**c, f**) Unpaired *t*-test. All data are presented as the mean values ± SEM. Results represent at least three independent experiments.
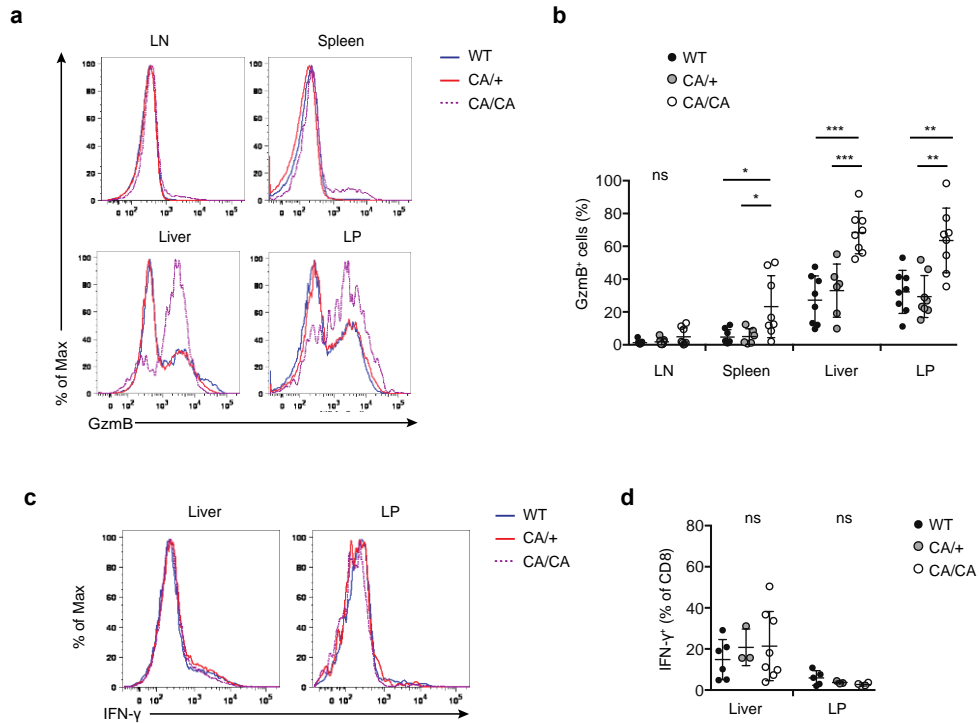
Figure 2-18: Heightened production of the cytolytic molecule granzyme B by CD8$^+$ T cells in *Foxp3^{Cre}Foxo1CA/Foxo1CA* mice. a, Flow cytometric analysis of granzyme B (GzmB) expression in CD8$^+$ cells from LN, spleen, liver and LP of wild-type (WT), *Foxp3^{Cre}Foxo1CA/+* (CA/+) or *Foxp3^{Cre}Foxo1CA/Foxo1CA* (CA/CA) mice.. **b**, Fractions of GzmB$^+$ cells in CD8$^+$ T cells from LN, spleen, liver and LP of WT, CA/+, CA/CA mice. WT, CA/CA, n=8; CA/+, n=6. **c**, Flow cytometric analysis of IFN-γ expression by CD8$^+$ T cells from liver and colon lamina propria (LP) of WT, CA/+, CA/CA mice. **d**, Quantification of the IFN-γ production by CD8$^+$ T cells. WT, n=6; CA/+, n=3; CA/CA, n=8. 4 to 6-week-old mice were included in the experiments. (**b, d**) All data are presented as the mean values $\pm$ SEM. Unpaired *t*-test. Results represent at least three independent experiments.
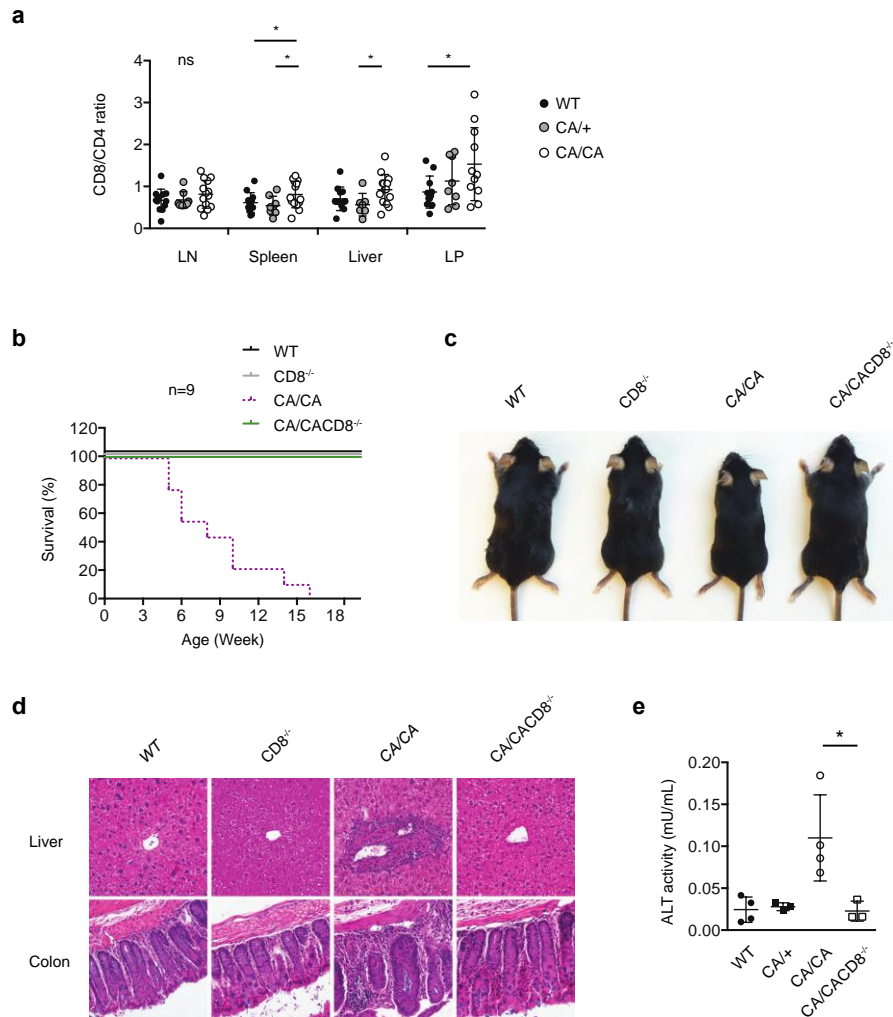
Figure 2-19: CD8$^+$ T cell depletion rescues the lethal disease in *Foxp3^{Cre}Foxo1CA/Foxo1CA* **mice. a**, CD8$^+$ to CD4$^+$ T cell ratio among lymph node (LN), spleen, liver, and LP T cells of wild-type (WT), *Foxp3^{Cre}Foxo1CA/+* (CA/+) or *Foxp3^{Cre}Foxo1CA/Foxo1CA* (CA/CA) mice. WT, n=10; CA/+, n=8; CA/CA, n=13. **b**, Survival of WT, *CD8$^{-/-}$* (CD8$^{-/-}$), CA/CA and *Foxp3^{Cre}Foxo1CA/Foxo1CACD8$^{-/-}$* (CA/CACD8$^{-/-}$) mice. **c**, A representative picture of WT, CD8$^{-/-}$, CA/CA, and CA/CACD8$^{-/-}$ mice. **d**, Haematoxylin and eosin staining of liver and colon sections from WT, CD8$^{-/-}$,CA/CA, and CA/CACD8$^{-/-}$ mice. Original magnification, ×20. **e**, Serum ALT activity from WT, CD8$^{-/-}$, CA/CA, and CA/CA CD8$^{-/-}$ mice. n=4. In all experiments, 4 to 6-week-old mice were used. (**a, e**) Mean values ± SEM are shown. Unpaired *t*-test.

2.2.6 Expression of Foxo1CA at a lower dose was sufficient to deplete tumor-associated Tregs

An interesting observation we made was that CA expression led to varying degrees of Treg reduction in different tissues, with the LP more affected than the liver (Fig. 2-13a). In fact, the magnitude of Treg loss in lymphoid organs and non-lymphoid tissues was inversely correlated with Foxo1 activity, as revealed by expression of two direct Foxo1 target genes (Fig. 2-20b).

Accumulation of Tregs in tumor sites has been reported in a number of cancers, and is associated with poor prognosis (*127, 216-218*). Many efforts have been made during the recent years aiming to limit excessive Treg activity to treat cancer, yet they mostly reply on non-specific and broadly acting reagents that deplete Tregs in a systematic manner (*126, 219*). To study how CA impacts tumor-infiltrating Tregs, we used the MMTV-PyMT (PyMT) spontaneous mammary tumor model (*220*). Tumor-infiltrating Tregs exhibited an activated phenotype that is similar as Tregs from the non-lymphoid tissues, liver and LP (Fig. 2-20a), yet they expressed the lowest level of Foxo1 targets (Fig. 2-20b).

The lowest expression of Foxo1 target genes in tumor-infiltrating Tregs implied that they might be the most sensitive to Foxo1 gain-of-function. To this end, we crossed CA/+ mice to the PyMT background. Tumor-infiltrating Tregs were diminished by 2.6-fold with CA expression from one allele (Fig. 2-21a and 21b), leading to a profound inhibition of tumor growth (Fig. 2-21c). Although CD8^{+} T cells were phenotypically indistinguishable in healthy tissues from CA/+ and WT mice (Fig. 2-18a and 18b),

tumor-infiltrating CD8$^+$ T cells from CA/+PyMT mice expressed higher amounts of GzmB (Fig. 5e-f).

Tumor progression in PyMT mice is accompanied with loss of genome stability, which induces time-dependent accumulation of gene mutations to foster oncogene-induced cell transformation (*221*). To determine whether CA expression in Tregs could inhibit growth of already transformed cells, we used syngeneic AT-3 cells derived from PyMT mice. Orthotopic implantation of AT-3 to the mammary fat pad resulted in aggressive tumor growth and lethality in WT mice, both of which were attenuated in CA/+ mice (Fig. 2-22a and 22b). Expression of CA triggered a 6.5-fold reduction of tumor-infiltrating Tregs (Fig. 2-22c and 22d), which was associated with increased expression of GzmB in tumor-infiltrating CD8$^+$ T cells (Fig. 2-22e). Importantly, depletion of CD8$^+$ T cells by crossing CA/+ mice to the CD8-deficient background restored the tumor growth (Fig. 2-22f), revealing a crucial function for CD8$^+$ T cells in tumor suppression.

To further investigate whether the CA effect was applicable to tumors of other tissue origin, we used B16 melanoma cells. Similar to AT-3, B16 tumor growth and lethality of tumor-bearing mice was inhibited in CA/+ mice (Fig. 2-23a and 23b), which was accompanied by an approximately 10-fold reduction of tumor-infiltrating Tregs and substantially increased GzmB production in CD8$^+$ T cells (Fig. 2-23c-23f). Collectively, these findings demonstrate that tumor-associated Tregs are generally more susceptible to CA-triggered depletion.
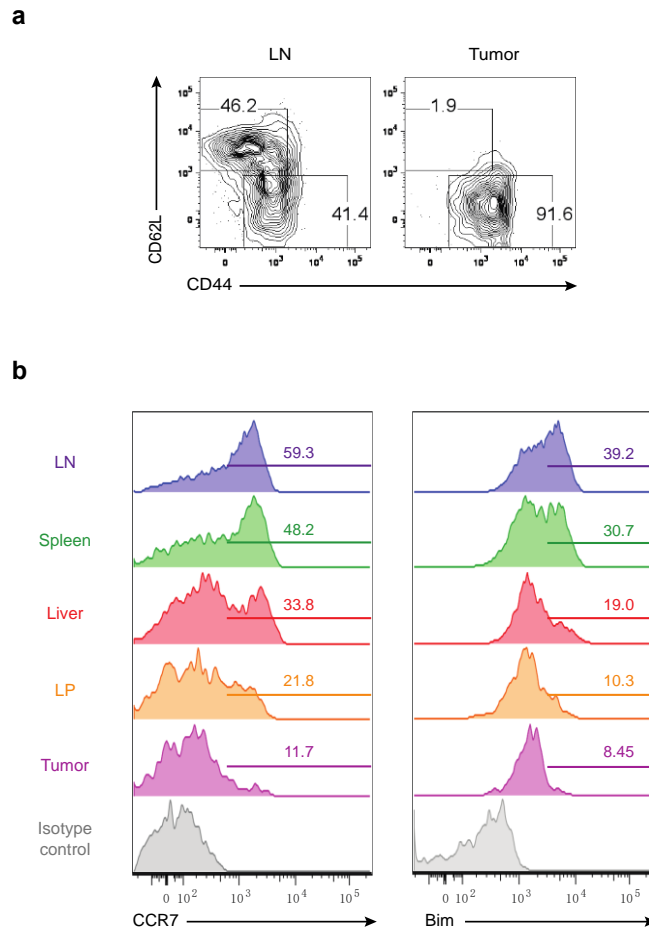
Figure 2-20: Tumor-infiltrating Tregs express lowest level of Foxo1 targets. a, Representative flow cytometric plots showing the CD44 and CD62L expression in Tregs (CD4$^+$Foxp3$^+$) from lymph node (LN) and tumor of PyMT tumor-bearing mice. **b**, Flow cytometric analysis of Foxo1-activated target genes CCR7 and Bim in Tregs from lymph node (LN), spleen, liver, colon lamina propria (LP), and tumor of 22 to 24-week-old PyMT mammary tumor-bearing mice. Numbers indicate percentage of CCR7- or Bim-positive cells shown in the gate.
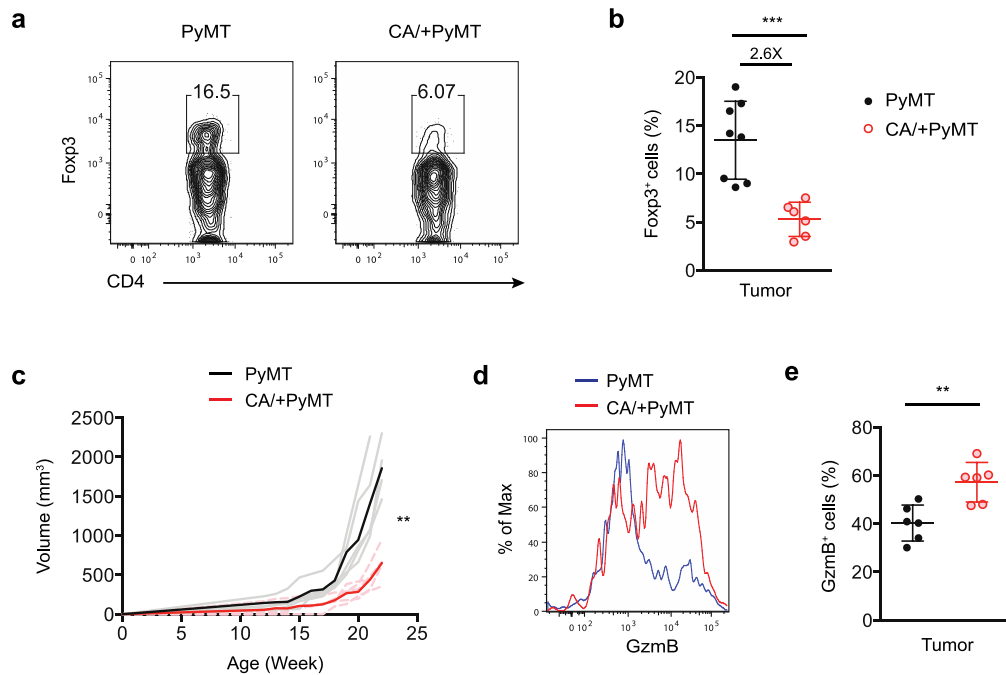
Figure 2-21: Tuned activation of Foxo1 in Tregs results in enhanced anti-tumor immunity without inflicting autoimmunity. a, Foxp3 expression in tumor-infiltrating CD4$^+$ T cells from PyMT or *Foxp3^{Cre}Foxo1CA/+PyMT* (CA/+PyMT) mice. **b**, The frequencies of Tregs among CD4$^+$ T cells in tumors of PyMT or CA/+PyMT mice. PyMT, n=8, CA/+PyMT, n=6. Number above plots indicates fold change in comparison to PyMT. **c,** Tumor growth curve of PyMT and CA/+PyMT mice. n=5. **d,** Flow cytometric analysis of GzmB expression in CD8$^+$ cells from tumors of PyMT and CA/+PyMT mice. **e**, Fractions of GzmB-expressing cells among the CD8$^+$ cells from tumors of PyMT and CA/+PyMT mice. n=6. Results represent at least three independent experiments. (**b, e**), Mean values ± SEM are shown. Unpaired *t*-test. (**c**), Light colored lines (grey and pink) in the background represent tumor growth curve of each individual mouse. Solid color lines (black and red) show the average tumor growth curve. Unpaired two-way ANOVA.
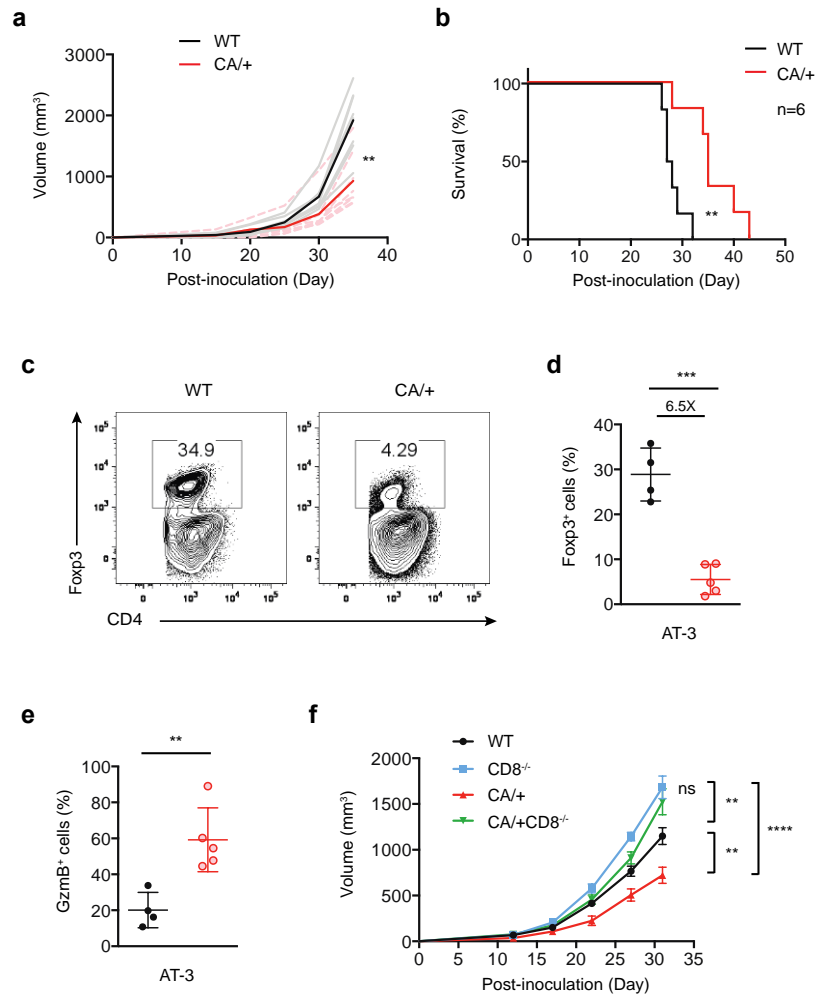
Figure 2-22: *Foxp3^Cre^Foxo1CA/+* **mice show enhanced anti-tumor immune responses. a**, 8 to 10-week-old wild-type (WT) or *Foxp3^Cre^Foxo1CA/+* (CA/+) mice received orthotopic inoculation of PyMT-derived mammary tumor cells (AT-3). **a**, Tumor growth curve of WT and CA/+ mice. n=8. **b**, Survival of WT and CA/+ mice received tumor implantation. **c**, Foxp3 expression in tumor-infiltrating CD4$^+$ T cells from cells from Day 30-35 AT-3 tumors. **d**, The frequencies of Tregs among CD4$^+$ T cells in tumors of WT- and CA/+ -tumor bearing mice. WT, n=4; CA/+, n=5. Number above plots indicates fold change in comparison to WT. **e**, Fractions of GzmB-expressing cells among the CD8$^+$ cells from tumors of WT and CA/+ mice. n=6. **f**, Tumor growth curve of WT, CD8$^{-/-}$, CA/+, or *Foxp3^Cre^Foxo1CA/+* CD8$^{-/-}$ (CA/+CD8$^{-/-}$) mice received orthotopic inoculation of AT-3 tumor cells. n=4. Results represent at least three independent experiments. (**d, e**), Mean values ± SEM are shown. Unpaired *t*-test. (**a**) Light colored lines (grey and pink) in the background represent tumor growth curve of each individual mouse. Solid color lines (black and red) show the average tumor growth curve. Unpaired two-way ANOVA. (**b**) Kaplan-Meier survival curves and the log-rank test performed. (**f**) Unpaired two-way ANOVA.
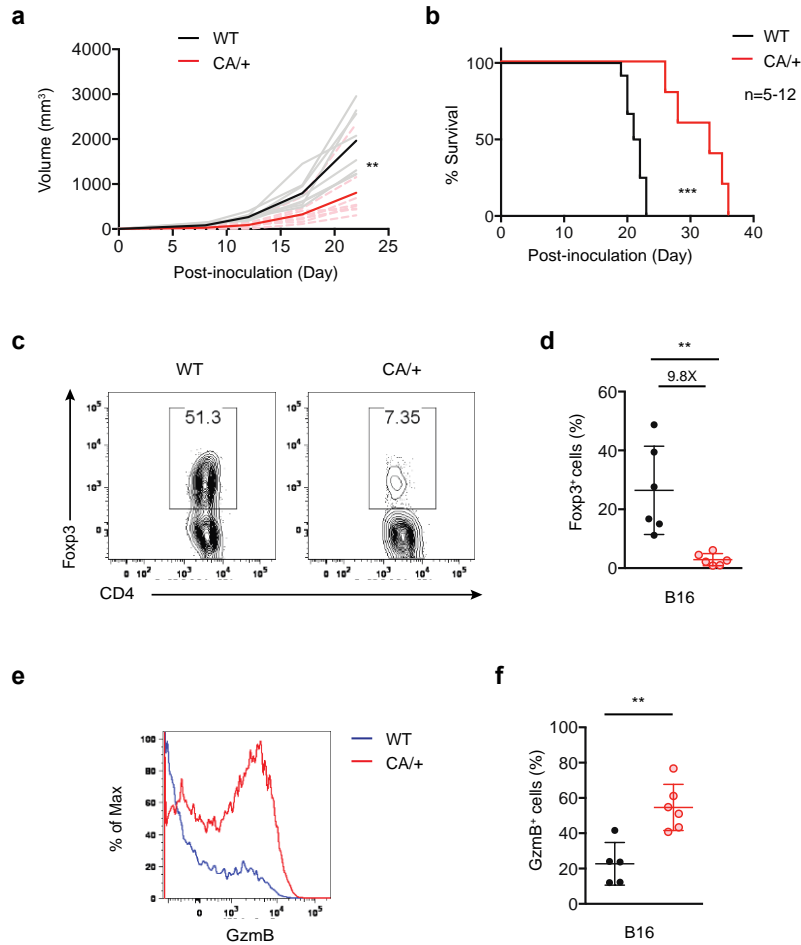
Figure 2-23: Expressing Foxo1CA one allele confers protection against tumor growth. a, 8 to 10-week-old wild-type (WT) or *Foxp3^{Cre}Foxo1CA/+* (CA/+) mice received subcutaneous injection of B16 melanoma cells. **a**, Tumor growth curve of WT and CA/+ mice. n=8. **b**, Survival of WT and CA/+ mice received tumor implantation. **c**, Foxp3 expression in tumor-infiltrating CD4$^+$ T cells from cells from Day 22-25 B16 tumors. **d**, The frequencies of Tregs among CD4$^+$ T cells in tumors of WT- and CA/+ -tumor bearing mice. n=6. Number above plots indicates fold change in comparison to WT. **e**, Flow cytometric analysis of GzmB expression in CD8$^+$ cells from tumors of WT and CA/+ mice. **f**, Fractions of GzmB-expressing cells among the CD8$^+$ cells from tumors of WT and CA/+ mice. n=6. Results represent at least three independent experiments. (**d, f**), Mean values ± SEM are shown. Unpaired *t*-test. (**a**) Light colored lines (grey and pink) in the background represent tumor growth curve of each individual mouse. Solid color lines (black and red) show the average tumor growth curve. Unpaired two-way ANOVA. (**b**) Kaplan-Meier survival curves and the log-rank test performed.

2.2.7 Foxo1 is a major downstream effector of the PI3K/Akt pathway in control of Treg function

As mentioned in the introduction, various components of the PI3K/Akt signaling pathway, such as Foxo1, mTORC1 and PTEN, have crucial roles in the regulation of mature Treg maintenance and suppressive function (*172, 186, 188, 190*). Heightened Akt signaling is observed in both Raptor- and PTEN-deficient Tregs (*186, 189*), and might contribute to the loss of Treg suppressive function. However, both mTORC1 and PTEN have PI3K/Akt-independent functions (*222, 223*), rendering the direct impact of PI3K-induced Akt activation in Tregs still unclear.

To directly stimulate Akt by hyperactive PI3K, we used a mouse model in which a constitutively active form of p110α, the catalytic subunit of PI3K, preceded by a loxP flanked STOP cassette is inserted into the ROSA26 locus, herein termed PI3KCA (*224*). Mice carrying the *PI3KCA* allele were crossed with *Foxp3^{Cre}* mice to induce Treg-specific expression of this mutant. As expected, *Foxp3^{Cre}PI3KCA/+* mice showed excessive Akt activation and Foxo1 phosphorylation in Treg cells (Fig. 2-24a). Moreover, those mice manifested a lethal autoimmune disorder, with massive infiltration of leukocytes in the salivary glad, lung, liver and colon (Fig. 2-26), which is similar as that seen in mice with Treg-specific Foxo1 ablation. In line with the severe immunopathology, T cell expansion and activation were also observed in *Foxp3^{Cre}PI3KCA/+* mice (Fig. 2-24b and 24c).

Similar as the *Foxp3^{Cre}Foxo1$^{f/f}$* mice, Treg proportions and numbers were not defective in mice with the mutant PI3K allele (Fig. 2-25a and 2-25b), suggesting that the

inflammatory disease is caused by a loss of Treg function rather than the Treg population. In addition, hyperactive PI3K signaling resulted in downregulation of Foxo1 target genes, such as CD62L and CCR7 (Fig. 2-25c), and induction of genes that is repressed by Foxo1, including IFN-γ (Fig. 2-25c), suggesting that the Foxo1-dependent transcriptional program is dysregulated by the expression of constitutively active PI3K.

Activated PI3K/Akt signaling stimulates multiple downstream effector molecules that affect Treg function. To test whether Foxo1 plays a crucial role in regulating Treg functionality in *Foxp3^{Cre}PI3KCA/+* mice, we ectopically expressed Foxo1CA in these Tregs. Foxo1CA rescued the inflammatory phenotype, including mice survival, scaly skin, splenomegaly and lymphoadenopathy (Fig. 2-26a and 26b). Moreover, the leukocyte infiltration phenotype was also corrected by the expression of nuclear Foxo1 (Fig. 2-26c). These findings demonstrate that Foxo1 acts as the major contributor downstream of PI3K/Akt signaling to the immunopathology developed in *Foxp3^{Cre}PI3KCA/+* mice.
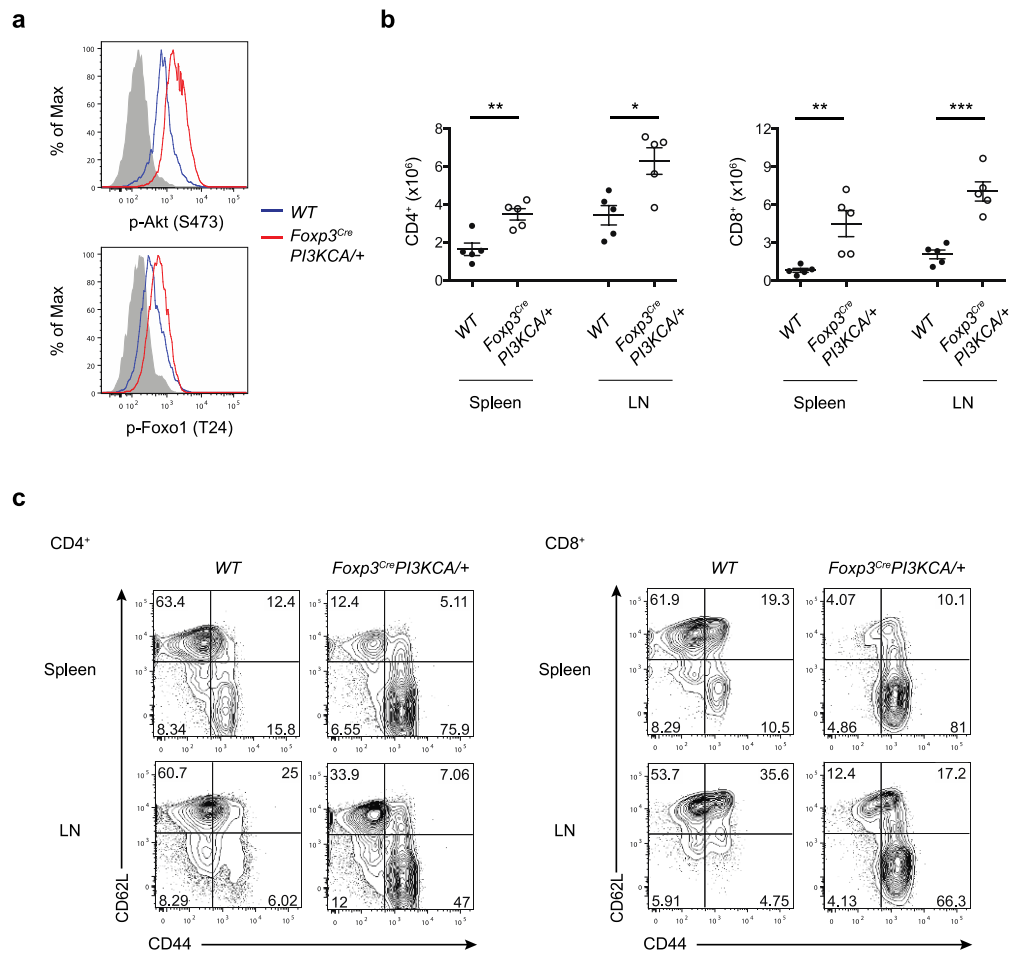
Figure 2-24: Expression of a constitutively active form of PI3K in Tregs triggers overt T cell responses. a, Flow cytometric analysis of phosphorylated Akt and Foxo1 proteins in splenic Tregs from *Foxp3^Cre^PI3KCA/+* mice or littermate control (wild-type, WT). **b**, CD4$^+$ and CD8$^+$ T cell-number from spleens and lymph nodes (axillary, brachial, inguinal) of 3-week-old *WT* and *Foxp3^Cre^PI3KCA/+* mice. **c**, Expression of CD44 and CD62L in CD4$^+$ and CD8$^+$ T cells from spleen and LNs of 3-week-old *WT* and *Foxp3^Cre^PI3KCA/+* mice. Data represent 5 mice per genotype analyzed in at least three independent experiments. All data are presented as the mean values $\pm$ SEM. Unpaired *t*-test.
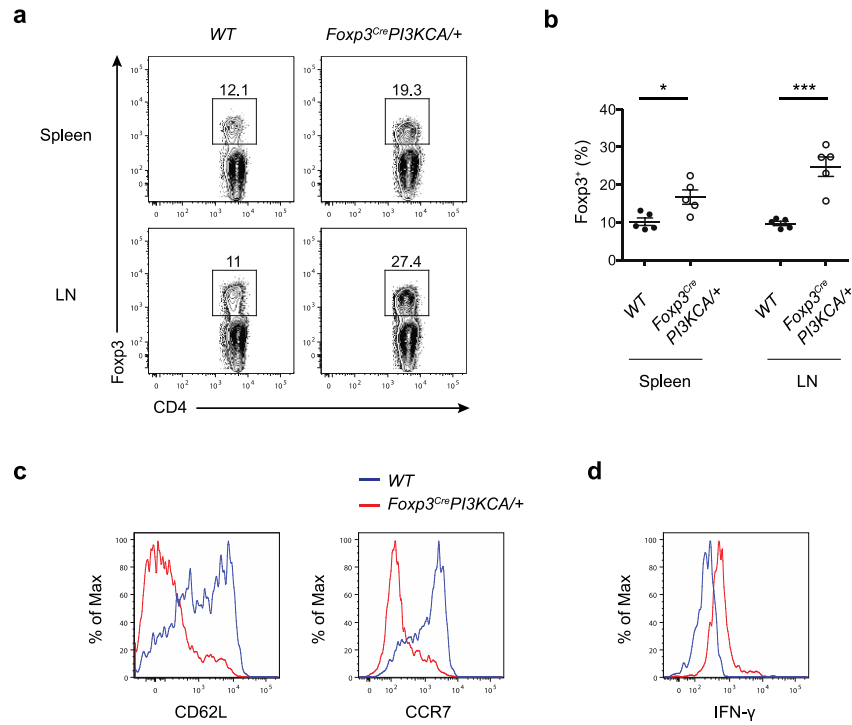
Figure 2-25: Tregs expressing hyperactive PI3K show similar phenotype as Foxo1-deficient Tregs. a-b, Flow cytometric analysis (**a**), and quantification (**b**) of Tregs in CD4$^+$ T cells from spleen and lymph nodes of 3-week-old *Foxp3^{Cre}PI3KCA/+* mice and littermate control (wild-type, WT). **c**, Expression of two Foxo1 targets, CD62L and CCR7, in splenic Tregs from WT and *Foxp3^{Cre}PI3KCA/+* mice. Data represent 7 mice per genotype analyzed in at least three independent experiments (mean $\pm$ SEM; unpaired *t*-test). **d**, Splenic Tregs from WT and *Foxp3^{Cre}PI3KCA/+* mice were restimulated with PMA and ionomycin for 4h, and analyzed for the expression of IFN-γ by intracellular cytokine staining. Data represent 5 mice per genotype analyzed in at least three independent experiments. All data are presented as the mean values $\pm$ SEM. Unpaired *t*-test.
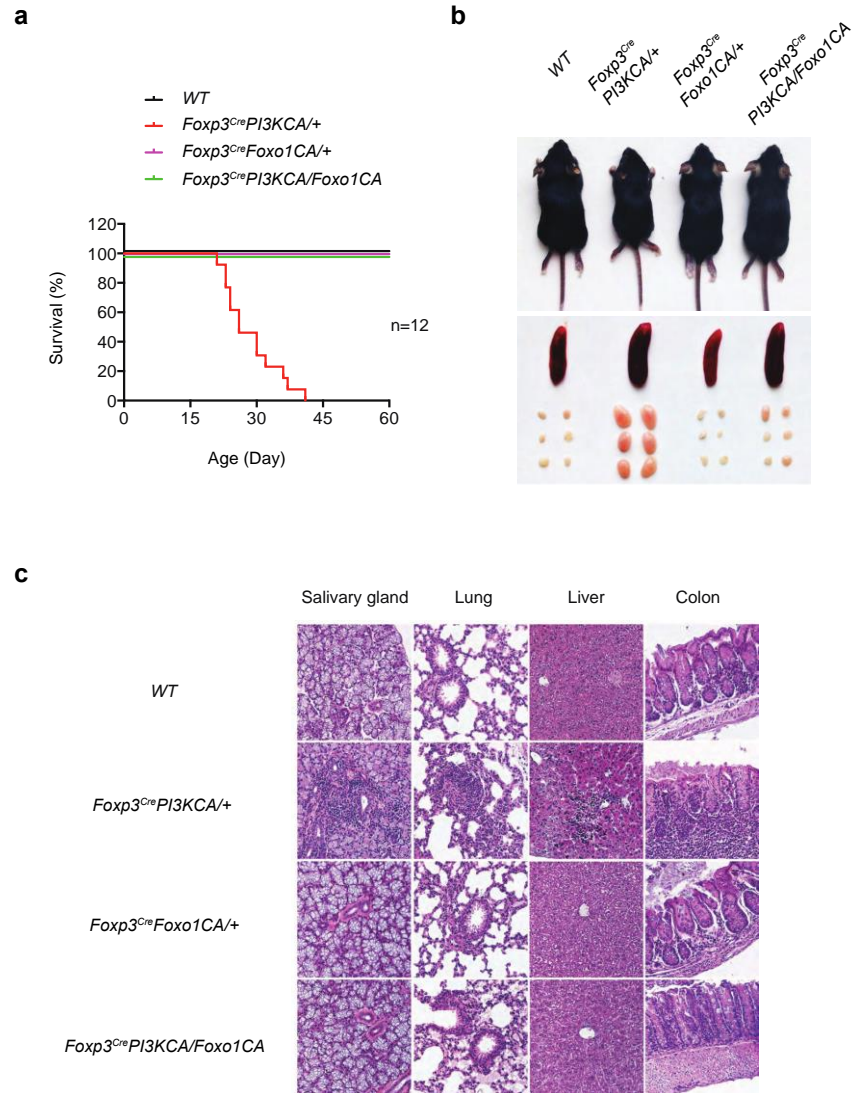
Figure 2-26: Ectopic expression of nuclear Foxo1 rescues the inflammatory disorder in $Foxp3^{Cre}PI3KCA/+$ mice. a, Survival of control (*WT*), $Foxp3^{Cre}PI3KCA/+$, $Foxp3^{Cre}Foxo1CA/+$, and $Foxp3^{Cre}PI3KCA/Foxo1CA$ mice. **b**, Representative pictures of 3-week-old *WT, $Foxp3^{Cre}$ PI3KCA/+, $Foxp3^{Cre}Foxo1CA/+$* and *$Foxp3^{Cre}$ PI3KCA/Foxo1CA* mice (upper), and their spleens and lymph nodes (axillary, brachial, inguinal) (lower). **c**, Hematoxylin and eosin staining of sections from lungs, livers, stomachs and colons. Original magnification, ×20.

2.3 Discussion

rTreg and aTreg subsets are identified in both humans and mice (*209, 210*), but their individual contributions to immune tolerance have been enigmatic. Our present study reveals that repression of Foxo1-dependent transcriptional program is a major reprogramming event associated with the differentiation of aTregs from rTregs. Under homeostatic conditions, both rTregs and aTregs recirculate through the blood, lymph and tissues, yet aTregs have a slower turnover rate, thus resembling effector memory T cells. The distinct migratory patterns between rTregs and aTregs are correlated with differential levels of Foxo1 activity – strong Foxo1 activity promotes expression of lymphoid organ homing molecules that are essential for rTregs, whereas downregulation of these proteins are required for the migration of aTregs to non-lymphoid organs. Using a gain-of-function model of Foxo1 that preferentially impairs aTreg populations in peripheral tissues, we could identify a prominent role for these cells in control of CD8$^+$ T cell tolerance. Importantly, tumor-associated aTregs show more substantial reduction of Foxo1-target genes compared with those residing in healthy tissues, and they are more susceptible to depletion caused by the constitutively active mutant of Foxo1.

A highly interesting observation we made was that mice expressing Foxo1CA specifically in Tregs developed a disease that was drastically different from those contained diminished or dysfunctional Treg pool. Our diseased mice didn't show crusty skins, scaly tails or enlarged secondary lymphoid organs. The CD4$^+$ and CD8$^+$ conventional T cells produced only mildly increased amounts of inflammatory cytokines. Nevertheless, the CD8$^+$ T cells in these mice showed markedly augmented cytotoxicity.

Depletion of CD8$^+$ T cells was able to rescue the fatal disorder, demonstrating a pivotal role of CD8$^+$ T cells in the immunopathology. Importantly, expression of Foxo1CA severely impaired aTreg populations in these mice, while leaving rTregs largely intact. These findings reveal a particular function of aTregs in suppressing CD8$^+$ T cell responses. The exact molecular mechanisms of how aTregs exert such specialized suppression await future investigation.

A number of different immunosuppression mechanisms have been ascribed to Tregs (*225*). They can either produce immunomodulatory cytokines, such as IL-10, IL-35 and TGF-β (*76, 226*), or "consume" local IL-2 via the high level of CD25 expression on their cell surface (*227*). Additionally, Tregs can disrupt effector T cell metabolism by generating adenosine, a reaction that is catalyzed by two ectoenzymes, CD39 and CD73 (*228*), or induce effector T cell death by releasing cytolytic molecules (*229*). Aside from the direct suppression on effector T cells, Tregs can also modulate the maturation and function of APCs. For instance, CTLA-4 expressed by Tregs dampens the costimulatory ligands, CD80 and CD86, on dendritic cells (*230, 231*). Therefore, the crucial suppression of CD8$^+$ T cell responses by aTregs can be accomplished by different mechanisms – aTregs direct inhibit CD8$^+$ T cell function through cell-cell contract; or aTregs repress CD4$^+$ helper T cells function that is required for optimal cytotoxic T cell responses; or aTregs suppress CD8$^+$ effector T cells by modulating APCs. Detailed characterization of distinct helper T cell populations as well as the dendritic cells and macrophages is needed to unveil the precise suppression mechanism(s).

Differential levels of Foxo1 activity are required for the proper migration and/or function of aTregs and rTregs. Intriguingly, emerging evidence suggests that Tregs adapt

to environmental cues and accomplish suppression via context-specific mechanisms. Ablation of IL-10 in Tregs causes aberrant immune responses in skin, lung and intestine, implying that IL-10-producing effector Tregs predominantly suppress effector responses at environmental interfaces (*208*). On the other hand, Tregs in the secondary lymphoid organs might primarily inhibit naive T cell priming, possibly through CTLA-4-mediated downregulation of costimulatory molecules on APC (*230*). Indeed, depletion of CTLA-4 in Tregs results in systemic autoimmunity associated with overt activation of T cells in secondary lymphoid organs and lymphoproliferation (*231*). It's therefore intriguing to speculate that modulation of Foxo1 activity is a key reprogramming event required for the tissue- and context-dependent adaptation. We will explore how Foxo1-regulated program contribute to immunosuppression-mediated by IL-10 and CTLA-4, and/or other mechanisms.

Importantly, tumor-associated aTregs are more susceptible to Foxo1-triggered depletion, permitting effective tumor immunity to be induced without overt spontaneous autoimmunity. The increased susceptibility likely is a consequence of higher antigen load in the tumor microenvironment and neoantigen generation by somatic mutations (*232-234*). Foxo1 activity is modulated by the PI3K/Akt signaling downstream of TCR, co-stimulation and cytokine ligation. Drugs that target the upstream signaling molecules, such as PI3K inhibitors and Akt inhibitors, may impinge on the Foxo1 pathway to selectively break Treg-mediated tumor immune tolerance.

2.4 Experimental procedures

Mice

The Foxo1CA (*Foxo1^{AAA}* knock-in) and Foxo1tag-GFP (*Foxo1^{tag}*) mouse models, as well as MMTV-PyMT on C57BL/6 background were previously described (*172, 220*). PI3KCA knock-in mouse strain was purchased from Jackson Laboratory (Strain: 012343) (*224*). C57BL/6, CD45.1^{+} and CD8$^{-/-}$ mice were purchased from Jackson Laboratory. Mice with Treg-cell-specific expression of Foxo1CA were generated by crossing *Foxo1^{AAA}* with *Foxp3^{Cre}* mice (*208*). *Foxp3^{Cre}* mice express YFP from the Foxp3 locus, and were used as a reporter for sorting experiments. To mark Treg cells with red fluorescent protein (RFP) in the Foxo1tag-GFP experiment, *Foxo1^{tag}* mice were bred with *Foxp3-IRES-RFP* mice (*235*). In all experiments, littermate controls were used when possible. Unless mentioned otherwise, both male and female mice were included. All mice were maintained under specific pathogen-free conditions, and animal experimentation was conducted in accordance with procedures approved by the Institutional Animal Care and Use Committee of Memorial Sloan Kettering Cancer Center. Investigators were not blinded to group allocation and outcome assessment. No statistical methods were used to predetermine sample size and the experiments were not randomized.

Parabiosis

Parabiosis and separation were done as reported with 6 to 8-week-old cogenically-marked female C57BL/6 mice that were matched for body weight (*236*). Briefly, matching skin incisions were made from the elbow to the knee of each mouse. Forelimb and hindlimb connections were made with sutures and skin incisions were closed using woundclips. For separation, connections between parabionts were disrupted and skin incisions were closed using woundclips. Parabionts were maintained for 4 weeks before surgical separation. Separated parabiont mice were analyzed up to 18 weeks post-surgery.

Tumor models

MMTV-PyMT spontaneous tumor model was previously described (*220*). AT-3 model: 8 to 10-week-old wild-type (WT), *Foxp3^{Cre}Foxo1CA/+* (CA/+), *CD8$^{-/-}$, or Foxp3^{Cre}Foxo1CA/+CD8$^{-/-}$* (CA/+CD8$^{-/-}$) mice were injected with AT-3 mammary tumor (2×10^5 cells into mammary fat pad) (*237*). B16 model: 8 to 10-week-old WT or CA/+ mice were injected with B16.F10 melanoma (1.25×10^5 cells subcutaneously). For all tumor models, tumors were measured regularly with a caliper. Tumor volume was calculated using the equation (L$\times$W^2) x 0.52 where "L"=length and "W"=width. The maximal tumor burden was 3,000 mm^3, and in none of the experiments was the limit exceeded. For PyMT, individual tumor volumes were added together to calculate total

tumor burden. Tumor bearing mice were sacrificed at 22 to 24-week old for PyMT model, 30 to 35-day post-inoculation for AT-3 model and 20 to 24-day post-inoculation for B16 model. In all flow cytometry experiments, tumors of similar sizes were used for comparison.

Cell isolation

After whole-body perfusion with 50 ml of heparinized PBS, lymphocytes were isolated as follows. Single-cell suspensions were prepared from spleens and peripheral (axillary, brachial, and inguinal) lymph nodes by tissue disruption with glass slides. To isolate cells from the liver, tissues were finely minced and digested with 1 mg/ml Collagenase D (Worthington) for 30 min at 37 ℃. For lamina propria lymphocytes isolation, colon was dissected and washed in HBSS. Intestinal pieces were stirred in 1 mM DTT in HBSS to release intraepithelial lymphocytes. The remaining intestinal tissues were finely minced and digested with RPMI plus 5% FBS and 1 mg/ml Collagenase D for 30 min at 37 ℃. For tumor-infiltrating immune cell isolation, tumor tissues were prepared by mechanical disruption followed by 1 hour treatment with 280 U/ml Collagenase Type 3 (Worthington) and 4 μg/ml DNase I (Sigma) at 37 °C. After the digestion steps, cells isolated from the liver, lamina propria and tumor were filtered through 70-μM cell strainer, layered in a 44% and 66% Percoll gradient (Sigma), and centrifuged at 3000 rpm for 30 min without brake. Cells at the interface were collected and analyzed by flow cytometry.

Flow cytometry

Flurochrome-conjugated, biotinylated antibodies against CD45.1 (clone 104), CD45.2 (A20), TCR-β (H57-595), CD4 (RM4-5), CD8 (17A2), CD44 (IM7), CD62L (MEL-14), CD69 (H1.2F3), CCR7 (4B12), Foxp3 (FJK-16s), ICOS (C398.4A), IFN-γ (XMG1.2), IL-4 (11B11), NK1.1 (PK136) were purchased from eBiocience. Antibodies against CD49a (Ha31/8), IL-17a (TC11-18H10.1) were purchased from BD Biosciences. Anti-GzmB (GB11) was purchased from Invitrogen. Purified antibodies against Bim (C34C5), p-Akt (S473) (736E11), p-Akt (T308) (C31E5E), p-Foxo1(T24), p-S6 (S240) were purchased from Cell Signaling. All antibodies were tested with their respective isotype controls. Cell surface staining was performed by incubating cells with specific antibodies for 30 min on ice in the presence of 2.4G2 mAb to block FcγR binding. CCR7 staining was incubated in 37 ℃ for 30 min prior to cell surface staining. Foxp3, Bim, GzmB, IFN-γ, IL-4, IL-17a staining was carried out using the intracellular transcription factor or cytokine staining kits from Tonbo or BD Biosciences. Phosphorylation staining was performed using BD phospho-protein kit. Secondary antibodies with flurochrome-conjugation were used for the staining of purified antibodies. To determine cytokine expression, isolated cells were stimulated with 50 ng/ml phorbol 12-myristate 13-acetate (Sigma), 1 mM ionomycin (Sigma) and GolgiStop (BD Biosciences) for 4 h prior to staining. Incorporation of EdU was measured using the Click-iT EdU flow cytometry assay kit according to the manufacturer's instructions (Invitrogen). Mice were injected i.p. with 50 μg/g body weight of EdU and sacrificed 18 hours later. For all stains, dead cells were excluded from analysis by means of Live/Dead Fixable Dye (Invitrogen), DAPI or

propidium iodide (PI) stain. All samples were acquired and analyzed with LSRII flow cytometer (Becton Dickson) and FlowJo software (TreeStar).

In vivo T cell labeling

2μg α-CD4-Biotin (RM4-4, BioLegend) was injected intravenously, and mice were sacrificed 5 minutes after injection. Splenocytes were prepared for flow cytometric analysis as described above. Streptavidin conjugated with fluorophore was used as the secondary labeling for α-CD4-Biotin, and a non-competing clone of CD4 antibody (RM4-5, eBioscience) was used to stain total CD4$^+$ cells.

In vitro T cell culture

Akt inhibitor experiment: CD4$^+$Foxp3$^+$CD62L^{hi}CD44^{lo} rTregs were purified from spleen and lymph nodes of *Foxp3$^{YFP/Cre}$* mice by flow cytometry sorting (BD FACS Aria) at Flow Cytometry Core Facility of Memorial Sloan Kettering Cancer Center (MSKCC). rTregs were cultured with plate bound α-CD3 (coated overnight, 5μg/mL), soluble α-CD28 (2μg/mL) and IL-2 (200U/mL) for 3 days. Akt inhibitor (MK-2206 2HCl, Selleckchem, 2μM final concentration) or DMSO solvent control was added to the culture. rTreg activation experiments: CD4$^+$Foxp3$^+$CD62L^{hi}CD44^{lo}CD69$^-$ICOS$^-$ rTregs were sorted out from *Foxp3^{Cre}*, *Foxp3^{Cre}Foxo1CA/+* or *Foxp3^{Cre}Foxo1CA/Foxo1CA* mice, and labeled with CellTrace Violet (Invitrogen). Cells were cultured with plate

bound α-CD3 (coated overnight, 5μg/mL), soluble α-CD28 (2μg/mL) and IL-2 (200U/mL) for 3 days.

In vitro Treg suppression

CD4$^+$CD25$^-$CD62L^{hi}CD44^{lo} conventional T cells purified by flow cytometry sorting were labeled with CellTrace Violet and used as responder cells. Responder T cells (5×10^4) were cultured for 72 hours with irradiated splenocytes (1×10^5) and α-CD3 (2μg/mL) in the presence or absence of various numbers of Tregs. Tregs (CD4$^+$Foxp3-YFP$^+$) were isolated by FACS sorting from *Foxp3^{Cre}*, *Foxp3^{Cre}Foxo1CA/+* or *Foxp3^{Cre}Foxo1CA/Foxo1CA* mice.

Gene-expression profiling

Splenic rTreg (CD4$^+$Foxp3-YFP$^+$CD62L^{hi}CD44^{lo}) and aTreg (CD4$^+$Foxp3-YFP$^+$CD62L^{lo}CD44^{hi}) cells were isolated from *Foxp3$^{YFP/Cre}$* mice by FACS sorting. RNA was prepared with the miRNeasy Mini Kit according to the manufacturer's instructions (Qiagen). Complementary DNA (cDNA) libraries were amplified using the SMARTer RACE Amplification Kit (Clontech), and were sequenced in replicate using 50 bp paired-end at Genomics Core Laboratory of MSKCC. Ribosomal RNA reads were quantified and filtered using the short-read aligner, Bowtie v2.1.0 (*238*). The remaining reads were aligned to the mouse genome (mm10) using the STAR v2.3.1 short-read aligner (*239*). Additional quality control was performed using RSeQC v2.3.7 (*240*). Gene abundance

was quantified by featureCounts (*241*) via the Subread analysis suite v1.4.3 (*242*). Differential gene expression was estimated using the DESeq2 R package with gene annotations curated in GENCODE version 2 for mouse reference genome GRCm38 (Ensembl 74) (*243*). RNA-sequencing data are available at Gene Expression Omnibus (GEO) (accession number GSE74957).

Quantitative PCR

RNA extraction was performed using RNeasy columns (Qiagen) and cDNA was generated using QuantiTect Reverse Transcription Kit (Qiagen) according to the manufacturer's instructions. RT^2 SYBR Green kit (Qiagen) and Stratagene Mx3500 (Agilent) were used in the qPCR experiments. mRNA levels of *Lamc1, Nid2, Mmp9, Cd69, Egr2, Il1r2*, and *Actb* were determined by the primers listed below. The mRNA amounts were normalized to those of *Actb*.

Lamc1: 5'-ggtggtctgtttcagccatt-3' and 5'-tgccacaaaatctcagcttg-3';

Nid2: 5'-tggatatggccaaggagaag-3' and 5'-caccgaggacagtttccatt-3';

Mmp9: 5'-accttccagtaggggcaact-3' and 5'-tgaatcagctggcttttgtg-3';

Actb: 5′-ttgctgacaggatgcagaag-3′ and 5′-acatctgctggaaggtggac-3′.

Immunofluorescence microscopy

Foxo1 localization experiment: Spleens from wild-type mice were immediately disrupted using glass slides into Cytofix/Cytoperm buffer (BD). After incubation for 30

min at room temperature, the cells were washed, resuspended in 90% methanol and incubated on ice for 30 min. After additional wash, cells were stained for surface and intracellular antigens, including CD4, CD44 and Foxp3, for 45 min at room temperature in the dark. rTregs ($CD4^+Foxp3^+CD44^{lo}$) and aTregs ($CD4^+Foxp3^+CD44^{hi}$) were then purified by FACS sorting, and spun to glass slides using Cytospin centrifuge (Thermo Scientific) at 1200 rpm for 5min. Cells on the glass slides were stained with 1:150 diluted α-Foxo1 (C29H4, Cell Signaling), followed by fluorophore-conjugated secondary antibody staining. Slides were mounted with gold anti-fading mounting buffer (Invitrogen). Images were acquired with a Leica TCS SP5-II confocal microscope at Molecular Cytology Core of MSKCC. For quantitative analysis, five fields were selected randomly and total cells in the field were manually counted and grouped with Volocity software (PerkinElmer Inc.), on the basis of their Foxo1 nuclear or cytosolic localization. For HA-Foxo1 staining, $CD4^+Foxp3-YFP^+$ cells were purified from *Foxp3^{Cre}*, *Foxp3^{Cre}Foxo1CA/+* or *Foxp3^{Cre}Foxo1CA/Foxo1CA* mice by FACS sorting, and were spun to glass slides using Cytospin centrifuge (Thermo Scientific) at 500 rpm, 1min. After fixation with 4% paraformaldehyde, cells were permeabilized with Foxp3 Fixation/Permeabilization buffer (eBioscience) according to the manufacturer's instructions. Cells were then blocked with Permeabilization buffer and 3% BSA, and incubated with 1:500 diluted α-HA (C29F4, Cell Signaling) and 1:150 diluted α-Foxp3 (FJK-16s, eBioscience), followed by fluorophore-conjugated secondary antibodies in Permeabilization buffer and 1% BSA.

Immunoblotting

Tregs (CD4$^+$Foxp3-YFP$^+$) were isolated from *Foxp3^{Cre}*, *Foxp3^{Cre}Foxo1CA/+* or *Foxp3^{Cre}Foxo1CA/Foxo1CA* mice by FACS sorting. Total protein extracts were dissolved in SDS sample buffer, separated on 12% SDS-PAGE gels and transferred to polyvinylidene difluoride membrane (Millipore). The membranes were probed with α-HA (6E2, Cell Signaling) and α-β-actin (AC-15, Sigma), and visualized with the Immobilon Western Chemiluminescent HRP Substrate (Millipore).

Histopathology

Liver and colon tissues were fixed in Safefix II (Protocol) and embedded in paraffin. 5-mm sections were stained with haematoxylin and eosin. The following grades were used to evaluate the colon pathology: 0, normal colonic crypt architecture; 1, mild inflammation: slight epithelial cell hyperplasia and increased numbers of leukocytes in the mucosa; 2, moderate colitis: pronounced epithelial hyperplasia, significant leukocyte infiltration, and decreased numbers of goblet cells; 3, severe colitis: marked epithelial hyperplasia with extensive leukocyte infiltration, significant depletion of goblet cells, occasional ulceration, or cryptic abscesses; 4, very severe colitis: marked epithelial hyperplasia with extensive transmural leukocyte infiltration, severe depletion of goblet cells, many crypt abscesses and severe ulceration.

Serum alanine aminotransferase activity

Blood was collected right after mice were euthanized and was stored at room temperature for 1 hour. The samples were then centrifuged for 15 min at 3,000 rpm, and the supernatant was obtained as serum. Alanine aminotransferase (ALT) activity was determined according to manufacturer's instructions (Sigma-Aldrich), using SpectraMax M5 plate reader (Molecular Devices).

Statistical analysis

All data are presented as the mean values $\pm$ SEM. Comparisons between groups were analyzed using unpaired or paired Student's t tests or analysis of variance (ANOVA), as appropriate. ns=not significant, *, $p<0.05$, **, $p<0.01$, ***, $p<0.001$, ****, $p<0.0001$.

CHAPTER III

GABP-DEPENDENT REGULATION OF EFFECTOR T CELL RESPONSES

AND REGULATORY T CELL FUNCTION

3.1 Introduction

3.1.1 Ets family of transcription factors

Ets (*E twenty-six*) proteins are a group of transcription factors containing the conserved Ets domain, a DNA-binding domain composed of 85 amino acids that binds to purine-rich DNA sequences with a core GGAA/T motif and additional flanking nucleotides (*244*). More than two dozens of Ets proteins have been identified from various organisms, and they are evolutionarily conserved within metazoan (*245, 246*). Ets family of transcription factors can be classified into several subfamilies on the basis of their structural composition, for instance, whether they contain the pointed (PNT) domain, and the location of the transactivation domain (*247*).

Ets transcription factors are expressed ubiquitously in mouse and human tissues, although different Ets proteins have distinct distribution patterns (*244*). Ets-1, the founding member of Ets family, as well as Ets-2, have a broad range of tissue distribution, whereas other Ets members, such as PU.1 and ESE-1, show tissue-specific expression (*244*). Ets factors interact with a multitude of co-regulatory factors to activate or repress the target gene expression, and to elicit gene-specific responses (*247*). They have crucial

functions in a variety of biological processes, including embryonic development, cellular differentiation, and oncogenic transformation (*247*).

3.1.2 GA-binding protein (GABP)

GA-binding protein (GABP) is unique among the large Ets transcription factor family as it is the only obligate multimeric complex (*248*). It is composed of two distinct subunits, GABPα and GABPβ (*249*). GABPα binds to DNA through its Ets domain, but lacks transactivation capability. GABPβ contains the transcription activation and nuclear localization signal domains, and it does not physically interact with DNA (*250*). GABPα has a single transcript isoform that is widely expressed across tissue types, whereas GABPβ is encoded by either *Gabpb1* or *Gabpb2* gene, and GABPβ1 contains multiple isoforms (*251, 252*). A subset of GABPβ isoforms, including GABPβ1L and GABPβ2, contain leucine zipper-like domains, which allow two GABPα/β heterodimers to form a heterotetramer complex. The GABPα$_2$/β$_2$ heterotetramer is capable of binding to GABPα motifs (core consensus CCGGAA) in proximity to each other, and further stimulates transcription (*253*).

GABP is ubiquitously expressed, and has been implicated in the regulation of many fundamental cellular processes, including ribosomal and mitochondrial biogenesis and cell cycle progression (*248*). It is also known as nuclear respiratory factor 2 (NRF2), a crucial transcriptional factor that controls the expression of both mitochondrial DNA and nuclear genes (*254*). Among the key genes that GABP regulates are the cytochrome c oxidase (COX) subunits IVii and Vb, which are important for electron transport and

oxidative phosphorylation (*255*). In addition to the "housekeeping" function, GABP regulates lineage-specific targets as well. For instance, GABP activates the expression of genes encoding acetylcholine receptors in the neuro-muscular synapse and the integrin *Itgb2* in myeloid cells (*256-258*). In order to exert the tissue-specific function, GABP interacts with a number of transcriptional regulators, including p300, c-Myb, C/EBP and Sp1, in a context-dependent manner, and is regulated by extracellular stimuli (*259-261*).

Constitutive inactivation of *Gabpa* gene leads to peri-implantation lethality in mice, suggesting a crucial role of GABP in early embryogenesis (*262, 263*). To circumvent the embryonic lethality, mice carrying loxP sites that flank Ets domain exons of *Gabpa* were generated by multiple groups (*264, 265*). Cre recombinase driven by different tissue-specific promoters was used to introduce conditional deletion of *Gabpa* gene. In studies focusing on mouse embryonic fibroblasts, GABP is shown to be required for cell cycle entry by regulating the activity of CDK inhibitors such as p27^{kip1} (*264, 266*). Additionally, loss of GABPα led to reduced mitochondrial mass, ATP production and oxygen consumption in fibroblasts, whereas mitochondrial structure and membrane potential were not disrupted (*255*).

GABP also impacts the hematopoietic system and various leukocyte populations. Using the Mx1-Cre and Poly I:C administration to induce *Gabpa* deletion in interferon-responsive cells, GABPα was shown to be required for the maintenance and differentiation of hematopoietic stem and progenitor cells, as well as for the differentiation of myeloid cells (*267, 268*). Moreover, GABP critically regulates B cell development, maturation and function by promoting Pax5 expression (*269*).

In cancer, Ets transcription factors are known to be frequently targeted by mutations, copy number alterations and translocations (*270*). Accordingly, constitutive disruption of the tetramer-forming GABPβ isoforms impaired self-renewal of hematopoietic and leukemia stem cells, and protected mice from Bcl-Abl-driven myeloproliferative disease, which resembles human chronic myeloid leukemia (CML) (*271*). Similarly, inducible depletion of *Gabpa* gene using Mx1-Cre, Poly I:C system also prevented the development of Bcl-Abl-driven CML in mice (*272*). In a study of liver cancer, increased expression and nuclear localization of GABPα and GABPβ were observed in liver cancer compared to the nontumorous liver tissue (*273*). GABP promotes cell cycle progression and inhibits cell death by positively regulating the expression of Yes-associated protein (YAP), a key component of the Hippo pathway (*273*).

3.1.3 GABP in T cells

Most studies exploring the roles of GABP in T cells focus on early T cell development. Examination of embryonic thymocytes at E14.5 of the *Gabpa* constitutively knockout mice showed that expression of IL-7Rα was completely abolished in the GABPα-null thymocytes (*263*). Later work used mice carrying Lck-Cre transgene to conditionally delete *Gabpa* gene in immature CD44$^+$CD4$^-$CD8$^-$ (DN1-DN2) thymocytes. In the *Lck-Cre Gabpa$^{f/f}$* mice, thymic cellularity was greatly diminished and thymocytes development was blocked at the DN3 stage (*274*). Intriguingly, those DN3 thymocytes expressed comparable levels of IL-7Rα as the GABPα-replete control, whereas the cells progressed to the DN4 stage had reduced expression of IL-7Rα (*274*).

These findings demonstrated a crucial function of GABPα in early T cell development, which is dependent on IL-7Rα.

Additionally, using P14 TCR transgenic CD8$^+$ T cells that specifically recognize a LCMV-derived peptide, knockdown of GABPα was associated with reduced IL-7Rα expression upon LCMV infection, which was antagonized by Gfi-1 (*275*).

3.2 Results

3.2.1 Thymocyte development in T cell-specific GABPα-deficient mice

Although GABPα has been reported as a crucial regulator of early T cell development, little is known about its function beyond thymocyte differentiation stage. To specifically dissect the functions of GABPα in mature T cells, we crossed *Gabpa$^{f/f}$* mice to mice carrying *CD4^{Cre}* transgene. The CD4-Cre recombinase was expressed in DP thymocytes, leading to efficient deletion of GABPα in SP thymocytes and mature T cells in the peripheral. Indeed, GABPα protein was not detectable in either CD4$^+$ or CD8$^+$ T cells isolated from spleen and lymph nodes (LNs) of *CD4^{Cre}Gabpa$^{f/f}$* mice, hereafter called KO mice (Fig. 3-1a). Thymic cellularity was similar in 5- to 8-week-old KO mice compared with *Gabpa$^{f/f}$* littermate controls, designated as wild-type (WT) (Fig. 3-1b). In addition, analysis of the proportions and numbers of DN, DP and SP subsets did not reveal drastic difference between KO and WT mice, with the exception that KO mice contained a slightly reduced CD8SP population (Fig. 3-1c and 1d). The largely

unperturbed thymocyte development in $CD4^{Cre}Gabpa^{f/f}$ mice permitted us to further investigate the roles of GABPα in peripheral CD4$^+$ and CD8$^+$ T cells.

3.2.2 GABPα is required for T cell activation and proliferation

GABPα-deficient mice showed a substantial decrease in the proportion and number of TCRβ$^+$ cells in the spleen and LNs compared with littermate controls (Fig. 3-2a-2c). Notably, while both CD4$^+$ and CD8$^+$ T cell subsets were diminished (Fig. 3-2f), CD8$^+$ T cells were more severely impaired by the loss of GABPα, as shown by the increased ratio of CD4$^+$ to CD8$^+$ T cells (Fig. 3-2d and 2e). Further phenotypic analysis of CD4$^+$ and CD8$^+$ T cells revealed that $CD4^{Cre}Gabpa^{f/f}$ mice possessed a significantly lower proportion of activated-memory phenotype (CD44^{hi}) cells compared to WT mice (Fig. 3-3). These observations suggest that GABPα-null T cells might be defective in antigen-stimulated activation and proliferation, which could explain the decrease in abundance.

To assess the cell proliferation of GABPα-deficient T cells *in vivo*, we measured the expression of Ki67, a proliferation marker, in 5- to 8- week-old mice. Surprisingly, CD4$^+$ T cells in the $CD4^{Cre}Gabpa^{f/f}$ mice expressed comparable amounts of Ki67 as that of the GABPα-replete CD4$^+$ T cells, and CD8$^+$ T cells in the GABPα-deficient mice contained higher expression of Ki67 compared to the wild-type counterparts (Fig. 3-3). These findings suggest that GABPα is dispensable for the homeostatic proliferation of T cells *in vivo*, and the increase in cell proliferation might be caused by compensatory mechanisms.
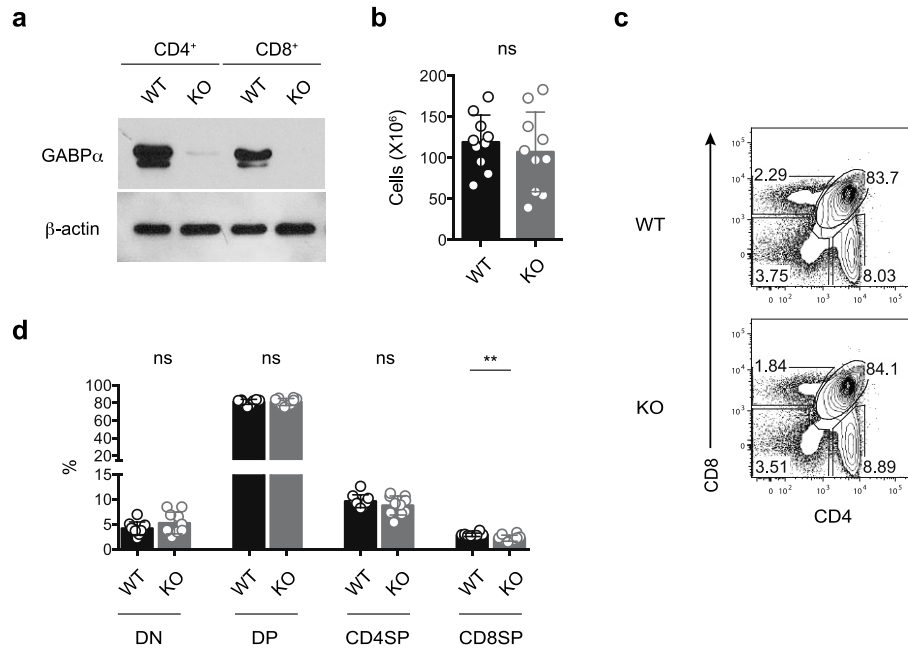
Figure 3-1: Thymocyte development in T cell-specific GABPα-deficient mice. a, Immunoblotting analysis of GABPα in purified CD4$^+$ and CD8$^+$ T cells from the spleens and LNs of *Gabpa$^{f/f}$* (wild-type, WT) and *CD4^{Cre}Gabpa$^{f/f}$* (KO) mice. β-actin was used as a loading control. **b**, Total numbers of thymocyte in WT and KO mice. **c**, Flow cytometric analysis of CD4 and CD8 expression on thymocytes of WT and KO mice. **d**, Percentages of CD4$^-$CD8$^-$ (double-negative, DN), CD4$^+$CD8$^+$ (double-positive, DP), CD4$^+$ or CD8$^+$ single-positive (SP) subsets. Mice of 5-8 week-old were used. Data represent 10 mice per genotype analyzed in at least three independent experiments (mean ±SEM; unpaired *t*-test).
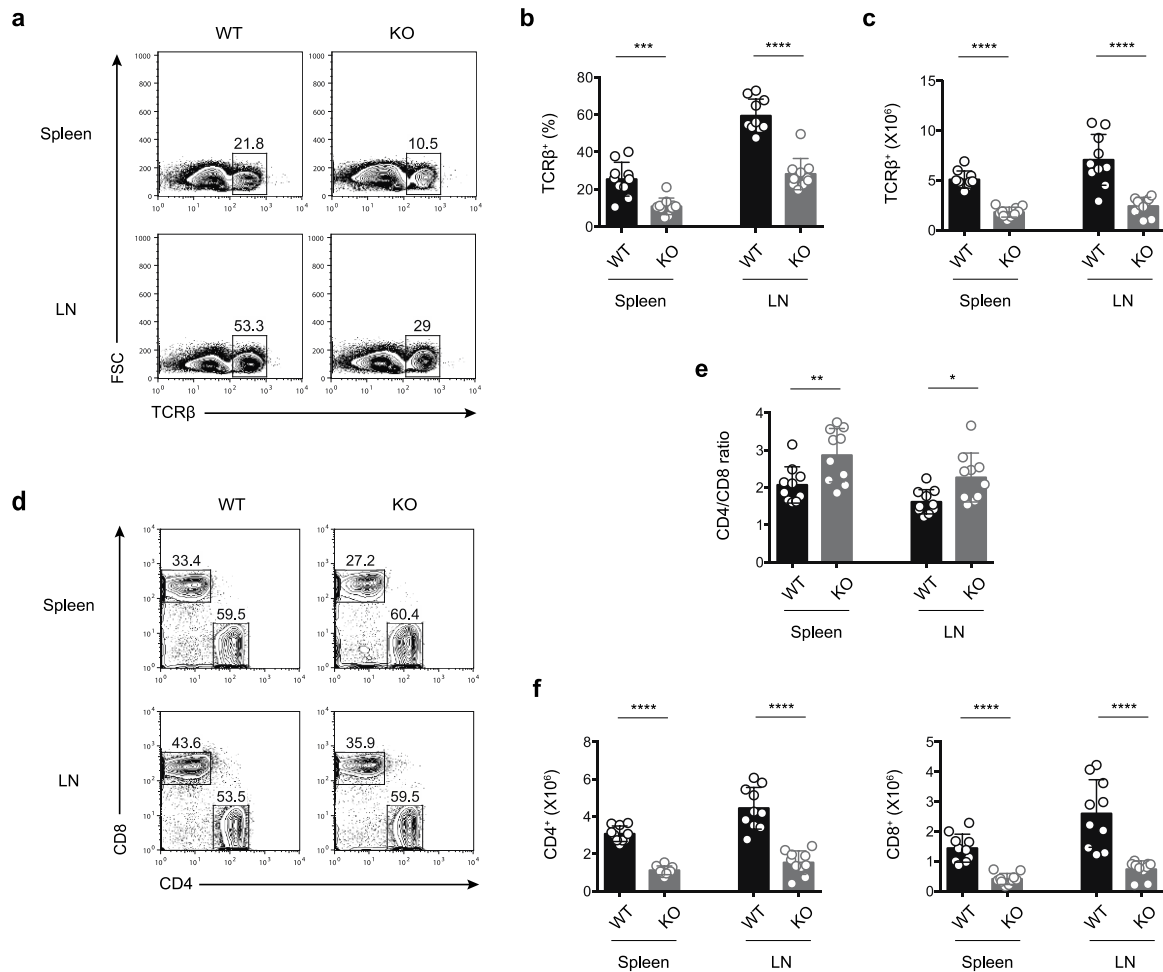
Figure 3-2: Mice with T cell-specific disruption of GABPα contain diminished T cell populations. a, Flow cytometric analysis of TCRβ expression on cells from spleen and peripheral lymph nodes (LNs) of *Gabpa^{f/f}* (wild-type, WT) and *CD4^{Cre}Gabpa^{f/f}* (KO) mice. **b-c**, Fractions of TCRβ$^+$ cells among total live cells (**b**), and numbers of TCRβ$^+$ cells (**c**) in the spleens and LNs of WT and KO mice. **d**, Expression of CD4 and CD8 on TCRβ$^+$ cells. **e**, Ratio of CD4$^+$ to CD8$^+$ cells. **f**, Numbers of CD4$^+$ to CD8$^+$ cells from spleen and LNs of WT and KO mice. Mice of 5-8 week-old were used. Data represent 10 mice per genotype analyzed in at least three independent experiments (mean ± SEM; unpaired *t*-test).
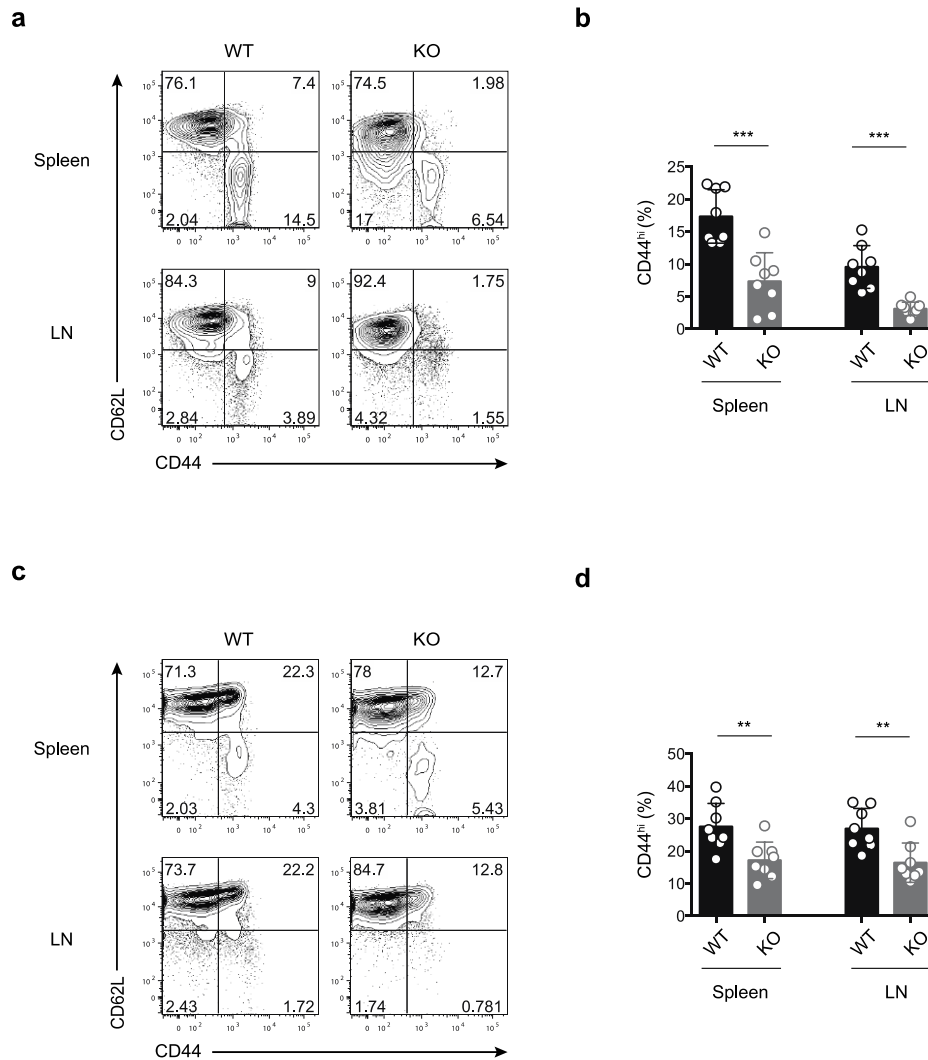
Figure 3-3: Antigen-experienced T cells are more severely impaired by the loss of GABPα. a, **c**, Flow cytometric analysis of CD44 and CD62L expression on CD4$^+$ (**a**) and CD8$^+$ (**c**) T cells from spleen and peripheral lymph nodes (LNs) of *Gabpa$^{f/f}$* (wild-type, WT) and *CD4^{Cre}Gabpa$^{f/f}$* (KO) mice. **b**, **d**, Fractions of CD44^{hi} cells among CD4$^+$ (**a**) and CD8$^+$ (**c**) in the spleens and LNs of WT and KO mice. Mice of 5-8 week-old were used. Data represent 8 mice per genotype analyzed in at least three independent experiments (mean ± SEM; unpaired *t*-test).
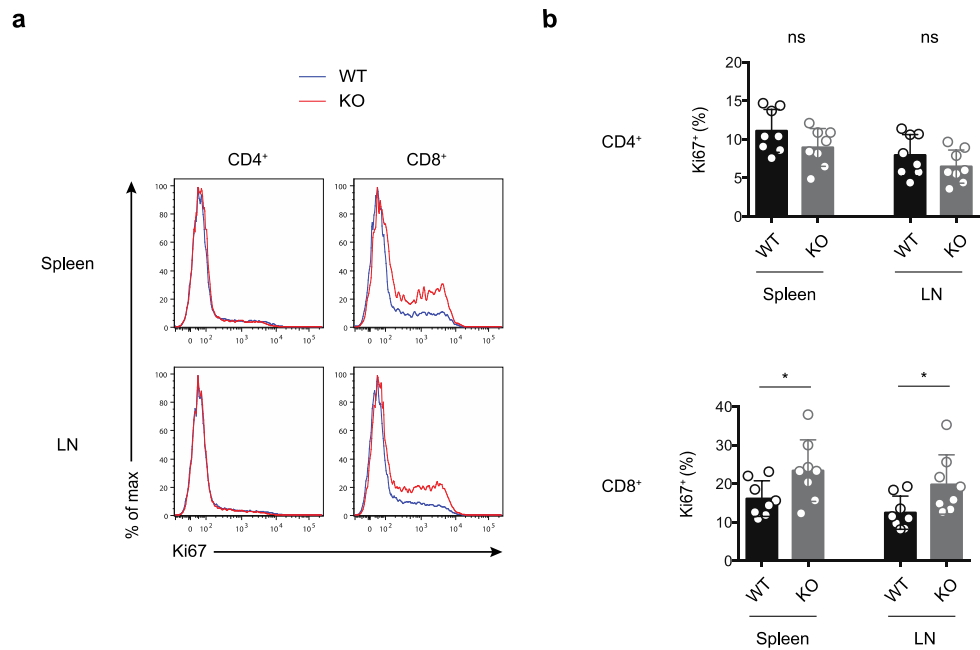
Figure 3-4: GABPα is dispensable for T cell homeostatic expansion. a, Flow cytometric analysis of Ki67 expression on CD4$^+$ and CD8$^+$ T cells from spleen and peripheral lymph nodes (LNs) of WT and KO mice. **b**, Enumeration of Ki67$^+$cells among CD4$^+$ and CD8$^+$ T cells in the spleens and LNs of WT and KO mice. Mice of 5-8 week-old were used. Data represent 8 mice per genotype analyzed in at least three independent experiments (mean $\pm$ SEM; unpaired *t*-test).

In order to determine whether GABPα plays a cell-intrinsic role in regulating T cell proliferation, we performed adoptive transfer experiments, in which CD4$^+$ and CD8$^+$ T cells were purified from congenically mismatched *CD4^{Cre}Gabpa$^{f/f}$* and *Gabpa$^{f/f}$* mice, mixed at 1:1 ratio, and intravenously injected into Rag1-deficent or sublethally irradiated C57/B6 wild-type recipients (Fig. 3-5a). We assessed the division of cells 7 days after transfer. In both Rag1$^{-/-}$ and the irradiated B6 recipients, WT CD4$^+$ or CD8$^+$ T cells underwent more cell division than did the GABPα-deficient T cells, suggesting that disruption of GABPα impairs cell proliferation in competitive settings (Fig. 3-5b).

The reduced activated-memory phenotype T cell subsets in *CD4^{Cre}Gabpa$^{f/f}$* mice and defective cell division in co-transfer experiments led us to examine the responses of GABPα-deficient T cells upon antigen stimulation *in vitro*. Briefly, we purified naive (CD62L^{hi} CD44^{lo}) CD4$^+$ and CD8$^+$ T cells from GABPα-deficient mice and littermate controls, and stimulated the cells with CD3 and CD28 antibodies in the presence of IL-2. At the early stages of stimulation, for instance, 12-hour post-stimulation, GABPα-knockout T cells showed similar kinetics of the induction of activation-associated molecules, CD69 and CD25 (Fig. 3-6a). However, these cells failed to further augment the expression of CD69 and CD25, as shown in the 36-hour time point (Fig. 3-6a). Disruption of GABPα prevented the cells from expanding their size as well (Fig. 3-6a). Additionally, GABPα-deficient T cells showed substantially diminished production of IL-2, which is a salient characteristic of activated effector T cells. In line with the activation defect, GABPα-deficient T cells did not undergo cell division in response to antigen stimulation (Fig. 3-6c). Together, these observations revealed an essential function of GABPα in control of T cell activation and antigen-stimulated proliferation.

We then sought to determine whether GABPα regulates the antigen-stimulated T cell responses *in vivo*. To this end, we infected *CD4^{Cre}Gabpa$^{f/f}$* mice and control littermates with a sublethal dose of *Listeria monocytogenes* expressing ovalbumin (OVA) as a model antigen (LM-OVA). Clearance of L. *monocytogenes* is mediated by T cells, among which CD8$^+$ T cells provide the most substantial contribution to protective immunity. An antigen-specific MHC class Ia-restricted T cell population reaches peak frequencies 7-8 days after inoculation. We measured the OVA-specific T cells in the spleen and liver, two major target organs of *L. monocytogenes*, at day 7 post infection. A substantial K^b-ova$^+$ CD8$^+$ T cell population was found in the WT mice, whereas this antigen-specific subset is barely detectable in the GABPα-deficient mice (Fig. 3-7), suggesting that GABPα is crucial for antigen-specific T cell proliferation *in vivo*.

Given that *CD4^{Cre}Gabpa$^{f/f}$* mice contained fewer CD8$^+$ T cells before the infection (Fig. 3-2f), we wanted to normalize the starting cell number and further assess the antigen-stimulated responses. We crossed the *Gabpa$^{f/f}$* mice to the OT-1 transgenic background to generate OVA-specific CD8$^+$ T cells (OT-1 cells), and subsequently bred the *Gabpa$^{f/f}$ OT-1* mice with mice carrying the *CD8-Cre* transgene. GABPα-deficient and –replete OT-1 cells were purified from cogenetically-marked mice (Fig. 3-8a), and transferred into the same recipients, which were challenged with LM-OVA 1 day after transfer. At day 3 post inoculation, a higher percentage of WT OT-1 cells underwent cell division than KO OT-1 cells (Fig. 3-8b and 8d), resulting in a larger population at day 7 post infection (Fig. 3-8c and 8e). Taken together, these observations demonstrate that GABPα has a cell-intrinsic role in promoting antigen-specific T responses to *L. monocytogenes* infection.
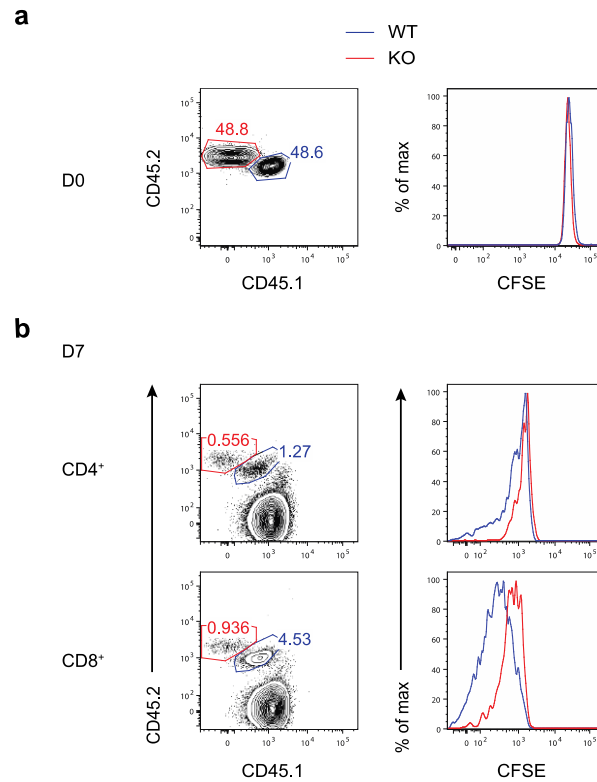
Figure 3-5: GABPα have a cell-intrinsic function in promoting T cell proliferation. CD4$^+$ or CD8$^+$ T cells from *Gabpa$^{f/f}$* (WT, CD45.1/CD45.2) and *CD4^{Cre}Gabpa$^{f/f}$* (KO, CD45.2/CD45.2) mice were mixed at a 1:1 ratio and transferred into Rag$^{-/-}$ or sublethally irradiated wild-type recipients (CD45.1/CD45.1). **a**, The WT and KO CD8$^+$ T cell populations before transfer. The staining of the cytosolic dye CFSE was comparable between WT and KO cells. **b**, Representative flow cytometric plots of transferred WT and KO cells in irradiated recipients at day 7 post transfer. Data represent at least three independent experiments.
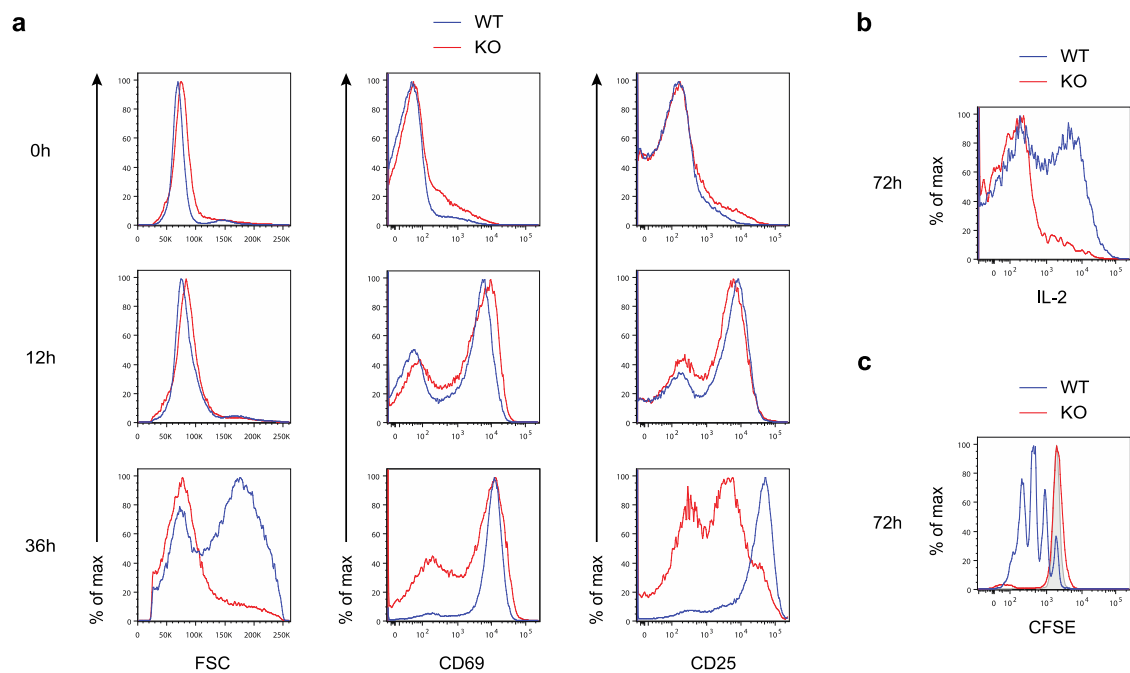
Figure 3-6: GABPα is required for antigen-stimulated activation and proliferation *in vitro*. Naive (CD62L^{hi} CD44^{lo}) CD4^{+} or CD8^{+} T cells from *Gabpa*[f/f] (WT) and *CD4*[Cre]*Gabpa*[f/f] (KO) mice were purified from flow cytometric sorting, and were subjected to anti-CD3 and CD28 stimulation in the presence of IL-2. Representative plots from CD8^{+} T cell culture were shown. **a**, Analysis of cell size (FSC) and activation markers, CD69 and CD25, at 0h, 12h and 36h post stimulation. **b**, 72h after cell culture, WT and KO cells were restimulated with PMA and ionomycin for 4h and analyzed for the expression of IL-2 by intracellular cytokine staining. **c**, WT and KO cells were labeled with the cytosolic dye CFSE, and cell division was assessed by the dilution of CFSE. Grey shaded line shows CFSE level of undivided cells. Data represent at least three independent experiments.
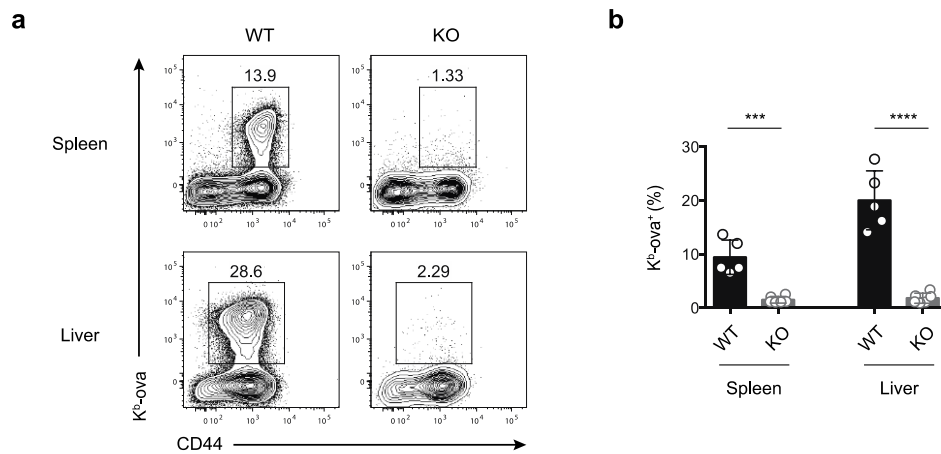
Figure 3-7: Defective antigen-specific T cell response in the absence of GABPα. *Gabpa*^{f/f} (WT) and *CD4*^{Cre}*Gabpa*^{f/f} (KO) mice were infected with 5×10^3 cfu of *L. Monocytogenes*-OVA. At Day 7-post infection, OVA-specific CD8$^+$ T cell responses were analyzed by the staining of K^b-ova tetramer. **a**, Representative flow cytometric blots of CD44 and K^b-ova staining in CD8$^+$ T cells from spleen and liver. **b**, Fractions of K^b-ova$^+$ T cells among the CD8$^+$ population. Data represent 5 mice per genotype analyzed in at least three independent experiments (mean $\pm$ SEM; unpaired *t*-test).
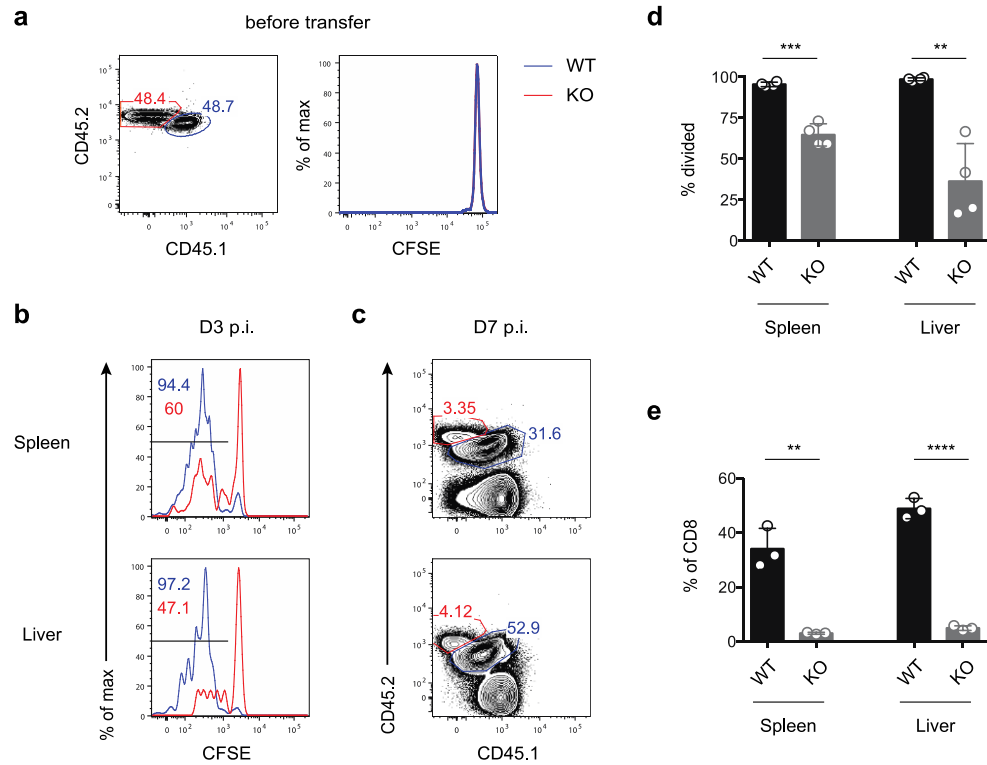
Figure 3-8: A cell-intrinsic role for GABPα in control of CD8$^+$ T cells responses to *L. monocytogene*s infection. OT-1 cells from *Gabpa$^{f/f}$ OT-1* (WT, CD45.1/CD45.2) and *CD8^{Cre}Gabpa$^{f/f}$ OT-1*   (KO, CD45.2/CD45.2) mice were mixed at a 1:1 ratio and transferred into wild-type recipients (CD45.1/CD45.1). The recipients were infected with LM-OVA a day after the cell transfer. **a**, The WT and KO OT-1 T cells before transfer. **b**, Dilution of CFSE at day 3 post infection. **c**, Representative flow cytometric plots of transferred WT and KO cells at day 7 after inoculation. **d**, Fractions of cells that have diluted CFSE at D3 p.i. **e**, Enumeration of WT and KO cells at D7 p.i. 4 mice (D3 p.i.) or 3 mice (D7 p.i.) were included. Data represented as mean $\pm$ SEM (unpaired *t*-test).

3.2.3 GABPα regulates cellular metabolism and cell cycle progression

To explore GABP-dependent molecular mechanisms in effector T cells, we performed microarray analysis to compare the transcriptome of WT and GABP-deficient T cells. Briefly, naive CD4$^+$ and CD8$^+$ T cells were purified from WT and *CD4^{Cre}Gabpa$^{f/f}$* mice. Half of the cells were subjected to TCR-stimulation *in vitro* for 18 hours, and the rest were untreated (considered as 0 hour). We compared the gene-expression profiles of WT and GABP-deficient T cells at both 0 hr (naive) and 18 hr (activated) time points, and looked for differentially expressed genes shared between CD4$^+$ and CD8$^+$ T cells. Comparison of data from WT and *CD4^{Cre}Gabpa$^{f/f}$* T cells revealed 112 and 84 genes downregulated or upregulated, respectively, by more than 1.5 fold and with a false discovery rate <0.05.

In order to identify direct transcriptional targets of GABP, we performed chromatin immunoprecipitation coupled to high-throughput sequencing (ChIP-seq) experiments with CD4$^+$ T cells from C57BL/6 mice. Using a cutoff of false discovery rate of 0.01, we identified 6825 genomic loci that were enriched in GABPα antibody pull down compared with the IgG control. Among the GABPα binding peaks, we could identify previously characterized binding sites of GABPα target genes, including the promoters of *Gabpa* and *Cox5b* (data not shown). GABPα binding sites were mostly enriched in the proximal promoter regions (Fig. 3-9a), and *de novo* motif prediction from the GABPα-binding peaks revealed a conserved GABPα recognition site that contains the GGAA core (Fig. 3-9b).

By cross-referencing the differentially expressed genes and the GABPα-bound genes, we identified 121 putative GABPα direct target genes, among which 92 and 39 were activated or repressed by GABPα, respectively. To gain insights into the general functional features of the GABPα regulated program, we analyzed the Gene Ontology and BioCarta pathway association of GABPα target genes. The putative GABPα direct target genes were strongly associated with cellular metabolic processes, vesicle transportation, mitochondrial biogenesis and function, stress responses, DNA replication, DNA repair, centrosome and cell cycle regulation, RNA processing, signal transduction and transcription (Fig. 3-9c).

Consistent with the critical regulation of GABPα in DNA replication and cell-cycle progression, GABPα-null T cells failed to incorporate EdU or enter the S phase upon TCR stimulation (Fig.3-10a). Among the DNA replication-associated genes regulated by GABPα include the minichromosome maintenance (Mcm) proteins (Fig. 3-9c, and 3-10b). Mcm family of proteins is composed of six related subunits, Mcm2-7, which are conversed in all eukaryotes (*276*). They form a hexameric complex that functions as a replicative helicase crucial for initiation and elongation of DNA replication (*277*). Expression of Mcm proteins was elevated in response to TCR stimulation, yet loss of GABPα impaired the induction of Mcms (Fig. 3-10c).

Additionally, inactivation of GABPα prevented the downregulation of p27^{kip1}, a negative regulator of cell cycle progression (Fig. 3-10c). Accumulation of p27^{kip1} in GABPα-deficient T cells also resulted in attenuated expression of cyclin E, which is induced at late G1 phase (Fig. 3-10c). Cyclin E, together with cyclin A and CDK2,

phosphorylates the retinoblastoma tumor suppressor (Rb), releasing the E2F transcription factor from the Rb-mediated inhibition, which is required for the transcription of S phase genes (*19*). Upon phosphorylation by the cyclin-CDK complexes, Rb could be subsequently degraded, which was prevented in GABPα-deficient T cells as well (Fig. 3-10c). In line with previous studies in fibroblasts (*264, 266*), expression of cyclin D and CDK6, the early S phase-associated molecules, were not affected by the disruption of GABPα (Fig. 3-10c). Together, these observations demonstrate that GABPα controls cell cycle progression by modulating Mcm- and p27-dependent pathways, rather than through the cyclin D/CDK6 axis.

Besides cell cycle progression, GABPα also functions as a critical regulator of cellular metabolism. Putative direct target genes of GABPα include genes encoding mitochondrial ribosomal proteins, *Mrpl16, Mrps35,* and essential components of electron transport chain and oxidative phosphorylation, such as *Ndufaf1, Idh3b* and *Ndufaf7* (Fig. 3-9c). In addition, GABPα target genes, *Romo1, Dera* and *Sdf2l1*, are involved in the modulation of reactive oxygen species (ROS) and endoplasmic reticulum (ER) stress responses (Fig. 3-9c). In agreement of the dysregulated cellular redox balance, GABPα-deficient T cells possessed heightened levels of both cellular and mitochondrial ROS, and were more prone to cell death in response to TCR stimulation (Fig.3-11).

Intriguingly, the expression of IL-7Rα was not defective in GABPα-deficient T cells in the peripheral (Fig.3-12a). In the ChIP-seq experiments, no GABPα-binding sites were found in *Il7r* gene locus or the regulatory elements (Fig.3-12b).
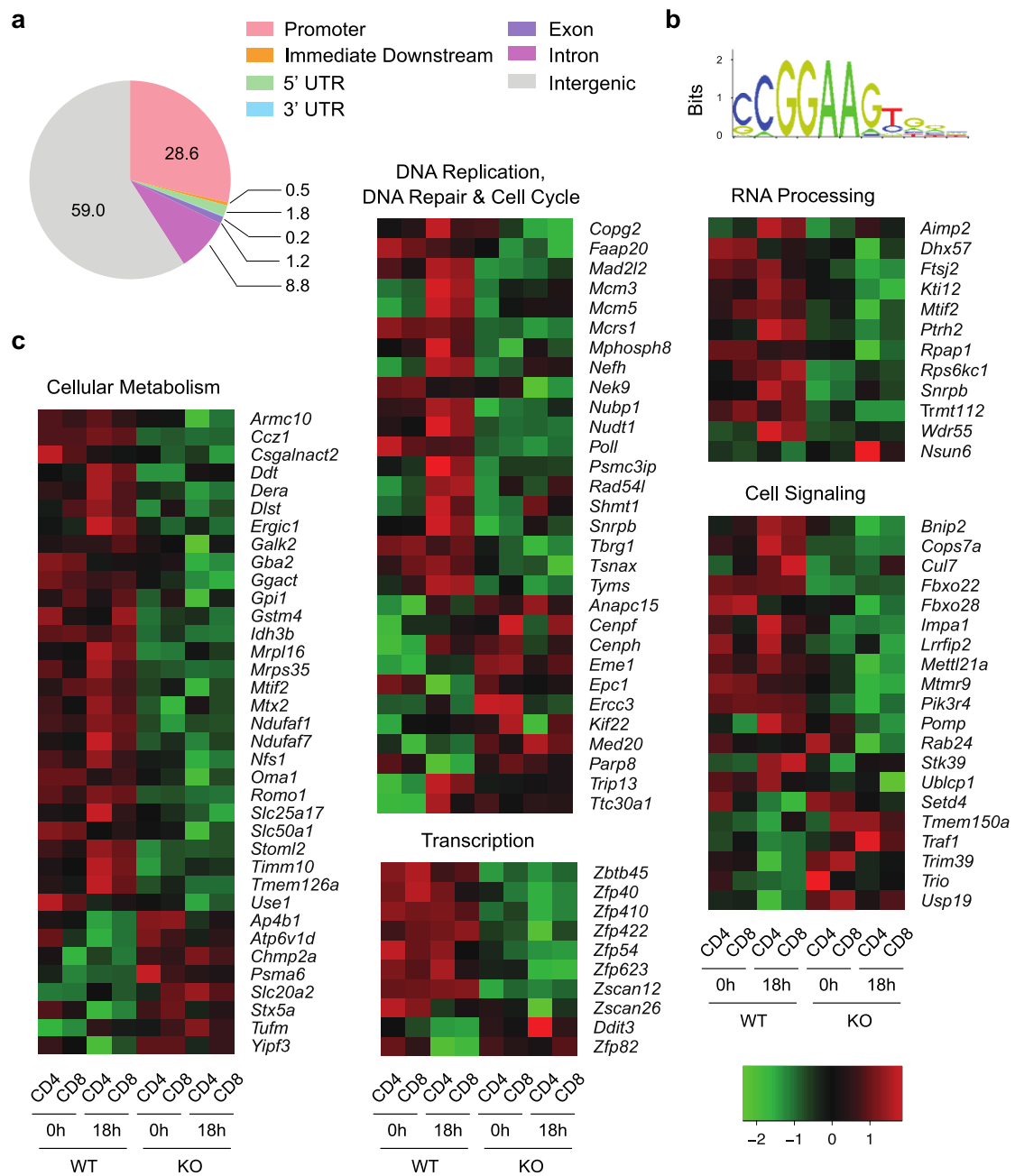
Figure 3-9: GABPα-dependent transcriptional program in T cells. a, Pie chart of distribution of GABPα binding peaks discovered from ChIP-seq. **b**, The consensus sequence motif identified in the GABPα binding sites by the MEME program. **c**, Heatmap of GABPα bound target genes differentially expressed between wild-type and GABPα-deficient CD4 and CD8 T cells.
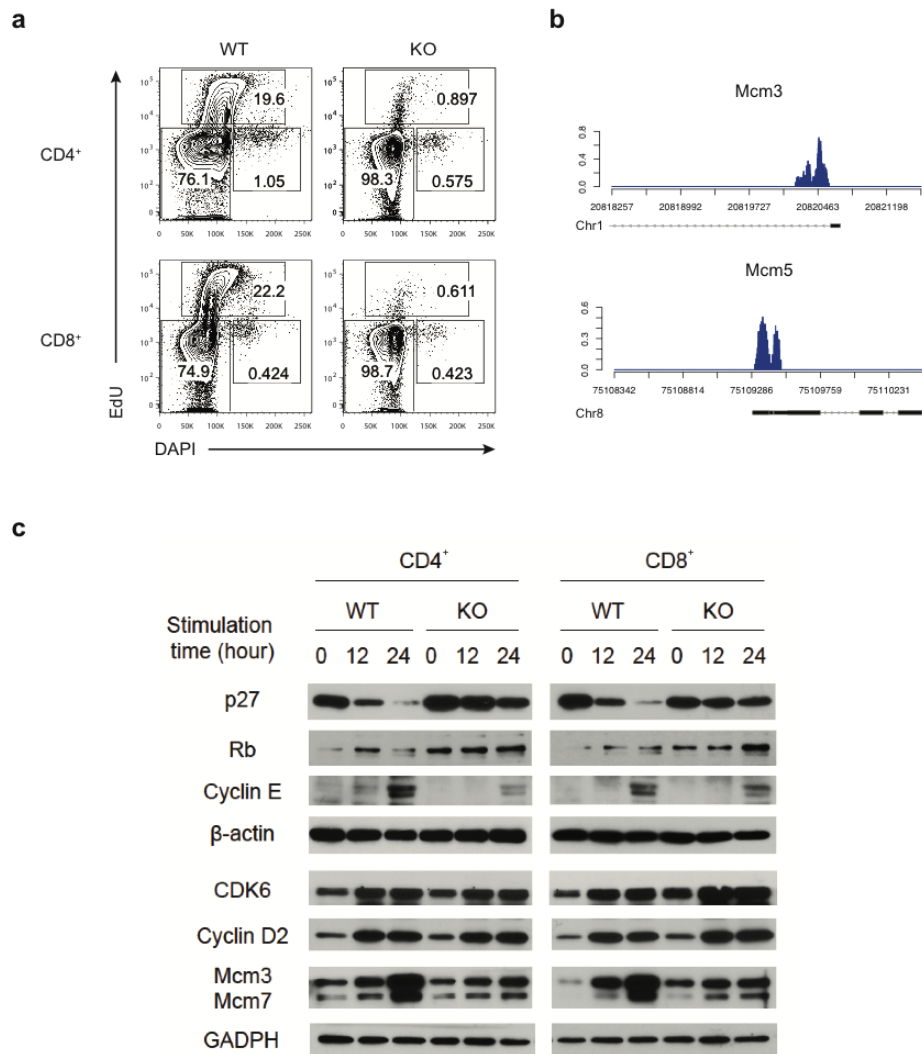
Figure 3-10: GABPα regulates DNA replication and cell-cycle progression. a, Naive (CD62L^{hi} CD44^{lo}) CD4$^+$ or CD8$^+$ T cells from *Gabpa$^{f/f}$* (WT) and *CD4^{Cre}Gabpa$^{f/f}$* (KO) mice were purified from flow cytometric sorting, and were subjected to anti-CD3 and CD28 stimulation in the presence of IL-2. After 22 hr, cells were pulsed with EdU for 2 hr. **b**, GABPα-bound regions in the *Mcm3* and *Mcm5* gene loci. **b**, Expression of Cyclin D, Cyclin E, CDK6, p27, Rb, Mcm3 and Mcm7 in CD4$^+$ or CD8$^+$ stimulated with α-CD3 and CD28.
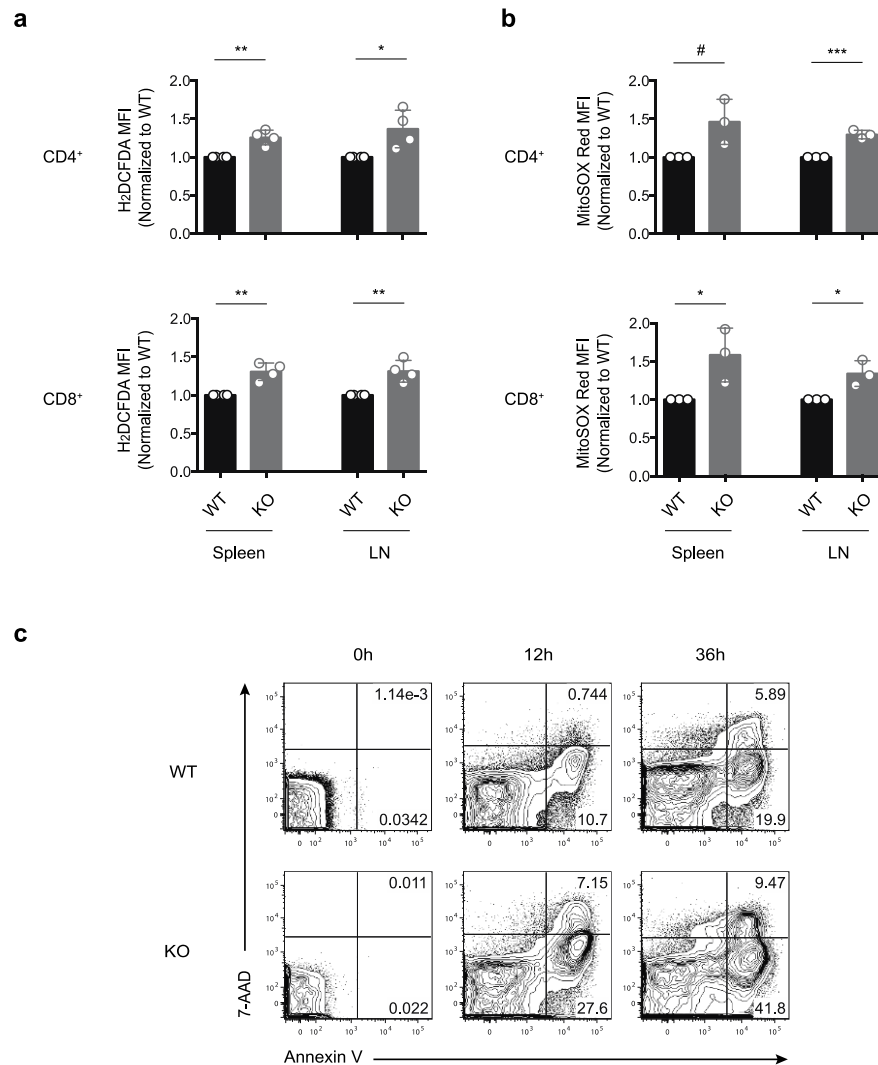
Figure 3-11: GABPα maintains cellular redox homeostasis. a-b, CD4^{+} or CD8^{+} T cells from spleen and lymph nodes (LN) of *Gabpa^{f/f}* (WT) and *CD4^{Cre}Gabpa^{f/f}* (KO) mice were analyzed. **a**, Ex vivo analysis of cellular ROS level by H_2DCFDA staining. **b**, Ex vivo analysis of mitochondrial ROS level by MitoSOX Red staining. **c**, Naive (CD62L^{hi}CD44^{lo}) CD4^{+} or CD8^{+} T cells from WT and KO mice were purified and were subjected to anti-CD3 and CD28 stimulation in the presence of IL-2. Cell death was assessed with Annexin V and 7-AAD staining. Representative plots from CD8^{+} T cell culture were shown.
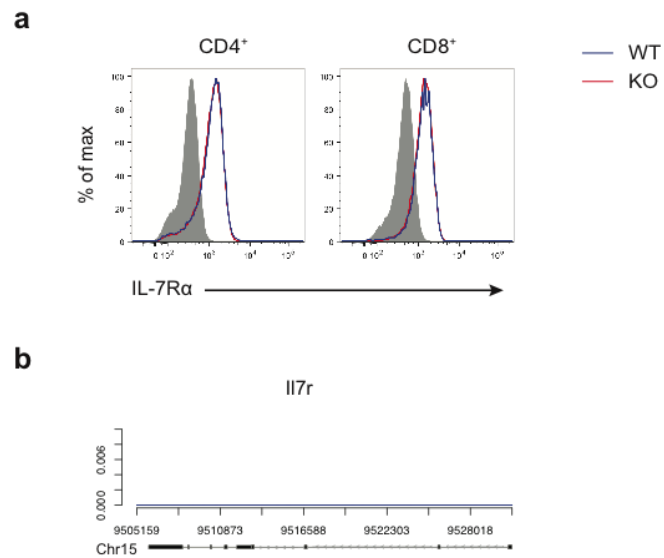
Figure 3-12: GABPα is dispensable for IL-7Rα expression in mature T cells. a, Flow cytometric analysis of IL-7Rα in CD4$^+$Foxp3$^-$ conventional CD4$^+$ and CD8$^+$ T cells from lymph nodes of *Gabpa$^{f/f}$* (WT) and *CD4^{Cre}Gabpa$^{f/f}$* (KO) mice **b**, Reads of GABPα ChIP-seq in *Il7r* gene locus.

3.2.4 GABPα is indispensible for Treg homeostasis and function

Considering the pivotal roles GABP play in antigen-stimulated responses in T cells and the strong TCR stimulation Tregs receive, we proceeded to evaluate the Treg phenotypes in $CD4^{Cre}Gabpa^{f/f}$ mice. The frequency and number of thymic Tregs in $CD4^{Cre}Gabpa^{f/f}$ mice were substantially reduced in comparison to littermate controls (Fig.3-13a and 13b). In addition, peripheral Treg populations were also diminished (Fig.3-13c and 13d), suggesting an important function of GABP in Treg development and/or maintenance.

To investigate the role of GABP in Tregs, we crossed $Gabpa^{fl/fl}$ mice to the $Foxp3^{Cre}$ mice. GABPα protein was barely detectable in Tregs from $Foxp3^{Cre}Gabp^{fl/fl}$ mice, whereas conventional $CD4^+$ T cells expressed comparable amount of GABPα protein to the wild-type counterpart (Fig. 3-14a). By 8 weeks of age, all mice with Treg-specific ablation of GABPα succumbed to a lymphoproliferative disorder (Fig. 3-14b), manifested by enlarged spleens and lymph nodes (Fig. 3-14d). In addition, sick $Foxp3^{Cre}Gabp^{fl/f}$ mice exhibited a hunched posture, scaly skin of ears and tails (Fig. 3-14c), and had massive lymphocytic and mononuclear infiltrates in multiple organs including lung, liver, stomach and colon (Fig. 3-14e). These phenotypes are reminiscent of those observed in mice carrying the scurfy mutation of *Foxp3* gene (*278*), indicating a loss of suppressive function in the remaining Tregs of $Foxp3^{Cre}Gabp^{fl/fl}$ mice.

The severe immunopathology in Treg-specific GABPα-deficient mice was associated with the expansion and activation of peripheral T cells (Fig, 3-15). Analysis of cytokine production by $CD4^+$ T cells from $Foxp3^{Cre}Gabp^{fl/f}$ mice showed a notable

increase in the numbers of CD4$^+$Foxp3$^-$ cells producing Th2 cytokines IL-4, IL-5 and IL-13, as well as Th1 cytokine IFN-γ (Fig. 3-16a and 16b). Consistent with the notion that IL-4 promotes IgG1 and IgE class-switch recombination, and IL-5 augments the production of IgA, sera from *Foxp3^{Cre}Gabp$^{fl/fl}$* mice contained dramatically increased amounts of IgG1, IgE and IgA (Fig. 3-16c). However, serum concentrations of IgG2a and IgG3, which are positively regulated by IFN-γ and are inhibited by IL-4, were not markedly affected (Fig. 3-16c), suggesting a predominant Th2 response in the mice.

In line with the impaired antigen-stimulated responses observed in GABPα-deficient conventional T cells, Tregs in the peripheral non-lymphoid organs, including lung and liver, were severely diminished (Fig. 3-17). Nevertheless, Tregs in the lymph node, which predominately exhibited a resting phenotype, were minimally affected (Fig. 3-17).
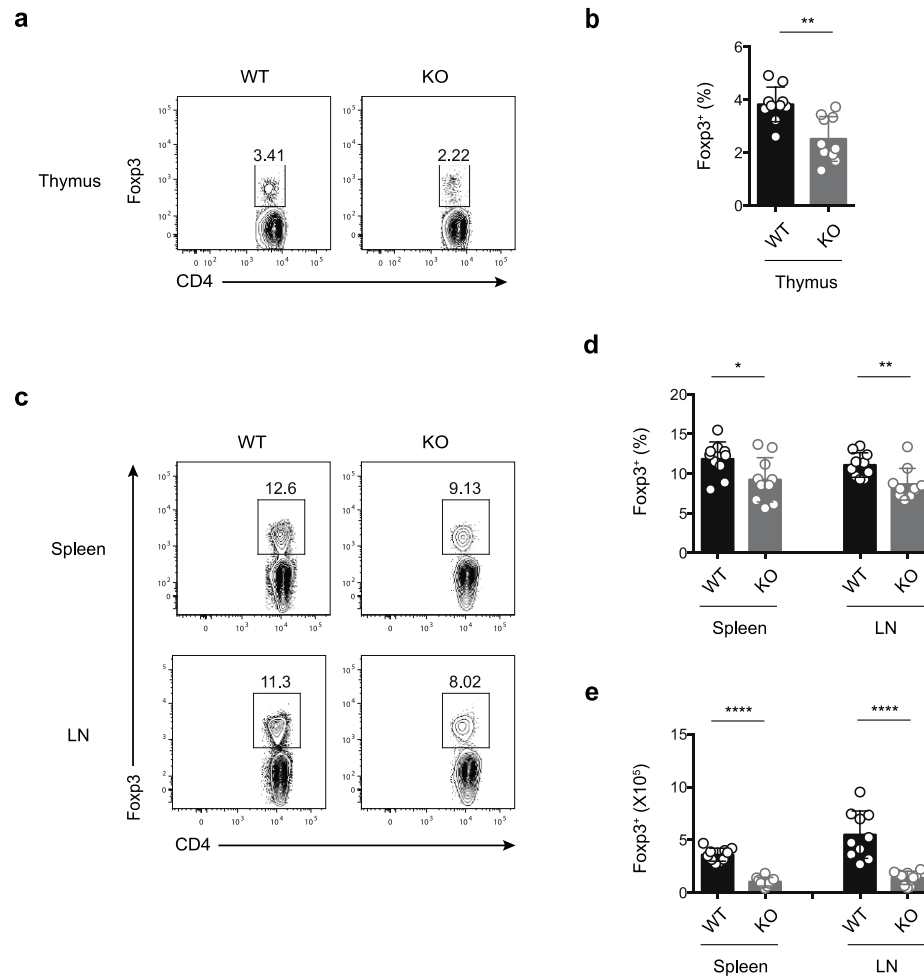
Figure 3-13: Mice with T cell-specific depletion of GABPα show reduced Tregs. a, **c**, Flow cytometric analysis of Foxp3^{+} cells within thymic CD4SP cells (**a**), and TCRβ^{+}CD4^{+} cells from the spleen and lymph nodes (LN) (**c**) of *CD4-CreGabp^{fl/fl}* mice and littermate controls. **d**, **e**, Percentages of Foxp3^{+} cells within thymic CD4SP cells (**b**), and TCRβ^{+}CD4^{+} cells from the spleen and LN (**d**). Mice of 5-8 week-old were used. Data represent 10 mice per genotype analyzed in at least three independent experiments (mean ±SEM; unpaired *t*-test).
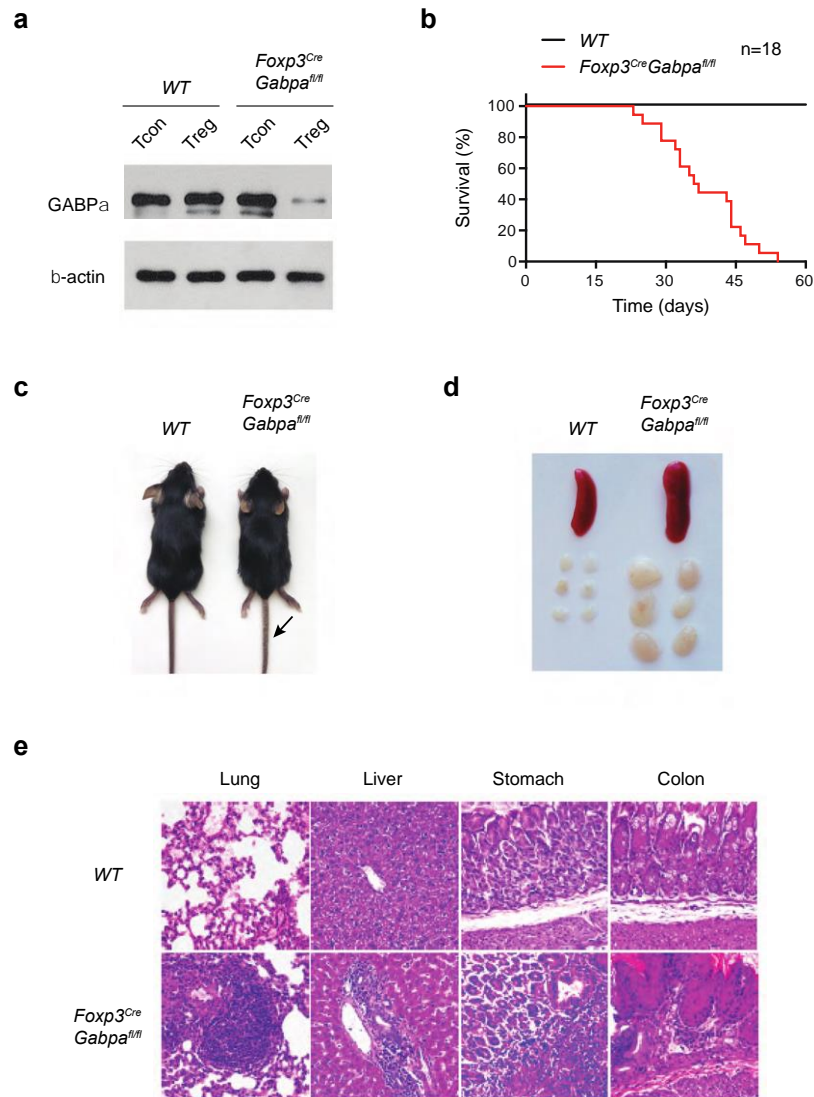
Figure 3-14: Depletion of GABPα in Tregs results in an aggressive autoimmune syndrome. a, GABPα protein in CD4^{+} Foxp3^{-} conventional T (Tcon) and Tregs of wild-type (WT) and *Foxp3^{Cre}Gabp$^{fl/fl}$* mice was determined by immunoblotting. **b**, Survival of *WT* and *Foxp3^{Cre}Gabp$^{fl/fl}$* mice. **c**, Images of 3-week-old *WT* and *Foxp3^{Cre}Gabp$^{fl/fl}$* mice. **d**, A representative picture of spleens and lymph nodes from 3-week-old *WT* and *Foxp3^{Cre}Gabp$^{fl/fl}$* mice. **e**, Hematoxylin and eosin staining of sections from lungs, livers, stomachs and colons of 3-week-old *WT* and *Foxp3^{Cre}Gabp$^{fl/fl}$* mice. Original magnification, ×20.

a

b

CD4⁺

WT   Foxp3^Cre Gabpa^fl/fl

CD8⁺

WT   Foxp3^Cre Gabpa^fl/fl
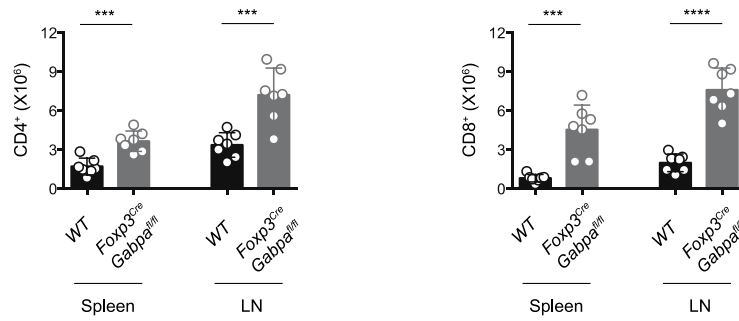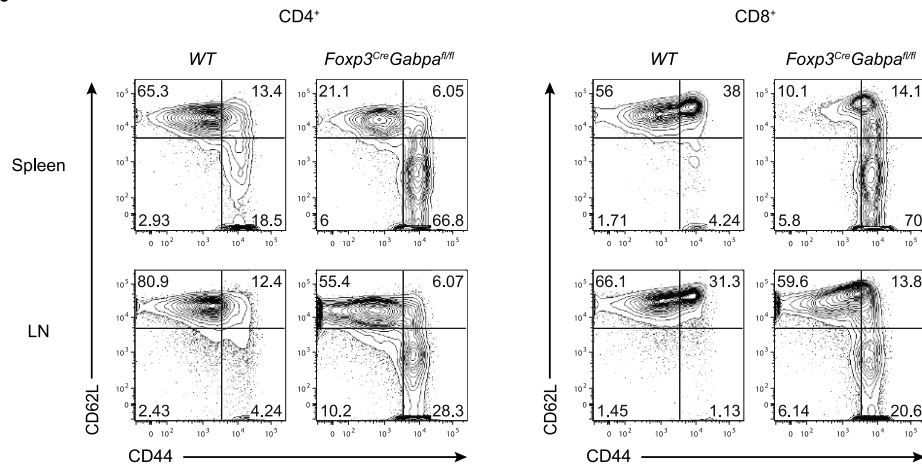
Figure 3-15: Expansion and hyper-activation of conventional T cells in *Foxp3^Cre Gabp^fl/fl* **mice. a,** CD4⁺ and CD8⁺ T cell-number from spleens and lymph nodes (axillary, brachial, inguinal) of 3-week-old *WT* and *Foxp3^Cre Gabp^fl/fl* mice. **b,** Flow cytometric analysis of CD44 and CD62L expression in CD4⁺ and CD8⁺ T cells from spleen and LNs of 3-week-old *WT* and *Foxp3^Cre Gabp^fl/fl* mice. Data represent 7 mice per genotype analyzed in at least three independent experiments (mean ± SEM; unpaired *t*-test).
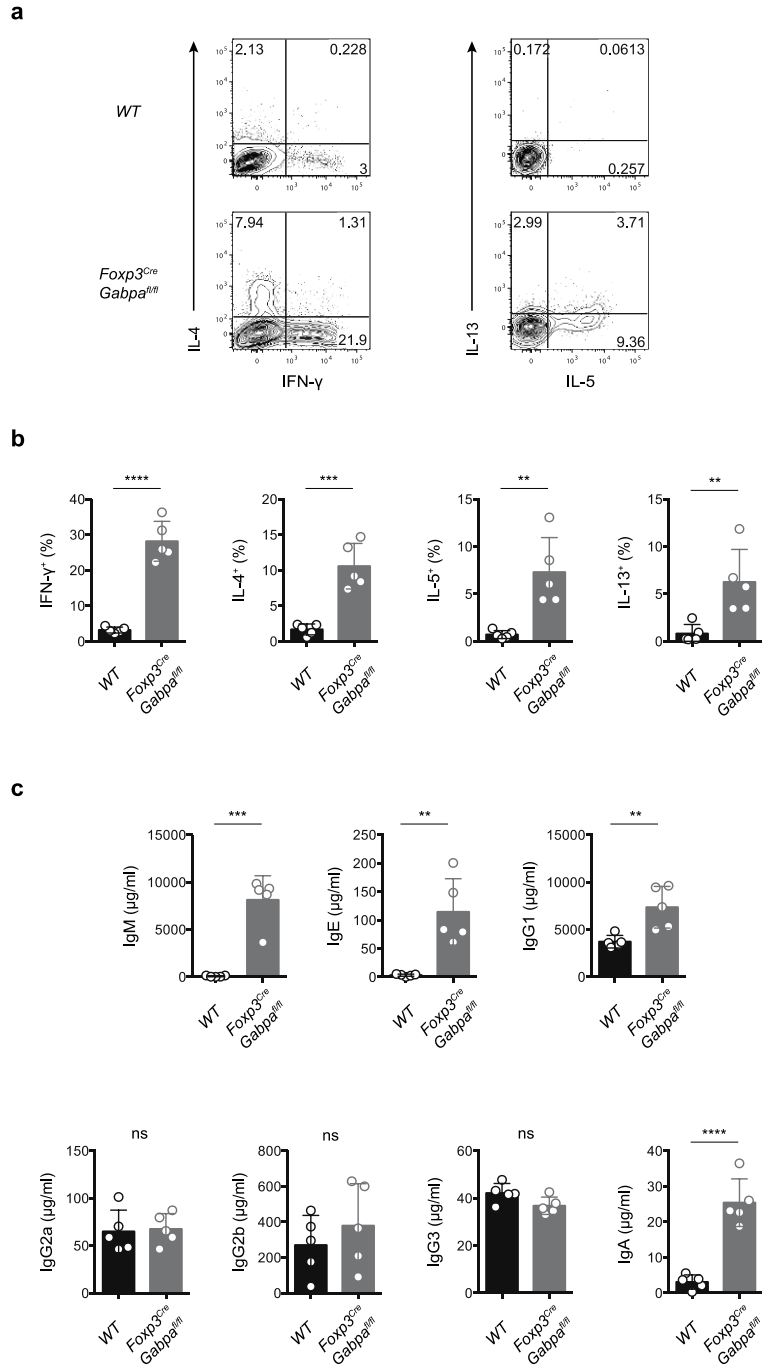
Figure 3-16: GABPα deficiency in Tregs leads to increased inflammatory cytokine production and augmented serum immunoglobulin levels. a, CD4$^+$ T cells isolated from the spleens of *WT* and *Foxp3^{Cre}Gabp$^{fl/fl}$* mice were stimulated with PMA and ionomycin for 4 hours and analyzed for the expression of IFN-γ, IL-4, IL-5, and IL-13 by intracellular staining. **b**, Percentage of cytokine-producing cells in total CD4$^+$Foxp3$^-$ Tcon cells. **c**, Analysis of immunoglobulin isotype amounts in sera of 3-week-old *WT* and *Foxp3^{Cre}Gabp$^{fl/fl}$* mice. Data represent 5 mice per genotype analyzed in at least three independent experiments (mean ± SEM; unpaired *t*-test).

a

b
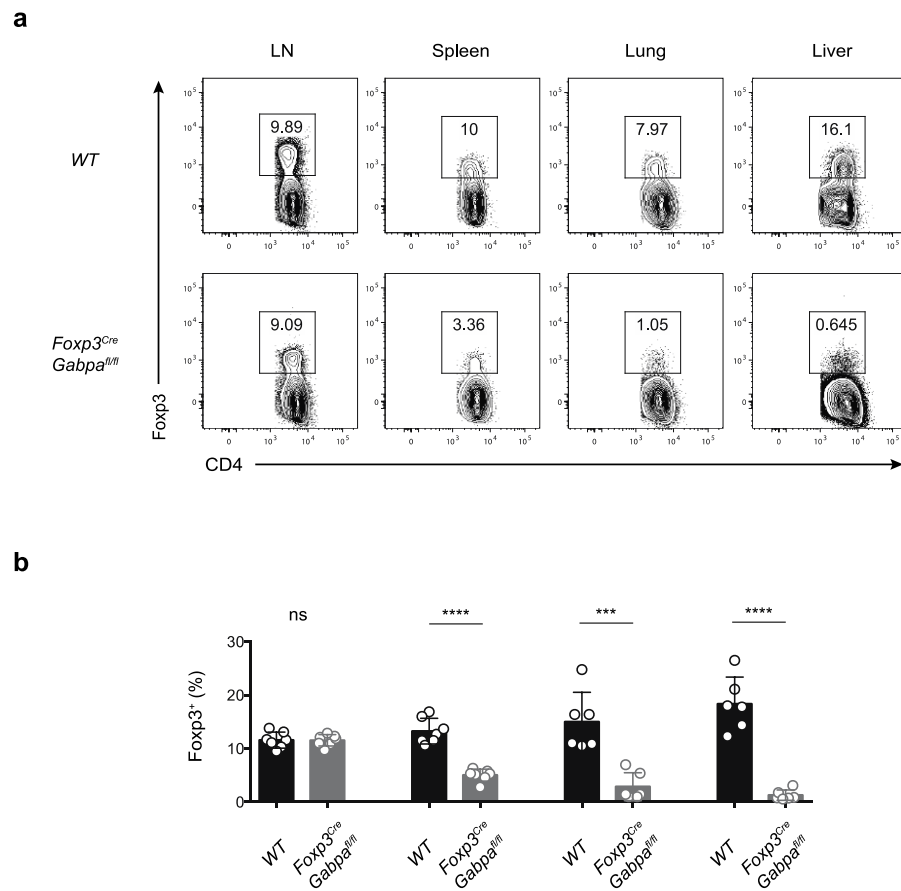
Figure 3-17: Effector-phenotype Tregs are preferentially affected by the loss of GABPα. Flow cytometric analysis (**a**), and quantification (**b**) of Tregs in CD4$^+$ T cells from spleen, lymph nodes, lung and liver of 3-week-old *WT* and *Foxp3^{Cre}Gabp$^{fl/fl}$* mice. Data represent 7 mice per genotype analyzed in at least three independent experiments (mean $\pm$ SEM; unpaired *t*-test).

3.3 Discussion

GABP has been shown to regulate early T cell development, in part, through modulating the expression of IL-7Rα (*263, 274*), yet its function in mature T cells has not been studied. Using a conditional knockout system that initiates depletion of *Gabpa* gene in DN thymocytes, we found that GABP was not essential for positive selection of CD4^{+} and CD8^{+} T cells, but was required for peripheral T cells homeostasis. GABPα deficiency led to diminished pool of CD4^{+} and CD8^{+} T cells in secondary lymphoid organs, with activated-memory phenotype T cells most severely affected. In response to antigen stimulation *in vitro*, GABPα-deficient T cells showed compromised proliferation, elevated reactive oxygen species levels, and impaired cell survival. In addition, mice lacking GABPα failed to mount an antigen-specific T cell response to *Listeria Monocytogenes* infection. Transcriptome analysis coupled with ChIP-seq identified GABPα as a key regulator of the DNA replication, cell cycle progression as well as cellular redox homeostasis. Collectively, these observations revealed a pivotal role GABPα in the control of TCR-stimulated metabolic reprogramming.

An interesting finding of this study was that the IL-7Rα chain was not differentially expressed in GABPα-deficient mature T cells compared with wild-type controls, nor was GABPα recruited to the gene locus of *Il7r*. GABPα was initially identified as a regulator of *Il7r* by motif analysis (*263*). GABPα interacted with the GGAA motif in the promoter region of *Il7r* gene in electrophoretic mobility shift assays (EMSA), and it induced the luciferase reporter activity in overexpression systems. IL-7Rα expression was completely abolished in embryonic thymocytes from *Gabpa[tp/tp]* mice

(*263*). In a later study using the *Lck-Cre Gabpa^{f/f}* mice, thymocytes development was blocked at the DN3 stage, yet the DN3 thymocytes didn't show any defect in IL-7Rα expression. Nevertheless, IL-7Rα expression was partially diminished in the DN4 cells (*274*). These observations raise the possibility that the requirement of GABPα in *Il7r* gene transcription becomes less stringent as T cell matures. One possible explanation could be the redundancy among the large family of Ets proteins. Indeed, genome-wide chromatin immunoprecipitation experiments revealed co-occupancy of the same genomic regions by multiple Ets proteins, in addition to the specific binding sites for each Ets protein (*279, 280*). An alternative explanation is that developing thymocytes and mature T cells require distinct transcriptional machineries for *Il7r* gene expression. Transcription factors including Foxo1 and Gfi-1 have been shown to regulate IL-7Rα expression under different conditions. The functional interaction between GABPα and these transcription factors awaits further investigation.

Intriguingly, the majority of GABPα-dependent transcriptional program is associated with fundamental cellular processes, including cell cycle progression, mitochondrial biogenesis and redox regulation. However, barely any putative GABPα targets are involved in T cell-specific responses, such as helper T cell or cytotoxic T cell differentiation, inflammatory cytokine production or chemoattractant receptor expression. Earlier studies revealed that GABPα was recruited to a distal enhancer of *Il2* locus, and TCR stimulation augmented GABPα-mediated IL-2 transcription (*281, 282*). However, we didn't find noticeable GABPα binding peaks in the enhancer or other regions of *Il2* gene. This might be attributed to differential levels of GABPα expression in the

experimental systems – we used wild-type T cells that contained much lower amounts of GABPα than the overexpression systems used in previous studies.

GABPα is indispensible for mature T cell proliferation in response to antigen stimulation. Cell cycle defects caused by loss of GABPα have been shown in mouse embryonic fibroblasts and a human liver carcinoma cell line (*264, 266, 273*). Consistent with these studies, our work reveals that GABPα doesn't impact the expression of D-type cyclins. Instead, it negatively regulates the CDK inhibitor p27[kip1] by promoting S-phase kinase-associated protein (Skp2) expression, which is an E3 ligase that controls the ubiquitination and degradation of p27[kip1] and p21[cip1] (*283*). However, other GABPα target genes discovered in these studies, such as the serine/threonine kinase KIS and the Hippo pathway effector molecule YAP, were not directly regulated by GABPα in mature T cells, which again could be explained by the different context-dependent regulation.

We also uncovered novel GABPα targets that are crucial for DNA replication and cell cycle progression, including *Mcm* genes and *Shmt1*. *Shmt1* encodes the cytoplasmic serine hydroxymethyltransferase, which functions in the folate-mediated one-carbon metabolism together with another well-established GABPα target, thymidylate synthase (Tyms) (*284*). One carbon metabolism is a metabolic network of interdependent pathways that occur in three cellular compartments: the cytoplasm, mitochondria, and nucleus (*285*). It is required for the *de novo* synthesis of purines and thymidylate, the remethylation of homocysteine to methionine and the interconversion of serine and glycine (*285*). Our present study, for the first time, describes the dysregulation of folate-dependent one-carbon metabolism in T lymphocytes and the functional consequences.

An interesting and somewhat surprising observation we made was that T cells in $CD4^{Cre}Gabpa^{f/f}$ mice expressed comparable levels of the proliferation marker Ki67 as that of littermate controls. Preliminary EdU incorporation in young $CD4^{Cre}Gabpa^{f/f}$ and control mice also revealed similar rates of T cell proliferation (data not shown). These findings suggest that GABPα-deficient T cells meet their biosynthetic demands necessary for proliferation under homeostatic condition *in vivo*. Indeed, different molecular mechanisms of lymphopenia-induced homeostatic proliferation versus antigen-driven proliferation have been described. IL-7R signaling together with weak TCR stimulation is required for homeostatic expansion, whereas strong TCR signaling triggers antigen-activated proliferation (*286, 287*). The intact homeostatic proliferation observed in $CD4^{Cre}Gabpa^{f/f}$ mice is consistent with the unperturbed IL-7Rα expression mentioned above. Moreover, the folate-mediated one-carbon metabolism was recently recognized to be an important source of NADPH to maintain redox balance and methyl groups for methylation, in addition to its long appreciated roles in nucleic acid biogenesis (*288*). Studies on tumors revealed that the one-carbon pathway has a vital function in cell proliferation and survival under harsh environmental conditions, such as nutrient scarcity and hypoxia (*289, 290*). During infection or strong antigen-stimulation, T cells might also experience nutrient-depleted or hypoxic environments (*291*), thereby necessitating GABPα-regulated one-carbon metabolism that is not required under homeostatic conditions.

In addition to the proteins involved in folate-dependent one carbon pathway, numerous other GABPα-targets contribute to cellular redox regulation and responses to ER stress. GABPα-deficient T cells contained elevated levels of total cellular ROS and

mitochondrial ROS, which was associated with augmented cell death. It remains to be investigated whether treating the cells with anti-oxidant reagents could correct the defects observed in GABPα-null T cells.

A number of Ets proteins, including the Ets and Tcf subfamilies, have been shown to be modulated by the Ras-MAPK pathway (*244*). An early study using a human T cell line revealed that activation of MAPK pathway by PMA and ionomycin treatment led to phosphorylation of GABP, which was correlated with enhanced transcriptional activity of the IL-2 distal enhancer (*282*). However, we didn't find GABPα-binding peaks in this *Il2* enhancer region in our ChIP-seq with total CD4$^+$ T cells. Future ChIP-seq experiments using activated T cells will determine if GABPα is recruited in response to TCR stimulation. Furthermore, whether TCR-induced signaling results in posttranslational modifications in GABPα and/or GABPβ, and whether that alters their subcellular localization, protein stability and transcriptional activity remain to be explored.

Depletion of GABPα in Tregs resulted in a fatal lymphoproliferative disease with a predominant type 2 response. The disease phenotype was reminiscent of that developed in Treg-specific IRF4-deficient mice (*206*). IRF-4 together with Blimp-1 regulates the differentiation and function of an effector Treg population that produces IL-10 (*207*). Future work will examine whether GABPα-null Tregs are capable of producing IL-10, and how GABPα-dependent transcriptional program in Tregs exerts selective control of type 2 effector T cell responses.

3.4 Experimental procedures

Mice

The *GABPa^{f/f}* mouse strain was kindly provided by Dr. Steve Burden (New York University) (*265*). The *CD4-Cre*, *Foxp3^{Cre}* and OT-1 transgenic mice were described previously (*157, 162, 172*). *CD8-Cre* (*292*) and CD45.1^{+} mice were purchased from Jackson Laboratory. In all experiments, littermate controls were used when possible. Both male and female mice were included. All mice were maintained under specific pathogen-free conditions, and animal experimentation was conducted in accordance with procedures approved by the Institutional Animal Care and Use Committee of Memorial Sloan Kettering Cancer Center.

Listeria monocytogenes infection

For the study of primary immune response, mice were intravenously infected with 5×10^3 colony-forming units (cfu) of *Listeria monocytogenes* expressing ovalbumin (LM-OVA), and spleens and livers were isolated for analysis 7 days after infection. For OT-1 transfer experiments, mice that had received OT-1 cells were intravenously infected with 1×10^5 cfu of LM-OVA 1 day after the adoptive T cell transfer. Spleens and livers of the infected mice were analyzed 3 days and 7 days post infection.

Adoptive transfer of T cells

CD4$^+$ or CD8$^+$ T cells from *Gabpa$^{f/f}$* (WT, CD45.1/CD45.2) and *CD4^{Cre}Gabpa$^{f/f}$* (KO, CD45.2/CD45.2) mice were purified by flow cytometric sorting (BD Aria 2), mixed at a 1:1 ratio, stained with CFSE (5μM final concentration at room temperature for 5 minutes), and transferred into Rag$^{-/-}$ or sublethally irradiated wild-type recipients (CD45.1/CD45.1) via intravenous injection. A total number of 2×10^6 cells were transferred into each recipient. Spleen and lymph nodes were analyzed 7 days after transfer.

For OT-1 transfer experiment: OT-1 cells from *Gabpa$^{f/f}$ OT-1* (WT, CD45.1/CD45.2) and *CD8^{Cre}Gabpa$^{f/f}$ OT-1* (KO, CD45.2/CD45.2) mice were purified by flow cytometric sorting (BD Aria 2), mixed at a 1:1 ratio, stained with CFSE (5μM final concentration), and intravenously transferred into wild-type recipients (CD45.1/CD45.1). A total number of 1.5×10^5 OT-1 cells were transferred (7.5×10^4 per genotype).

Cell isolation

After whole-body perfusion with 50 ml of heparinized PBS, lymphocytes were isolated as follows. Single-cell suspensions were prepared from spleens and peripheral (axillary, brachial, and inguinal) lymph nodes by tissue disruption with glass slides. To isolate cells from the liver and lung, tissues were finely minced and digested with 1 mg/ml Collagenase D (Worthington) for 30 min at 37 ℃. After the digestion, cells were

filtered through 70-μM cell strainer, layered in a 44% and 66% Percoll gradient (Sigma), and centrifuged at 3000 rpm for 30 min without brake. Cells at the interface were collected and analyzed by flow cytometry.

Flow cytometry

Flurochrome-conjugated, biotinylated antibodies against CD45.1 (clone 104), CD45.2 (A20), TCR-β (H57-595), CD4 (RM4-5), CD8 (17A2), CD25 (PC61.5), CD44 (IM7), CD62L (MEL-14), CD69 (H1.2F3), IL-7Rα (A7R34), Foxp3 (FJK-16s), IFN-γ (XMG1.2), IL-2 (JES605H4), IL-4 (11B11), IL-13 (eBio13A), Ki67 (MOPC-21) were purchased from eBiocience. Antibody against IL-5 (TRFK5) was purchased from BD Biosciences. All antibodies were tested with their respective isotype controls. Cell surface staining was performed by incubating cells with specific antibodies for 30 min on ice in the presence of 2.4G2 mAb to block FcγR binding. Foxp3, Ki67, IFN-γ, IL-2, IL-4, IL-5, IL-13 staining was carried out using the intracellular transcription factor or cytokine staining kits from Tonbo or BD Biosciences. To determine cytokine expression, isolated cells were stimulated with 50 ng/ml phorbol 12-myristate 13-acetate (Sigma), 1 mM ionomycin (Sigma) and GolgiStop (BD Biosciences) for 4 h prior to staining. K^b-ova tetramer staining. Apoptotic cell death staining was performed with Annexin V staining kit (BD) according the manufacturer's instructions. Mitochondrial mass, cellular reactive oxygen species (ROS) and mitochondrial ROS levels were determined by MitoTracker Green, 2',7'-dichlorodihydrofluorescein diacetate (H2DCFDA) and MitoSOX Red staining, respectively (ThermoFisher). Incorporation of EdU was measured using the

Click-iT EdU flow cytometry assay kit (Invitrogen). For all stains, dead cells were excluded from analysis by means of Live/Dead Fixable Dye (Invitrogen), DAPI or propidium iodide (PI) stain. All samples were acquired and analyzed with LSRII flow cytometer (Becton Dickson) and FlowJo software (TreeStar).

In vitro T cell culture

Naive (CD25$^-$CD62L^{hi}CD44^{lo}) CD4$^+$ and CD8$^+$ T cells were purified from spleen and lymph nodes of *Gabpa$^{f/f}$* (WT) and *CD4^{Cre}Gabpa$^{f/f}$* (KO) mice by flow cytometry sorting (BD FACS Aria). Sorted T cells were cultured with plate bound α-CD3 (coated overnight, 5μg/mL), soluble α-CD28 (2μg/mL) and IL-2 (100U/mL) for indicated time periods. For EdU incorporation experiments, the cells stimulated with were α-CD3/28 and IL-2 for 22 hours and EdU (10 μM) was added into the culture for 2 hours.

Gene-expression profiling

Naive (CD25$^-$CD62L^{hi}CD44^{lo}) CD4$^+$ and CD8$^+$ T cells were purified from spleen and lymph nodes of *Gabpa$^{f/f}$* (WT) and *CD4^{Cre}Gabpa$^{f/f}$* (KO) mice by FACS sorting. Extract RNA from half of the sorted naive cells, which was considered as 0h time point. The other half of cells was subject to the α-CD3/28 and IL-2 stimulation for 18 hours before cell lysis using QIAZol reagent (Qiagen). RNA extraction was prepared with the miRNeasy Mini Kit according to the manufacturer's instructions (Qiagen). Two rounds of RNA amplification, labeling, and hybridization to M430 2.0 chips (Affymetrix) were

carried out at the Genomics Core of Memorial Sloan Kettering Cancer Center. All data analyses were done with R Console. The genes with 1.5 fold or more change of expression, and adjusted p value smaller than 0.05 were considered as GABPα-dependent genes.

Chromatin Immunoprecipitation

CD4+ T cells of wild-type mice were purified by MACS beads (Miltenyi) and fixed for 10 minutes at room temperature with 10% formaldehyde. Glycine was added to a final concentration of 0.125M to quench the formaldehyde. Cells were pelleted, washed twice and ice-cold PBS and lysed with hypotonic lysis buffer. Chromatin was sheared with Bioruptor sonicator (Diagenode) to 200-500 base pairs (bp) in length. The prepared chromatin was incubated with 5μg anti-GABPα (sc-22810 X, Santa Cruz) or control rabbit immunoglobulin (2729, Cell Signaling) overnight. Immune complexes were washed, and eluted. Precipitated DNA ChIP DNA and input DNA were incubated at 65°C to reverse the crosslinking. After digestion with RNase and proteinase K, the ChIP and input DNA were purified with phenol/chloroform extraction and ethanol precipitation. The purified DNA was repaired, ligated with adaptor, and amplified by PCR for 15-20 cycles. The amplified DNA was size selected by gel extraction and used for sequencing. Paired ends 36bp sequencing was performed at the Genomics Core of Memorial Sloan Kettering Cancer Center using HiSeq (Illumina). Reads were first processed with Trimmomatic to remove the adaptor sequences and bases with quality scores below 20, and reads with less than 30 remaining bases were discarded (*293*). Trimmed reads were

then aligned to mm10 mouse genome with the bowtie aligner (*238*). GABP peaks were called using MACS2 using q value cut-off 0.01 (*294*). The distribution of the peaks around the TSS was calculated using the ChIPpeakAnno package (*295*). DNA motif analysis was performed with the MEME software suite.

Enzyme-linked immunosorbent assay (ELISA)

The serum immunoglobulins in *Gabpa*$^{f/f}$ and *Foxp3*^{Cre}*Gabpa*$^{f/f}$ mice were determined with enzyme-linked immunosorbent assay kits from Southern Biotech according to manufacturer's instructions at multiple dilutions.

Immunoblotting

CD4$^+$ and CD8$^+$ T cells were purified from spleen and lymph nodes of *CD4*^{Cre}*Gabpa*$^{f/f}$ mice and littermate controls, and Tregs (CD4$^+$Foxp3-YFP$^+$) were purified from *Foxp3*^{Cre}*Gabpa*$^{f/f}$ mice and littermate controls by FACS sorting (BD, Aria). In the time course culture experiment, naive cells were purified, subject to α-CD3/28 and IL-2 culture and harvested at indicated time points. Total protein extracts were dissolved in SDS sample buffer, separated on 12% SDS-PAGE gels and transferred to polyvinylidene difluoride membrane (Millipore). The membranes were probed with antibodies against GABPα (sc-22810, Santa Cruz), p27 (3688, Cell Signaling), Rb (9313, Cell Signaling), Cyclin E (4132, Cell Signaling), CDK6 (3136, Cell Signaling), Cyclin D2 (3741, Cell Signaling), Mcm3 (4003, Cell Signaling), Mcm7 (4018, Cell Signaling), GADPH

(ab9485, Abcam) and β-actin (AC-15, Sigma), and visualized with the Immobilon Western Chemiluminescent HRP Substrate (Millipore).

Histopathology

Lung, liver, stomach and colon tissues from $Gabpa^{f/f}$ and $Foxp3^{Cre}Gabpa^{f/f}$ mice were fixed in Safefix II (Protocol) and embedded in paraffin. 5-mm sections were stained with haematoxylin and eosin.

Statistical analysis

All data are presented as the mean values $\pm$ SEM. Comparisons between groups were analyzed using unpaired Student's t tests. ns=not significant, #, p<0.01, *, p<0.05, **, p<0.01, ***, p<0.001, ****, p<0.0001.

CONCLUDING REMARKS

Over the recent years, our understanding of T cell activation, differentiation, proliferation, survival, trafficking and function has significantly expanded, providing a greater appreciation of the signals and pathways that regulate these processes. Evolutionarily conserved pathways that regulate cellular metabolism and stress responses have been implicated to play crucial and specific roles in the control of T cell responses. In this dissertation, we discuss the functions of the PI3K/Akt/Foxo signaling and the MAPK/Ets pathway in the regulation of conventional and regulatory T lymphocytes. These signaling pathways integrate immunological inputs, including antigen recognition, costimulatory ligand engagement and cytokine stimulation, and translate them into coordinately regulated gene expression. In depth molecular understanding of these signaling events and transcriptional programs will enhance our ability to manipulate T cell responses in autoimmunity, allograft transplantation, infectious diseases and cancer.

REFERENCES

1. M. A. Yui, E. V. Rothenberg, Developmental gene networks: a triathlon on the course to T cell identity. *Nat Rev Immunol* **14**, 529-545 (2014).

2. U. Koch, F. Radtke, Mechanisms of T cell development and transformation. *Annual review of cell and developmental biology* **27**, 539-562 (2011).

3. Q. Yang, J. Jeremiah Bell, A. Bhandoola, T-cell lineage determination. *Immunol Rev* **238**, 12-22 (2010).

4. T. K. Starr, S. C. Jameson, K. A. Hogquist, Positive and negative selection of T cells. *Annu Rev Immunol* **21**, 139-176 (2003).

5. R. N. Germain, T-cell development and the CD4-CD8 lineage decision. *Nat Rev Immunol* **2**, 309-322 (2002).

6. S. Z. Josefowicz, L. F. Lu, A. Y. Rudensky, Regulatory T cells: mechanisms of differentiation and function. *Annu Rev Immunol* **30**, 531-564 (2012).

7. D. Masopust, J. M. Schenkel, The integration of T cell migration, differentiation and function. *Nat Rev Immunol* **13**, 309-320 (2013).

8. C. D. Surh, J. Sprent, Homeostasis of naive and memory T cells. *Immunity* **29**, 848-862 (2008).

9. K. Takada, S. C. Jameson, Naive T cell homeostasis: from awareness of space to a sense of place. *Nat Rev Immunol* **9**, 823-832 (2009).

10. S. Takeda, H. R. Rodewald, H. Arakawa, H. Bluethmann, T. Shimizu, MHC class II molecules are not required for survival of newly generated CD4+ T cells, but affect their long-term life span. *Immunity* **5**, 217-228 (1996).

11. C. Tanchot, F. A. Lemonnier, B. Perarnau, A. A. Freitas, B. Rocha, Differential requirements for survival and proliferation of CD8 naive or memory T cells. *Science* **276**, 2057-2062 (1997).

12. J. C. Rathmell, E. A. Farkash, W. Gao, C. B. Thompson, IL-7 enhances the survival and maintains the size of naive T cells. *J Immunol* **167**, 6869-6876 (2001).

13. S. Wojciechowski *et al.*, Bim/Bcl-2 balance is critical for maintaining naive and memory T cell homeostasis. *J Exp Med* **204**, 1665-1675 (2007).

14. K. Akashi, M. Kondo, U. von Freeden-Jeffry, R. Murray, I. L. Weissman, Bcl-2 rescues T lymphopoiesis in interleukin-7 receptor-deficient mice. *Cell* **89**, 1033-1041 (1997).

15. K. Murali-Krishna *et al.*, Persistence of memory CD8 T cells in MHC class I-deficient mice. *Science* **286**, 1377-1381 (1999).

16. J. H. Cho *et al.*, An intense form of homeostatic proliferation of naive CD8+ cells driven by IL-2. *J Exp Med* **204**, 1787-1801 (2007).

17. N. J. MacIver, R. D. Michalek, J. C. Rathmell, Metabolic regulation of T lymphocytes. *Annu Rev Immunol* **31**, 259-283 (2013).

18. O. Boyman, J. Sprent, The role of interleukin-2 during homeostasis and activation of the immune system. *Nat Rev Immunol* **12**, 180-190 (2012).

19. E. A. Rowell, A. D. Wells, The role of cyclin-dependent kinases in T-cell development, proliferation, and function. *Critical reviews in immunology* **26**, 189-212 (2006).

20. E. L. Pearce, E. J. Pearce, Metabolic pathways in immune cell activation and quiescence. *Immunity* **38**, 633-643 (2013).

21. K. N. Pollizzi, J. D. Powell, Integrating canonical and metabolic signalling programmes in the regulation of T cell responses. *Nat Rev Immunol* **14**, 435-446 (2014).

22. M. G. Vander Heiden, L. C. Cantley, C. B. Thompson, Understanding the Warburg effect: the metabolic requirements of cell proliferation. *Science* **324**, 1029-1033 (2009).

23. R. Wang *et al.*, The transcription factor Myc controls metabolic reprogramming upon T lymphocyte activation. *Immunity* **35**, 871-882 (2011).

24. M. D. Buck, D. O'Sullivan, E. L. Pearce, T cell metabolism drives immunity. *J Exp Med* **212**, 1345-1360 (2015).

25. R. D. Michalek *et al.*, Cutting edge: distinct glycolytic and lipid oxidative metabolic programs are essential for effector and regulatory CD4+ T cell subsets. *J Immunol* **186**, 3299-3303 (2011).

26. J. J. O'Shea, W. E. Paul, Mechanisms underlying lineage commitment and plasticity of helper CD4+ T cells. *Science* **327**, 1098-1102 (2010).

27. J. Zhu, H. Yamane, W. E. Paul, Differentiation of effector CD4 T cell populations (*). *Annu Rev Immunol* **28**, 445-489 (2010).

28. N. S. Joshi, S. M. Kaech, Effector CD8 T cell development: a balancing act between memory cell potential and terminal differentiation. *J Immunol* **180**, 1309-1315 (2008).

29. S. Sarkar *et al.*, Functional and genomic profiling of effector CD8 T cell subsets with distinct memory fates. *J Exp Med* **205**, 625-640 (2008).

30. X. Bao *et al.*, Endothelial heparan sulfate controls chemokine presentation in recruitment of lymphocytes and dendritic cells to lymph nodes. *Immunity* **33**, 817-829 (2010).

31. S. D. Rosen, Ligands for L-selectin: homing, inflammation, and beyond. *Annu Rev Immunol* **22**, 129-156 (2004).

32. B. Johansson-Lindbom, W. W. Agace, Generation of gut-homing T cells and their localization to the small intestinal mucosa. *Immunol Rev* **215**, 226-242 (2007).

33. Y. Reiss, A. E. Proudfoot, C. A. Power, J. J. Campbell, E. C. Butcher, CC chemokine receptor (CCR)4 and the CCR10 ligand cutaneous T cell-attracting chemokine (CTACK) in lymphocyte trafficking to inflamed skin. *J Exp Med* **194**, 1541-1547 (2001).

34. S. M. Kaech, W. Cui, Transcriptional control of effector and memory CD8+ T cell differentiation. *Nat Rev Immunol* **12**, 749-761 (2012).

35. S. N. Mueller, T. Gebhardt, F. R. Carbone, W. R. Heath, Memory T cell subsets, migration patterns, and tissue residence. *Annu Rev Immunol* **31**, 137-161 (2013).

36. T. Gebhardt *et al.*, Memory T cells in nonlymphoid tissue that provide enhanced local immunity during infection with herpes simplex virus. *Nat Immunol* **10**, 524-530 (2009).

37. D. Masopust, V. Vezys, A. L. Marzo, L. Lefrancois, Preferential localization of effector memory cells in nonlymphoid tissue. *Science* **291**, 2413-2417 (2001).

38. F. Sallusto, D. Lenig, R. Forster, M. Lipp, A. Lanzavecchia, Two subsets of memory T lymphocytes with distinct homing potentials and effector functions. *Nature* **401**, 708-712 (1999).

39. J. E. Smith-Garvin, G. A. Koretzky, M. S. Jordan, T cell activation. *Annu Rev Immunol* **27**, 591-619 (2009).

40. L. P. Kane, J. Lin, A. Weiss, Signal transduction by the TCR for antigen. *Current opinion in immunology* **12**, 242-249 (2000).

41. L. E. Samelson, Signal transduction mediated by the T cell antigen receptor: the role of adapter proteins. *Annu Rev Immunol* **20**, 371-394 (2002).

42. G. A. Koretzky, F. Abtahian, M. A. Silverman, SLP76 and SLP65: complex regulation of signalling in lymphocytes and beyond. *Nat Rev Immunol* **6**, 67-78 (2006).

43. E. Genot, D. A. Cantrell, Ras regulation and function in lymphocytes. *Current opinion in immunology* **12**, 289-294 (2000).

44. K. Hayashi, A. Altman, Protein kinase C theta (PKCtheta): a key player in T cell life and death. *Pharmacological research* **55**, 537-544 (2007).

45. S. Vallabhapurapu, M. Karin, Regulation and function of NF-kappaB transcription factors in the immune system. *Annu Rev Immunol* **27**, 693-733 (2009).

46. J. Schulze-Luehrmann, S. Ghosh, Antigen-receptor signaling to nuclear factor kappa B. *Immunity* **25**, 701-715 (2006).

47. M. Cargnello, P. P. Roux, Activation and function of the MAPKs and their substrates, the MAPK-activated protein kinases. *Microbiology and molecular biology reviews : MMBR* **75**, 50-83 (2011).

48. M. Oh-hora, A. Rao, Calcium signaling in lymphocytes. *Current opinion in immunology* **20**, 250-258 (2008).

49. J. Liou *et al.*, STIM is a Ca2+ sensor essential for Ca2+-store-depletion-triggered Ca2+ influx. *Current biology : CB* **15**, 1235-1241 (2005).

50. J. Roos *et al.*, STIM1, an essential and conserved component of store-operated Ca2+ channel function. *The Journal of cell biology* **169**, 435-445 (2005).

51. S. Feske *et al.*, A mutation in Orai1 causes immune deficiency by abrogating CRAC channel function. *Nature* **441**, 179-185 (2006).

52. M. Savignac, B. Mellstrom, J. R. Naranjo, Calcium-dependent transcription of cytokine genes in T lymphocytes. *Pflugers Archiv : European journal of physiology* **454**, 523-533 (2007).

53. C. R. Beals, C. M. Sheridan, C. W. Turck, P. Gardner, G. R. Crabtree, Nuclear export of NF-ATc enhanced by glycogen synthase kinase-3. *Science* **275**, 1930-1934 (1997).

54. K. Okkenhaug, M. Turner, M. R. Gold, PI3K Signaling in B Cell and T Cell Biology. *Front Immunol* **5**, 557 (2014).

55. B. A. Hemmings, D. F. Restuccia, PI3K-PKB/Akt pathway. *Cold Spring Harb Perspect Biol* **4**, a011189 (2012).

56. A. Eijkelenboom, B. M. Burgering, FOXOs: signalling integrators for homeostasis maintenance. *Nat Rev Mol Cell Biol* **14**, 83-97 (2013).

57. R. Zoncu, A. Efeyan, D. M. Sabatini, mTOR: from growth signal integration to cancer, diabetes and ageing. *Nat Rev Mol Cell Biol* **12**, 21-35 (2011).

58. P. Narayan, B. Holt, R. Tosti, L. P. Kane, CARMA1 is required for Akt-mediated NF-kappaB activation in T cells. *Mol Cell Biol* **26**, 2327-2336 (2006).

59. X. P. Zhong, R. Guo, H. Zhou, C. Liu, C. K. Wan, Diacylglycerol kinases in immune cell function and self-tolerance. *Immunol Rev* **224**, 249-264 (2008).

60. O. Acuto, F. Michel, CD28-mediated co-stimulation: a quantitative support for TCR signalling. *Nat Rev Immunol* **3**, 939-951 (2003).

61. L. Chen, D. B. Flies, Molecular mechanisms of T cell co-stimulation and co-inhibition. *Nat Rev Immunol* **13**, 227-242 (2013).

62. A. Hutloff *et al.*, ICOS is an inducible T-cell co-stimulator structurally and functionally related to CD28. *Nature* **397**, 263-266 (1999).

63. T. H. Watts, TNF/TNFR family members in costimulation of T cell responses. *Annu Rev Immunol* **23**, 23-68 (2005).

64. H. Nishimura *et al.*, Autoimmune dilated cardiomyopathy in PD-1 receptor-deficient mice. *Science* **291**, 319-322 (2001).

65. P. Waterhouse *et al.*, Lymphoproliferative disorders with early lethality in mice deficient in Ctla-4. *Science* **270**, 985-988 (1995).

66. W. A. Teft, M. G. Kirchhof, J. Madrenas, A molecular perspective of CTLA-4 function. *Annu Rev Immunol* **24**, 65-97 (2006).

67. J. J. O'Shea, P. J. Murray, Cytokine signaling modules in inflammatory responses. *Immunity* **28**, 477-487 (2008).

68. J. J. O'Shea *et al.*, The JAK-STAT pathway: impact on human disease and therapeutic intervention. *Annual review of medicine* **66**, 311-328 (2015).

69. A. V. Villarino, Y. Kanno, J. R. Ferdinand, J. J. O'Shea, Mechanisms of Jak/STAT signaling in immunity and disease. *J Immunol* **194**, 21-27 (2015).

70. Y. Rochman, R. Spolski, W. J. Leonard, New insights into the regulation of T cells by gamma(c) family cytokines. *Nat Rev Immunol* **9**, 480-490 (2009).

71. L. C. Platanias, Mechanisms of type-I- and type-II-interferon-mediated signalling. *Nat Rev Immunol* **5**, 375-386 (2005).

72. A. Yoshimura, T. Naka, M. Kubo, SOCS proteins, cytokine signalling and immune regulation. *Nat Rev Immunol* **7**, 454-465 (2007).

73. D. Brenner, H. Blaser, T. W. Mak, Regulation of tumour necrosis factor signalling: live or let die. *Nat Rev Immunol* **15**, 362-374 (2015).

74.   H. Wajant, K. Pfizenmaier, P. Scheurich, Tumor necrosis factor signaling. *Cell death and differentiation* **10**, 45-65 (2003).

75.   J. Massague, TGFbeta signalling in context. *Nat Rev Mol Cell Biol* **13**, 616-630 (2012).

76.   M. O. Li, R. A. Flavell, Contextual regulation of inflammation: a duet by transforming growth factor-beta and interleukin-10. *Immunity* **28**, 468-476 (2008).

77.   M. O. Li, Y. Y. Wan, S. Sanjabi, A. K. Robertson, R. A. Flavell, Transforming growth factor-beta regulation of immune responses. *Annu Rev Immunol* **24**, 99-146 (2006).

78.   Y. Xing, K. A. Hogquist, T-cell tolerance: central and peripheral. *Cold Spring Harb Perspect Biol* **4**, (2012).

79.   T. M. McCaughtry, K. A. Hogquist, Central tolerance: what have we learned from mice? *Seminars in immunopathology* **30**, 399-409 (2008).

80.   M. S. Anderson, M. A. Su, Aire and T cell development. *Current opinion in immunology* **23**, 198-206 (2011).

81.   J. M. Gardner *et al.*, Deletional tolerance mediated by extrathymic Aire-expressing cells. *Science* **321**, 843-847 (2008).

82.   C. Benoist, D. Mathis, Treg cells, life history, and diversity. *Cold Spring Harb Perspect Biol* **4**, a007021 (2012).

83.   S. Sakaguchi, T. Yamaguchi, T. Nomura, M. Ono, Regulatory T cells and immune tolerance. *Cell* **133**, 775-787 (2008).

84.   M. A. McGargill, J. M. Derbinski, K. A. Hogquist, Receptor editing in developing T cells. *Nat Immunol* **1**, 336-341 (2000).

85.   P. Chappert, R. H. Schwartz, Induction of T cell anergy: integration of environmental cues and infectious tolerance. *Current opinion in immunology* **22**, 552-559 (2010).

86.   P. L. Cohen, R. A. Eisenberg, Lpr and gld: single gene models of systemic autoimmunity and lymphoproliferative disease. *Annu Rev Immunol* **9**, 243-269 (1991).

87.   C. L. Bennett *et al.*, The immune dysregulation, polyendocrinopathy, enteropathy, X-linked syndrome (IPEX) is caused by mutations of FOXP3. *Nature genetics* **27**, 20-21 (2001).

88.   M. E. Brunkow *et al.*, Disruption of a new forkhead/winged-helix protein, scurfin, results in the fatal lymphoproliferative disorder of the scurfy mouse. *Nature genetics* **27**, 68-73 (2001).

89.   R. S. Wildin *et al.*, X-linked neonatal diabetes mellitus, enteropathy and endocrinopathy syndrome is the human equivalent of mouse scurfy. *Nature genetics* **27**, 18-20 (2001).

90.   M. A. Burchill, J. Yang, K. B. Vang, M. A. Farrar, Interleukin-2 receptor signaling in regulatory T cell development and homeostasis. *Immunology letters* **114**, 1-8 (2007).

91.   M. A. Burchill, J. Yang, C. Vogtenhuber, B. R. Blazar, M. A. Farrar, IL-2 receptor beta-dependent STAT5 activation is required for the development of Foxp3+ regulatory T cells. *J Immunol* **178**, 280-290 (2007).

92.   S. Kano *et al.*, The contribution of transcription factor IRF1 to the interferon-gamma-interleukin 12 signaling axis and TH1 versus TH-17 differentiation of CD4+ T cells. *Nat Immunol* **9**, 34-41 (2008).

93.   O. Filipe-Santos *et al.*, Inborn errors of IL-12/23- and IFN-gamma-mediated immunity: molecular, cellular, and clinical features. *Seminars in immunology* **18**, 347-361 (2006).

94.   I. C. Ho, T. S. Tai, S. Y. Pai, GATA3 and the T-cell lineage: essential functions before and after T-helper-2-cell differentiation. *Nat Rev Immunol* **9**, 125-135 (2009).

95.   W. E. Paul, J. Zhu, How are T(H)2-type immune responses initiated and amplified? *Nat Rev Immunol* **10**, 225-235 (2010).

96.   H. Van Esch *et al.*, GATA3 haplo-insufficiency causes human HDR syndrome. *Nature* **406**, 419-422 (2000).

97.   C. Doucet *et al.*, IL-4 and IL-13 specifically increase adhesion molecule and inflammatory cytokine expression in human lung fibroblasts. *International immunology* **10**, 1421-1433 (1998).

98.   H. Takeda *et al.*, Effect of 5-fluorouracil on cell cycle regulatory proteins in human colon cancer cell line. *Japanese journal of cancer research : Gann* **90**, 677-684 (1999).

99.   M. Veldhoen, R. J. Hocking, C. J. Atkins, R. M. Locksley, B. Stockinger, TGFbeta in the context of an inflammatory cytokine milieu supports de novo differentiation of IL-17-producing T cells. *Immunity* **24**, 179-189 (2006).

100. N. Manel, D. Unutmaz, D. R. Littman, The differentiation of human T(H)-17 cells requires transforming growth factor-beta and induction of the nuclear receptor RORgammat. *Nat Immunol* **9**, 641-649 (2008).

101. E. Volpe *et al.*, A critical function for transforming growth factor-beta, interleukin 23 and proinflammatory cytokines in driving and modulating human T(H)-17 responses. *Nat Immunol* **9**, 650-657 (2008).

102. L. de Beaucoudrey *et al.*, Mutations in STAT3 and IL12RB1 impair the development of human IL-17-producing T cells. *J Exp Med* **205**, 1543-1550 (2008).

103. S. Okada *et al.*, IMMUNODEFICIENCIES. Impairment of immunity to Candida and Mycobacterium in humans with bi-allelic RORC mutations. *Science* **349**, 606-613 (2015).

104. R. H. Duerr *et al.*, A genome-wide association study identifies IL23R as an inflammatory bowel disease gene. *Science* **314**, 1461-1463 (2006).

105. P. Miossec, T. Korn, V. K. Kuchroo, Interleukin-17 and type 17 helper T cells. *The New England journal of medicine* **361**, 888-898 (2009).

106. D. D. Patel, V. K. Kuchroo, Th17 Cell Pathway in Human Immunity: Lessons from Genetics and Therapeutic Interventions. *Immunity* **43**, 1040-1051 (2015).

107. S. Crotty, T follicular helper cell differentiation, function, and roles in disease. *Immunity* **41**, 529-542 (2014).

108. H. Ueno, J. Banchereau, C. G. Vinuesa, Pathophysiology of T follicular helper cells in humans and mice. *Nat Immunol* **16**, 142-152 (2015).

109. L. M. Fahey *et al.*, Viral persistence redirects CD4 T cell differentiation toward T follicular helper cells. *J Exp Med* **208**, 987-999 (2011).

110. H. T. Khong, Q. J. Wang, S. A. Rosenberg, Identification of multiple antigens recognized by tumor-infiltrating lymphocytes from a single patient: tumor escape by antigen loss and loss of MHC expression. *Journal of immunotherapy* **27**, 184-190 (2004).

111. R. M. Maizels, K. A. Smith, Regulatory T cells in infection. *Advances in immunology* **112**, 73-136 (2011).

112. H. Ebinuma *et al.*, Identification and in vitro expansion of functional antigen-specific CD25+ FoxP3+ regulatory T cells in hepatitis C virus infection. *J Virol* **82**, 5043-5053 (2008).

113. L. Pace *et al.*, Regulatory T cells increase the avidity of primary CD8+ T cell responses and promote memory. *Science* **338**, 532-536 (2012).

114. Y. Belkaid, C. A. Piccirillo, S. Mendez, E. M. Shevach, D. L. Sacks, CD4+CD25+ regulatory T cells control Leishmania major persistence and immunity. *Nature* **420**, 502-507 (2002).

115. M. D. Vesely, M. H. Kershaw, R. D. Schreiber, M. J. Smyth, Natural innate and adaptive immunity to cancer. *Annu Rev Immunol* **29**, 235-271 (2011).

116. R. D. Schreiber, L. J. Old, M. J. Smyth, Cancer immunoediting: integrating immunity's roles in cancer suppression and promotion. *Science* **331**, 1565-1570 (2011).

117. A. M. Engel, I. M. Svane, J. Rygaard, O. Werdelin, MCA sarcomas induced in scid mice are more immunogenic than MCA sarcomas induced in congenic, immunocompetent mice. *Scandinavian journal of immunology* **45**, 463-470 (1997).

118. M. Girardi *et al.*, The distinct contributions of murine T cell receptor (TCR)gammadelta+ and TCRalphabeta+ T cells to different stages of chemically induced skin cancer. *J Exp Med* **198**, 747-755 (2003).

119. J. F. Bromberg, C. M. Horvath, Z. Wen, R. D. Schreiber, J. E. Darnell, Jr., Transcriptionally active Stat1 is required for the antiproliferative effects of both interferon alpha and interferon gamma. *Proc Natl Acad Sci U S A* **93**, 7673-7678 (1996).

120. E. Cretney *et al.*, Increased susceptibility to tumor initiation and metastasis in TNF-related apoptosis-inducing ligand-deficient mice. *J Immunol* **168**, 1356-1361 (2002).

121. W. F. Davidson, T. Giese, T. N. Fredrickson, Spontaneous development of plasmacytoid tumors in mice with defective Fas-Fas ligand interactions. *J Exp Med* **187**, 1825-1838 (1998).

122. M. J. Smyth *et al.*, Perforin-mediated cytotoxicity is critical for surveillance of spontaneous lymphoma. *J Exp Med* **192**, 755-760 (2000).

123. J. M. Park *et al.*, Early role of CD4+ Th1 cells and antibodies in HER-2 adenovirus vaccine protection against autochthonous mammary carcinomas. *J Immunol* **174**, 4228-4236 (2005).

124. H. Matsushita *et al.*, Cancer exome analysis reveals a T-cell-dependent mechanism of cancer immunoediting. *Nature* **482**, 400-404 (2012).

125. H. Nishikawa, S. Sakaguchi, Regulatory T cells in cancer immunotherapy. *Current opinion in immunology* **27**, 1-7 (2014).

126. P. D. Bos, G. Plitas, D. Rudra, S. Y. Lee, A. Y. Rudensky, Transient regulatory T cell ablation deters oncogene-driven breast cancer and enhances radiotherapy. *J Exp Med* **210**, 2435-2466 (2013).

127. T. J. Curiel *et al.*, Specific recruitment of regulatory T cells in ovarian carcinoma fosters immune privilege and predicts reduced survival. *Nat Med* **10**, 942-949 (2004).

128. E. Sato *et al.*, Intraepithelial CD8+ tumor-infiltrating lymphocytes and a high CD8+/regulatory T cell ratio are associated with favorable prognosis in ovarian cancer. *Proc Natl Acad Sci U S A* **102**, 18538-18543 (2005).

129. S. A. Rosenberg, J. C. Yang, N. P. Restifo, Cancer immunotherapy: moving beyond current vaccines. *Nat Med* **10**, 909-915 (2004).

130. B. C. Carthon *et al.*, Preoperative CTLA-4 blockade: tolerability and immune monitoring in the setting of a presurgical clinical trial. *Clinical cancer research : an official journal of the American Association for Cancer Research* **16**, 2861-2871 (2010).

131. F. S. Hodi *et al.*, Immunologic and clinical effects of antibody blockade of cytotoxic T lymphocyte-associated antigen 4 in previously vaccinated cancer patients. *Proc Natl Acad Sci U S A* **105**, 3005-3010 (2008).

132. J. C. Yang *et al.*, Ipilimumab (anti-CTLA4 antibody) causes regression of metastatic renal cell cancer associated with enteritis and hypophysitis. *Journal of immunotherapy* **30**, 825-830 (2007).

133. S. A. Rosenberg, N. P. Restifo, Adoptive cell transfer as personalized immunotherapy for human cancer. *Science* **348**, 62-68 (2015).

134. L. G. Radvanyi *et al.*, Specific lymphocyte subsets predict response to adoptive cell therapy using expanded autologous tumor-infiltrating lymphocytes in metastatic melanoma patients. *Clinical cancer research : an official journal of the American Association for Cancer Research* **18**, 6758-6770 (2012).

135. M. Sadelain, R. Brentjens, I. Riviere, The basic principles of chimeric antigen receptor design. *Cancer discovery* **3**, 388-398 (2013).

136. T. Tsukahara *et al.*, CD19 target-engineered T-cells accumulate at tumor lesions in human B-cell lymphoma xenograft mouse models. *Biochem Biophys Res Commun* **438**, 84-89 (2013).

137. J. N. Kochenderfer *et al.*, Eradication of B-lineage cells and regression of lymphoma in a patient treated with autologous T cells genetically engineered to recognize CD19. *Blood* **116**, 4099-4102 (2010).

138. R. J. Brentjens *et al.*, CD19-targeted T cells rapidly induce molecular remissions in adults with chemotherapy-refractory acute lymphoblastic leukemia. *Science translational medicine* **5**, 177ra138 (2013).

139. Y. H. Huang, K. Sauer, Lipid signaling in T-cell development and function. *Cold Spring Harb Perspect Biol* **2**, a002428 (2010).

140. J. M. Han, S. J. Patterson, M. K. Levings, The Role of the PI3K Signaling Pathway in CD4(+) T Cell Differentiation and Function. *Front Immunol* **3**, 245 (2012).

141. P. T. Bhaskar, N. Hay, The two TORCs and Akt. *Dev Cell* **12**, 487-502 (2007).

142. E. Fayard, G. Xue, A. Parcellier, L. Bozulic, B. A. Hemmings, Protein kinase B (PKB/Akt), a key mediator of the PI3K signaling pathway. *Curr Top Microbiol Immunol* **346**, 31-56 (2010).

143. W. Ouyang, M. O. Li, Foxo: in command of T lymphocyte homeostasis and tolerance. *Trends Immunol* **32**, 26-33 (2011).

144. J. Huang, B. D. Manning, A complex interplay between Akt, TSC2 and the two mTOR complexes. *Biochem Soc Trans* **37**, 217-222 (2009).

145. S. J. Harris, R. V. Parry, J. Westwick, S. G. Ward, Phosphoinositide lipid phosphatases: natural regulators of phosphoinositide 3-kinase signaling in T lymphocytes. *J Biol Chem* **283**, 2465-2469 (2008).

146. J. Brognard, A. C. Newton, PHLiPPing the switch on Akt and protein kinase C signaling. *Trends Endocrinol Metab* **19**, 223-230 (2008).

147. M. Wang, X. Zhang, H. Zhao, Q. Wang, Y. Pan, FoxO gene family evolution in vertebrates. *BMC Evol Biol* **9**, 222 (2009).

148. F. M. Jacobs *et al.*, FoxO6, a novel member of the FoxO class of transcription factors with distinct shuttling dynamics. *J Biol Chem* **278**, 35959-35967 (2003).

149. T. Furuyama *et al.*, Abnormal angiogenesis in Foxo1 (Fkhr)-deficient mice. *J Biol Chem* **279**, 34741-34749 (2004).

150. T. Hosaka *et al.*, Disruption of forkhead transcription factor (FOXO) family members in mice reveals their functional diversification. *Proc Natl Acad Sci U S A* **101**, 2975-2980 (2004).

151. Y. M. Kerdiles *et al.*, Foxo1 links homing and survival of naive T cells by regulating L-selectin, CCR7 and interleukin 7 receptor. *Nat Immunol* **10**, 176-184 (2009).

152.   D. H. Castrillon, L. Miao, R. Kollipara, J. W. Horner, R. A. DePinho, Suppression of ovarian follicle activation in mice by the transcription factor Foxo3a. *Science* **301**, 215-218 (2003).

153.   D. R. Calnan, A. Brunet, The FoxO code. *Oncogene* **27**, 2276-2288 (2008).

154.   K. E. van der Vos, P. J. Coffer, FOXO-binding partners: it takes two to tango. *Oncogene* **27**, 2289-2299 (2008).

155.   A. Brunet *et al.*, Protein kinase SGK mediates survival signals by phosphorylating the forkhead transcription factor FKHRL1 (FOXO3a). *Mol Cell Biol* **21**, 952-965 (2001).

156.   S. Fabre *et al.*, FOXO1 regulates L-Selectin and a network of human T cell homing molecules downstream of phosphatidylinositol 3-kinase. *J Immunol* **181**, 2980-2989 (2008).

157.   W. Ouyang, O. Beckett, R. A. Flavell, M. O. Li, An essential role of the Forkhead-box transcription factor Foxo1 in control of T cell homeostasis and tolerance. *Immunity* **30**, 358-371 (2009).

158.   A. Laine *et al.*, Foxo1 Is a T Cell-Intrinsic Inhibitor of the RORgammat-Th17 Program. *J Immunol* **195**, 1791-1803 (2015).

159.   C. Wu *et al.*, Induction of pathogenic TH17 cells by inducible salt-sensing kinase SGK1. *Nature* **496**, 513-517 (2013).

160.   R. Hess Michelini, A. L. Doedens, A. W. Goldrath, S. M. Hedrick, Differentiation of CD8 memory T cells depends on Foxo1. *J Exp Med* **210**, 1189-1200 (2013).

161.   E. H. Kim *et al.*, Signal integration by Akt regulates CD8 T cell effector and memory differentiation. *J Immunol* **188**, 4305-4314 (2012).

162.   M. V. Kim, W. Ouyang, W. Liao, M. Q. Zhang, M. O. Li, The transcription factor Foxo1 controls central-memory CD8+ T cell responses to infection. *Immunity* **39**, 286-297 (2013).

163.   J. A. Sullivan, E. H. Kim, E. H. Plisch, S. L. Peng, M. Suresh, FOXO3 regulates CD8 T cell memory by T cell-intrinsic mechanisms. *PLoS Pathog* **8**, e1002533 (2012).

164.   J. A. Sullivan, E. H. Kim, E. H. Plisch, M. Suresh, FOXO3 regulates the CD8 T cell response to a chronic viral infection. *J Virol* **86**, 9025-9034 (2012).

165.   M. M. Tejera, E. H. Kim, J. A. Sullivan, E. H. Plisch, M. Suresh, FoxO1 controls effector-to-memory transition and maintenance of functional CD8 T cell memory. *J Immunol* **191**, 187-199 (2013).

166. R. R. Rao, Q. Li, M. R. Gubbels Bupp, P. A. Shrikant, Transcription factor Foxo1 represses T-bet-mediated effector functions and promotes memory CD8(+) T cell differentiation. *Immunity* **36**, 374-387 (2012).

167. S. Togher, A. Larange, S. P. Schoenberger, S. Feau, FoxO3 is a negative regulator of primary CD8+ T-cell expansion but not of memory formation. *Immunol Cell Biol* **93**, 120-125 (2015).

168. M. M. Staron *et al.*, The transcription factor FoxO1 sustains expression of the inhibitory receptor PD-1 and survival of antiviral CD8(+) T cells during chronic infection. *Immunity* **41**, 802-814 (2014).

169. Y. Harada *et al.*, Transcription factors Foxo3a and Foxo1 couple the E3 ligase Cbl-b to the induction of Foxp3 expression in induced regulatory T cells. *J Exp Med* **207**, 1381-1391 (2010).

170. Y. M. Kerdiles *et al.*, Foxo transcription factors control regulatory T cell development and function. *Immunity* **33**, 890-904 (2010).

171. W. Ouyang *et al.*, Foxo proteins cooperatively control the differentiation of Foxp3+ regulatory T cells. *Nat Immunol* **11**, 618-627 (2010).

172. W. Ouyang *et al.*, Novel Foxo1-dependent transcriptional programs control T(reg) cell function. *Nature* **491**, 554-559 (2012).

173. S. J. Bensinger *et al.*, Distinct IL-2 receptor signaling pattern in CD4+CD25+ regulatory T cells. *J Immunol* **172**, 5287-5296 (2004).

174. R. Zeiser *et al.*, Differential impact of mammalian target of rapamycin inhibition on CD4+CD25+Foxp3+ regulatory T cells compared with conventional CD4+ T cells. *Blood* **111**, 453-462 (2008).

175. S. J. Patterson *et al.*, Cutting edge: PHLPP regulates the development, function, and molecular signaling pathways of regulatory T cells. *J Immunol* **186**, 5533-5537 (2011).

176. A. Zanin-Zhorov *et al.*, Scaffold protein Disc large homolog 1 is required for T-cell receptor-induced activation of regulatory T-cell function. *Proc Natl Acad Sci U S A* **109**, 1625-1630 (2012).

177. G. M. Delgoffe *et al.*, The mTOR kinase differentially regulates effector and regulatory T cell lineage commitment. *Immunity* **30**, 832-844 (2009).

178. S. Haxhinasto, D. Mathis, C. Benoist, The AKT-mTOR axis regulates de novo differentiation of CD4+Foxp3+ cells. *J Exp Med* **205**, 565-574 (2008).

179. D. T. Patton *et al.*, Cutting edge: the phosphoinositide 3-kinase p110 delta is critical for the function of CD4+CD25+Foxp3+ regulatory T cells. *J Immunol* **177**, 6598-6602 (2006).

180. S. Sauer *et al.*, T cell receptor signaling controls Foxp3 expression via PI3K, Akt, and mTOR. *Proc Natl Acad Sci U S A* **105**, 7797-7802 (2008).

181. G. Liu *et al.*, The receptor S1P1 overrides regulatory T cell-mediated immune suppression through Akt-mTOR. *Nat Immunol* **10**, 769-777 (2009).

182. G. Liu, K. Yang, S. Burns, S. Shrestha, H. Chi, The S1P(1)-mTOR axis directs the reciprocal differentiation of T(H)1 and T(reg) cells. *Nat Immunol* **11**, 1047-1056 (2010).

183. S. P. Cobbold *et al.*, Infectious tolerance via the consumption of essential amino acids and mTOR signaling. *Proc Natl Acad Sci U S A* **106**, 12055-12060 (2009).

184. X. Chang, A. S. Lazorchak, D. Liu, B. Su, Sin1 regulates Treg-cell development but is not required for T-cell growth and proliferation. *Eur J Immunol* **42**, 1639-1647 (2012).

185. P. T. Walsh *et al.*, PTEN inhibits IL-2 receptor-mediated expansion of CD4+ CD25+ Tregs. *J Clin Invest* **116**, 2521-2531 (2006).

186. H. Zeng *et al.*, mTORC1 couples immune signals and metabolic programming to establish T(reg)-cell function. *Nature* **499**, 485-490 (2013).

187. G. M. Delgoffe *et al.*, Stability and function of regulatory T cells is maintained by a neuropilin-1-semaphorin-4a axis. *Nature* **501**, 252-256 (2013).

188. A. Huynh *et al.*, Control of PI(3) kinase in Treg cells maintains homeostasis and lineage stability. *Nat Immunol* **16**, 188-196 (2015).

189. S. Shrestha *et al.*, Treg cells require the phosphatase PTEN to restrain TH1 and TFH cell responses. *Nat Immunol* **16**, 178-187 (2015).

190. M. D. Sharma *et al.*, The PTEN pathway in Tregs is a critical driver of the suppressive tumor microenvironment. *Sci Adv* **1**, e1500845 (2015).

191. A. Chaudhry, A. Y. Rudensky, Control of inflammation by integration of environmental cues by regulatory T cells. *J Clin Invest* **123**, 939-944 (2013).

192. X. Yuan, G. Cheng, T. R. Malek, The importance of regulatory T-cell heterogeneity in maintaining self-tolerance. *Immunol Rev* **259**, 103-114 (2014).

193. M. A. Curotto de Lafaille, J. J. Lafaille, Natural and adaptive foxp3+ regulatory T cells: more of the same or a division of labor? *Immunity* **30**, 626-635 (2009).

194. I. K. Gratz, D. J. Campbell, Organ-specific and memory treg cells: specificity, development, function, and maintenance. *Front Immunol* **5**, 333 (2014).

195. A. Iellem, L. Colantonio, D. D'Ambrosio, Skin-versus gut-skewed homing receptor expression and intrinsic CCR4 expression on human peripheral blood CD4+CD25+ suppressor T cells. *Eur J Immunol* **33**, 1488-1496 (2003).

196. B. Singh *et al.*, Control of intestinal inflammation by regulatory T cells. *Immunol Rev* **182**, 190-200 (2001).

197. A. M. Thornton *et al.*, Expression of Helios, an Ikaros transcription factor family member, differentiates thymic-derived from peripherally induced Foxp3+ T regulatory cells. *J Immunol* **184**, 3433-3441 (2010).

198. J. M. Weiss *et al.*, Neuropilin 1 is expressed on thymus-derived natural regulatory T cells, but not mucosa-generated induced Foxp3+ T reg cells. *J Exp Med* **209**, 1723-1742, S1721 (2012).

199. M. Yadav *et al.*, Neuropilin-1 distinguishes natural and inducible regulatory T cells among regulatory T cell subsets in vivo. *J Exp Med* **209**, 1713-1722, S1711-1719 (2012).

200. N. Arpaia *et al.*, Metabolites produced by commensal bacteria promote peripheral regulatory T-cell generation. *Nature* **504**, 451-455 (2013).

201. Y. Furusawa *et al.*, Commensal microbe-derived butyrate induces the differentiation of colonic regulatory T cells. *Nature* **504**, 446-450 (2013).

202. P. M. Smith *et al.*, The microbial metabolites, short-chain fatty acids, regulate colonic Treg cell homeostasis. *Science* **341**, 569-573 (2013).

203. S. K. Lathrop *et al.*, Peripheral education of the immune system by colonic commensal microbiota. *Nature* **478**, 250-254 (2011).

204. A. Chaudhry *et al.*, CD4+ regulatory T cells control TH17 responses in a Stat3-dependent manner. *Science* **326**, 986-991 (2009).

205. M. A. Koch *et al.*, The transcription factor T-bet controls regulatory T cell homeostasis and function during type 1 inflammation. *Nat Immunol* **10**, 595-602 (2009).

206. Y. Zheng *et al.*, Regulatory T-cell suppressor program co-opts transcription factor IRF4 to control T(H)2 responses. *Nature* **458**, 351-356 (2009).

207. E. Cretney *et al.*, The transcription factors Blimp-1 and IRF4 jointly control the differentiation and function of effector regulatory T cells. *Nat Immunol* **12**, 304-311 (2011).

208. Y. P. Rubtsov *et al.*, Regulatory T cell-derived interleukin-10 limits inflammation at environmental interfaces. *Immunity* **28**, 546-558 (2008).

209. J. Huehn *et al.*, Developmental stage, phenotype, and migration distinguish naive- and effector/memory-like CD4+ regulatory T cells. *J Exp Med* **199**, 303-313 (2004).

210. M. Miyara *et al.*, Functional delineation and differentiation dynamics of human CD4+ T cells expressing the FoxP3 transcription factor. *Immunity* **30**, 899-911 (2009).

211. D. Sugiyama *et al.*, Anti-CCR4 mAb selectively depletes effector-type FoxP3+CD4+ regulatory T cells, evoking antitumor immune responses in humans. *Proc Natl Acad Sci U S A* **110**, 17945-17950 (2013).

212. K. S. Smigiel *et al.*, CCR7 provides localized access to IL-2 and defines homeostatically distinct regulatory T cell subsets. *J Exp Med* **211**, 121-136 (2014).

213. H. Peng *et al.*, Liver-resident NK cells confer adaptive immunity in skin-contact inflammation. *J Clin Invest* **123**, 1444-1456 (2013).

214. S. M. Hedrick, R. Hess Michelini, A. L. Doedens, A. W. Goldrath, E. L. Stone, FOXO transcription factors throughout T cell biology. *Nat Rev Immunol* **12**, 649-661 (2012).

215. C. T. Luo, M. O. Li, Transcriptional control of regulatory T cell development and function. *Trends Immunol* **34**, 531-539 (2013).*

* Reprinted from Trends in Immunology, 34(11), Luo C.T., Li M.O., Transcriptional control of regulatory T cell development and function, 531-9, Copyright 2013, with permission from Elsevier.

216. H. Nishikawa, S. Sakaguchi, Regulatory T cells in tumor immunity. *Int J Cancer* **127**, 759-767 (2010).

217. S. A. Quezada, K. S. Peggs, T. R. Simpson, J. P. Allison, Shifting the equilibrium in cancer immunoediting: from tumor tolerance to eradication. *Immunol Rev* **241**, 104-118 (2011).

218. W. Zou, Regulatory T cells, tumour immunity and immunotherapy. *Nat Rev Immunol* **6**, 295-307 (2006).

219. S. Onizuka *et al.*, Tumor rejection by in vivo administration of anti-CD25 (interleukin-2 receptor alpha) monoclonal antibody. *Cancer Res* **59**, 3128-3133 (1999).

220. R. A. Franklin *et al.*, The cellular and molecular origin of tumor-associated macrophages. *Science* **344**, 921-925 (2014).

221. J. R. Stringer *et al.*, Modeling variation in tumors in vivo. *Proc Natl Acad Sci U S A* **102**, 2408-2413 (2005).

222. M. Laplante, D. M. Sabatini, mTOR signaling in growth control and disease. *Cell* **149**, 274-293 (2012).

223. M. S. Song *et al.*, Nuclear PTEN regulates the APC-CDH1 tumor-suppressive complex in a phosphatase-independent manner. *Cell* **144**, 187-199 (2011).

224. L. Srinivasan *et al.*, PI3 kinase signals BCR-dependent mature B cell survival. *Cell* **139**, 573-586 (2009).

225. D. A. Vignali, L. W. Collison, C. J. Workman, How regulatory T cells work. *Nat Rev Immunol* **8**, 523-532 (2008).

226. L. W. Collison *et al.*, The inhibitory cytokine IL-35 contributes to regulatory T-cell function. *Nature* **450**, 566-569 (2007).

227. N. Oberle, N. Eberhardt, C. S. Falk, P. H. Krammer, E. Suri-Payer, Rapid suppression of cytokine transcription in human CD4+CD25 T cells by CD4+Foxp3+ regulatory T cells: independence of IL-2 consumption, TGF-beta, and various inhibitors of TCR signaling. *J Immunol* **179**, 3578-3587 (2007).

228. S. Deaglio *et al.*, Adenosine generation catalyzed by CD39 and CD73 expressed on regulatory T cells mediates immune suppression. *J Exp Med* **204**, 1257-1265 (2007).

229. X. Cao *et al.*, Granzyme B and perforin are important for regulatory T cell-mediated suppression of tumor clearance. *Immunity* **27**, 635-646 (2007).

230. O. S. Qureshi *et al.*, Trans-endocytosis of CD80 and CD86: a molecular basis for the cell-extrinsic function of CTLA-4. *Science* **332**, 600-603 (2011).

231. K. Wing *et al.*, CTLA-4 control over Foxp3+ regulatory T cell function. *Science* **322**, 271-275 (2008).

232. M. M. Gubin *et al.*, Checkpoint blockade cancer immunotherapy targets tumour-specific mutant antigens. *Nature* **515**, 577-581 (2014).

233. C. Linnemann *et al.*, High-throughput epitope discovery reveals frequent recognition of neo-antigens by CD4+ T cells in human melanoma. *Nat Med* **21**, 81-85 (2015).

234. E. Tran *et al.*, Cancer immunotherapy based on mutation-specific CD4+ T cells in a patient with epithelial cancer. *Science* **344**, 641-645 (2014).

235. Y. Y. Wan, H. Chi, M. Xie, M. D. Schneider, R. A. Flavell, The kinase TAK1 integrates antigen and cytokine receptor signaling for T cell development, survival and function. *Nat Immunol* **7**, 851-858 (2006).

236. D. E. Wright, A. J. Wagers, A. P. Gulati, F. L. Johnson, I. L. Weissman, Physiological migration of hematopoietic stem and progenitor cells. *Science* **294**, 1933-1936 (2001).

237. T. J. Stewart, S. I. Abrams, Altered immune function during long-term host-tumor interactions can be modulated to retard autochthonous neoplastic growth. *J Immunol* **179**, 2851-2859 (2007).

238. B. Langmead, C. Trapnell, M. Pop, S. L. Salzberg, Ultrafast and memory-efficient alignment of short DNA sequences to the human genome. *Genome Biol* **10**, R25 (2009).

239. A. Dobin *et al.*, STAR: ultrafast universal RNA-seq aligner. *Bioinformatics* **29**, 15-21 (2013).

240. L. Wang, S. Wang, W. Li, RSeQC: quality control of RNA-seq experiments. *Bioinformatics* **28**, 2184-2185 (2012).

241. Y. Liao, G. K. Smyth, W. Shi, featureCounts: an efficient general purpose program for assigning sequence reads to genomic features. *Bioinformatics* **30**, 923-930 (2014).

242. Y. Liao, G. K. Smyth, W. Shi, The Subread aligner: fast, accurate and scalable read mapping by seed-and-vote. *Nucleic Acids Res* **41**, e108 (2013).

243. J. Harrow *et al.*, GENCODE: producing a reference annotation for ENCODE. *Genome Biol* **7 Suppl 1**, S4 1-9 (2006).

244. A. D. Sharrocks, The ETS-domain transcription factor family. *Nat Rev Mol Cell Biol* **2**, 827-837 (2001).

245. B. M. Degnan, S. M. Degnan, T. Naganuma, D. E. Morse, The ets multigene family is conserved throughout the Metazoa. *Nucleic Acids Res* **21**, 3479-3484 (1993).

246. V. Laudet, C. Niel, M. Duterque-Coquillaud, D. Leprince, D. Stehelin, Evolution of the ets gene family. *Biochem Biophys Res Commun* **190**, 8-14 (1993).

247. T. Oikawa, T. Yamada, Molecular biology of the Ets family of transcription factors. *Gene* **303**, 11-34 (2003).

248. A. G. Rosmarin, K. K. Resendes, Z. Yang, J. N. McMillan, S. L. Fleming, GA-binding protein transcription factor: a review of GABP as an integrator of

intracellular signaling and protein-protein interactions. *Blood Cells Mol Dis* **32**, 143-154 (2004).

249. K. LaMarco, C. C. Thompson, B. P. Byers, E. M. Walton, S. L. McKnight, Identification of Ets- and notch-related subunits in GA binding protein. *Science* **253**, 789-792 (1991).

250. A. H. Batchelor, D. E. Piper, F. C. de la Brousse, S. L. McKnight, C. Wolberger, The structure of GABPalpha/beta: an ETS domain- ankyrin repeat heterodimer bound to DNA. *Science* **279**, 1037-1041 (1998).

251. F. C. de la Brousse, E. H. Birkenmeier, D. S. King, L. B. Rowe, S. L. McKnight, Molecular and genetic characterization of GABP beta. *Genes Dev* **8**, 1853-1865 (1994).

252. S. Gugneja, J. V. Virbasius, R. C. Scarpulla, Four structurally distinct, non-DNA-binding subunits of human nuclear respiratory factor 2 share a conserved transcriptional activation domain. *Mol Cell Biol* **15**, 102-111 (1995).

253. J. Sawada, M. Goto, C. Sawa, H. Watanabe, H. Handa, Transcriptional activation through the tetrameric complex formation of E4TF1 subunits. *EMBO J* **13**, 1396-1402 (1994).

254. J. V. Virbasius, C. A. Virbasius, R. C. Scarpulla, Identity of GABP with NRF-2, a multisubunit activator of cytochrome oxidase expression, reveals a cellular role for an ETS domain activator of viral promoters. *Genes Dev* **7**, 380-392 (1993).

255. Z. F. Yang, K. Drumea, S. Mott, J. Wang, A. G. Rosmarin, GABP transcription factor (nuclear respiratory factor 2) is required for mitochondrial biogenesis. *Mol Cell Biol* **34**, 3194-3201 (2014).

256. E. P. Bottinger, C. S. Shelley, O. C. Farokhzad, M. A. Arnaout, The human beta 2 integrin CD18 promoter consists of two inverted Ets cis elements. *Mol Cell Biol* **14**, 2604-2615 (1994).

257. A. Briguet, M. A. Ruegg, The Ets transcription factor GABP is required for postsynaptic differentiation in vivo. *J Neurosci* **20**, 5989-5996 (2000).

258. A. G. Rosmarin, D. G. Caprio, D. G. Kirsch, H. Handa, C. P. Simkevich, GABP and PU.1 compete for binding, yet cooperate to increase CD18 (beta 2 leukocyte integrin) transcription. *J Biol Chem* **270**, 23627-23633 (1995).

259. M. Gyrd-Hansen, T. O. Krag, A. G. Rosmarin, T. S. Khurana, Sp1 and the ets-related transcription factor complex GABP alpha/beta functionally cooperate to activate the utrophin promoter. *J Neurol Sci* **197**, 27-35 (2002).

260. I. Nuchprayoon, C. P. Simkevich, M. Luo, A. D. Friedman, A. G. Rosmarin, GABP cooperates with c-Myb and C/EBP to activate the neutrophil elastase promoter. *Blood* **89**, 4546-4554 (1997).

261. K. K. Resendes, A. G. Rosmarin, GA-binding protein and p300 are essential components of a retinoic acid-induced enhanceosome in myeloid cells. *Mol Cell Biol* **26**, 3060-3070 (2006).

262. S. Ristevski *et al.*, The ETS transcription factor GABPalpha is essential for early embryogenesis. *Mol Cell Biol* **24**, 5844-5849 (2004).

263. H. H. Xue *et al.*, GA binding protein regulates interleukin 7 receptor alpha-chain gene expression in T cells. *Nat Immunol* **5**, 1036-1044 (2004).

264. Z. F. Yang, S. Mott, A. G. Rosmarin, The Ets transcription factor GABP is required for cell-cycle progression. *Nat Cell Biol* **9**, 339-346 (2007).

265. A. Jaworski, C. L. Smith, S. J. Burden, GA-binding protein is dispensable for neuromuscular synapse formation and synapse-specific gene expression. *Mol Cell Biol* **27**, 5040-5046 (2007).

266. M. F. Crook *et al.*, GA-binding protein regulates KIS gene expression, cell migration, and cell cycle progression. *FASEB J* **22**, 225-235 (2008).

267. Z. F. Yang *et al.*, GABP transcription factor is required for myeloid differentiation, in part, through its control of Gfi-1 expression. *Blood* **118**, 2243-2253 (2011).

268. S. Yu *et al.*, GABP controls a critical transcription regulatory module that is essential for maintenance and differentiation of hematopoietic stem/progenitor cells. *Blood* **117**, 2166-2178 (2011).

269. H. H. Xue *et al.*, The transcription factor GABP is a critical regulator of B lymphocyte development. *Immunity* **26**, 421-431 (2007).

270. A. Seth, D. K. Watson, ETS transcription factors and their emerging roles in human cancer. *Eur J Cancer* **41**, 2462-2478 (2005).

271. S. Yu, X. Jing, J. D. Colgan, D. M. Zhao, H. H. Xue, Targeting tetramer-forming GABPbeta isoforms impairs self-renewal of hematopoietic and leukemic stem cells. *Cell Stem Cell* **11**, 207-219 (2012).

272. Z. F. Yang *et al.*, GABP transcription factor is required for development of chronic myelogenous leukemia via its control of PRKD2. *Proc Natl Acad Sci U S A* **110**, 2312-2317 (2013).

273. H. Wu *et al.*, The Ets transcription factor GABP is a component of the hippo pathway essential for growth and antioxidant defense. *Cell Rep* **3**, 1663-1677 (2013).

274. S. Yu, D. M. Zhao, R. Jothi, H. H. Xue, Critical requirement of GABPalpha for normal T cell development. *J Biol Chem* **285**, 10179-10188 (2010).

275. A. Chandele *et al.*, Formation of IL-7Ralphahigh and IL-7Ralphalow CD8 T cells during infection is regulated by the opposing functions of GABPalpha and Gfi-1. *J Immunol* **180**, 5309-5319 (2008).

276. S. D. Bell, M. R. Botchan, The minichromosome maintenance replicative helicase. *Cold Spring Harb Perspect Biol* **5**, a012807 (2013).

277. M. L. Bochman, A. Schwacha, The Mcm complex: unwinding the mechanism of a replicative helicase. *Microbiology and molecular biology reviews : MMBR* **73**, 652-683 (2009).

278. S. Kanangat *et al.*, Disease in the scurfy (sf) mouse is associated with overexpression of cytokine genes. *Eur J Immunol* **26**, 161-165 (1996).

279. J. Boros *et al.*, Elucidation of the ELK1 target gene network reveals a role in the coordinate regulation of core components of the gene regulation machinery. *Genome Res* **19**, 1963-1973 (2009).

280. P. C. Hollenhorst, A. A. Shah, C. Hopkins, B. J. Graves, Genome-wide analyses reveal properties of redundant and specific promoter occupancy within the ETS gene family. *Genes Dev* **21**, 1882-1894 (2007).

281. A. Avots *et al.*, GABP factors bind to a distal interleukin 2 (IL-2) enhancer and contribute to c-Raf-mediated increase in IL-2 induction. *Mol Cell Biol* **17**, 4381-4389 (1997).

282. A. Hoffmeyer *et al.*, The GABP-responsive element of the interleukin-2 enhancer is regulated by JNK/SAPK-activating pathways in T lymphocytes. *J Biol Chem* **273**, 10112-10119 (1998).

283. H. Imaki *et al.*, Cell cycle-dependent regulation of the Skp2 promoter by GA-binding protein. *Cancer Res* **63**, 4607-4613 (2003).

284. T. L. Rudge, L. F. Johnson, Synergistic activation of the TATA-less mouse thymidylate synthase promoter by the Ets transcription factor GABP and Sp1. *Exp Cell Res* **274**, 45-55 (2002).

285. J. T. Fox, P. J. Stover, Folate-mediated one-carbon metabolism. *Vitam Horm* **79**, 1-44 (2008).

286. O. Boyman, S. Letourneau, C. Krieg, J. Sprent, Homeostatic proliferation and survival of naive and memory T cells. *Eur J Immunol* **39**, 2088-2094 (2009).

287. A. W. Goldrath, C. J. Luckey, R. Park, C. Benoist, D. Mathis, The molecular program induced in T cells undergoing homeostatic proliferation. *Proc Natl Acad Sci U S A* **101**, 16885-16890 (2004).

288. J. Fan *et al.*, Quantitative flux analysis reveals folate-dependent NADPH production. *Nature* **510**, 298-302 (2014).

289. D. Kim *et al.*, SHMT2 drives glioma cell survival in ischaemia but imposes a dependence on glycine clearance. *Nature* **520**, 363-367 (2015).

290. J. Ye *et al.*, Serine catabolism regulates mitochondrial redox control during hypoxia. *Cancer discovery* **4**, 1406-1417 (2014).

291. E. L. Pearce, M. C. Poffenberger, C. H. Chang, R. G. Jones, Fueling immunity: insights into metabolism and lymphocyte function. *Science* **342**, 1242454 (2013).

292. Y. Maekawa *et al.*, Notch2 integrates signaling by the transcription factors RBP-J and CREB1 to promote T cell cytotoxicity. *Nat Immunol* **9**, 1140-1147 (2008).

293. A. M. Bolger, M. Lohse, B. Usadel, Trimmomatic: a flexible trimmer for Illumina sequence data. *Bioinformatics* **30**, 2114-2120 (2014).

294. Y. Zhang *et al.*, Model-based analysis of ChIP-Seq (MACS). *Genome Biol* **9**, R137 (2008).

295. L. J. Zhu *et al.*, ChIPpeakAnno: a Bioconductor package to annotate ChIP-seq and ChIP-chip data. *BMC Bioinformatics* **11**, 237 (2010).